Entropica Labs Apprenticeship Report: Solving MaxCut Problem using Quantum Approximate Optimisation Algorithm (QAOA) under a proposed Hybrid Quantum-Classical Parameter Optimisation Strategy

Chee Chong Hian[1]

Entropica Labs
Odeon Towers, Singapore 188720,
Singapore

School of Physical and Mathematical Sciences
Nanyang Technological University, Singapore 637371,
Singapore

26th June 2020

[1]Email: chee0122@ntu.edu.sg

Abstract

In this project, a new greedy-based Hybrid Quantum-Classical Parameter Optimisation Strategy is proposed, Greedy Newton combines the practicality of Greedy-based heuristics and the efficiency of Newton's method of optimisation to improve the parameter optimisation performance in QAOA to solve the unweighted MaxCut problem. It promises to generate a candidate quantum state, which maximises the expectation of the MaxCut Hamiltonian, that has the best possible probability to solve MaxCut. However, its implementation was not without its difficulties as finding the gradient and Hessian of the expectation, with respect to the local QAOA parameters, necessitates an unconventional method of calculating it. By the results of a numerical experiment, it was found that the Greedy Newton strategy performs better than the conventional ones such as Standard Greedy Search and Greedy Subsearch in terms of total number of quantum computer calls needed and the total amount of simulated computational time required, by an order of magnitude of at most 2, with comparable candidate state MaxCut solution quality, under specific graphs types and cases of small $g \leq 3$ regularity and small $n \leq 8$ number of vertices.

Contents

Acknowledgements

I would like to thank my mentor, Ewan Munro, for giving technical advice and research guidance that helped me to bring forth my personal ideas that carried this projects through. I am also grateful to my supervisor, Tommaso Demarie, for giving objective feedback and comments with regards to my project progress which helped me to plan and craft my project flow effectively.

In addition, I would like to express gratitude to SGInnovate Programme Manager, Shiangker Wong, who had organised the SGInnovate Summation Programme which provided me a wonderful opportunity to work in the Quantum Computing industry and interact with other talented apprentices from other deep tech industries.

Finally, I would also like to thank my supervising professor Mile Gu from the School of Physical and Mathematical Sciences (SPMS) at Nanyang Technological University (NTU), and his research colleague Dr Jayne Thompson from the Centre for Quantum Technologies (CQT) at National University of Singapore (NUS) for expressing support in me undertaking this Apprenticeship as a non credit-bearing internship under the NTU's Bachelor of Science (Honours) in Physics degree programme.

Project Funding

This project was carried out in the year 2020 from January to June, fully funded by both SGInnovate and Entropica Labs, under the SGInnovate's Summation Programme. The contents of this project are solely the responsibility of the project author and do not represent the official views of SGInnovate, Entropica Labs, SPMS, NTU, CQT and NUS.

List of Figures

List of Tables

Chapter 1

Project Introduction

Quantum computing has received tremendous attention in the recent decade, fuelled by its exciting and powerful potential to solve difficult computational problems in a faster and more efficient manner than a classical computer would. However, to achieve and deliver such a promise is an extremely difficult task due to the sheer complexity and scale of building a working quantum computer. Currently, most of the quantum computers that exist today are in the Noisy Intermediate-Scale Quantum (NISQ) regime [Pre18], which means that researchers today can test state-of-the-art quantum algorithms that use up to 100 noisy and sparsely connected qubits. NISQ computers are incapable of running powerful quantum algorithms such as Shor's Factoring [Sho94] or Grover's Database Search [Gro96] that requires noiseless and densely connected qubits. Both algorithms are powerful as they have theoretically proven high efficiencies and speedups against their classical counterparts, which may one day revolutionise the computing industry. It may take several more decades of development in quantum computer engineering to supersede NISQ and achieve Full Quantum Error-Correction/Mitigation regime [NC10].

Fortunately, there exist useful, though less powerful, quantum algorithms are suited for NISQ computers. It may have debatable efficiencies and speedups in solving certain class of computational problems. One of these NISQ algorithms is called Quantum Approximate Optimisation Algorithm (QAOA) that was designed to solve combinatorial problems approximately [FGG14b]. It solves by generating a candidate quantum state that has a high probability of collapsing into a solution state, which solves the combinatorial problem. To generate the candidate state, QAOA applies a series of parametrised unitary operators on a starting initial state. By optimally adjusting the parameters of the unitary operators, QAOA would therefore output the desired candidate state. The issue of finding optimal parameters may be resolved either by solving for it analytically or numerically using a classical optimisation strategy. As the analytical method is usually difficult, the numerical approach is often preferred. The use of a classical optimisation strategy for optimising any parameters for a parametrised quantum algorithm is called the Hybrid Quantum-Classical Parameter Optimisation Strategy[Per+13]. Implementing different hybrid strategies would therefore yield different efficiencies and speedups of QAOA.

However, regardless of any hybrid strategies, a theoretically optimal QAOA has a proven theoretical lower and upper bounds in the ability to solve certain combinatorial problems under several specific cases [FGG14b; FGG14a; LZ16]. There have been numerous theoretical work done on analysing the performance of QAOA to solve many of these problems, under many different hybrid strategies. For example, there are hybrid strategies that implement gradient-based optimisers such as

gradient descent [Cro18; Pag+19; Swe+19], quasi-Newton methods (BFGS) [Ans+18; Zho+18; Oh+19; Vik+19; UBP20; WMS20; WGK20], non-gradient based optimizers such as Nelder Mead [GM18; Li+19; Ben+19; Vik+19; MCD20; UBP20; Tom+20] and machine learning inspired optimisers such as neural networks [McC+18; Ver+19] and reinforcement learning [McK+19; Kha+19b; Kha+19a; GSR19; Wau+20]. While there are strong efforts and progress made in developing new sophisticated hybrid strategies for QAOA, there seems to be an insufficient development on greedy-based hybrid strategies due to its perceived poor performance in terms of computational time and quality of the candidate state generated. In an attempt to improve its performance, a new greedy-based hybrid strategy, called Greedy Newton will be proposed to solve for a combinatorial MaxCut Graph problem. Its computational solving performance will be compared against two other conventional greedy-based hybrid strategy: Standard Greedy Search & Greedy Subsearch.

1.0.1 Project Aim

In this project, we aim to investigate the performance of Greedy Newton and compare against two other conventional greedy-based hybrid strategy for QAOA parameter optimisation.

1.0.2 Project Objectives

1. Describe and explain the development of the Greedy Newton hybrid strategy.
2. Describe and elaborate two other conventional greedy-based hybrid strategies: Standard Greedy Search & Greedy Subsearch
3. Define the key performance indicators (KPI) that will be used in comparing the performance of the greedy-based hybrid strategies.
4. Program and run a custom numerical quantum simulation experiment that implements the aforementioned hybrid strategies.
5. Analyse and discuss the results obtained from the numerical simulation.

1.0.3 Project Overview

This project consists of three parts. The first part is the project background, where the basics of quantum mechanics, quantum computing and the variational quantum algorithm will be briefly introduced. The second part is the main project that consists of several chapters which will elaborate in detail on QAOA, the MaxCut problem, the aforementioned hybrid strategies, the implementation of the numerical quantum simulation experiment and a discussion on the numerical results. The third part is the project conclusion which contains a write up on the apprenticeship experience and future research on this project. Other additional, but inapplicable, information such as curious extensions of the theoretical results are kept in the appendix section.

Part I

Project Background

Chapter 2

Quantum Mechanics

This chapter is appropriately modified from an earlier work by the same author [Che20]. Quantum mechanics is a theory that attempts to explain the non-classical behaviours of quantum systems, by modelling quantum systems and operations using mathematical concepts found in linear algebra and probability. In the computational context, quantum mechanics is analogous to classical mechanics. Classical mechanics involves classical operations acting on classical states while quantum mechanics involves quantum operations acting on quantum states. Specifically, classical operations are algebraic arithmetic and measurements that seems to mirror the behaviour of quantum operations, which are unitary transformation and quantum measurements, mathematically represented by unitary and hermitian matrix respectively. Classical states are collections of n-level classical systems, mathematically represented as bits or digits, defined under a binary or a decimal number system. On the other hand, a quantum state is a collection of n-level quantum systems that is mathematically represented as tensor products of n-level quantum systems. The summary of the basic structure of classical mechanics and quantum mechanics in the computation context is given in figures 2.0.1 and 2.0.2 respectively.

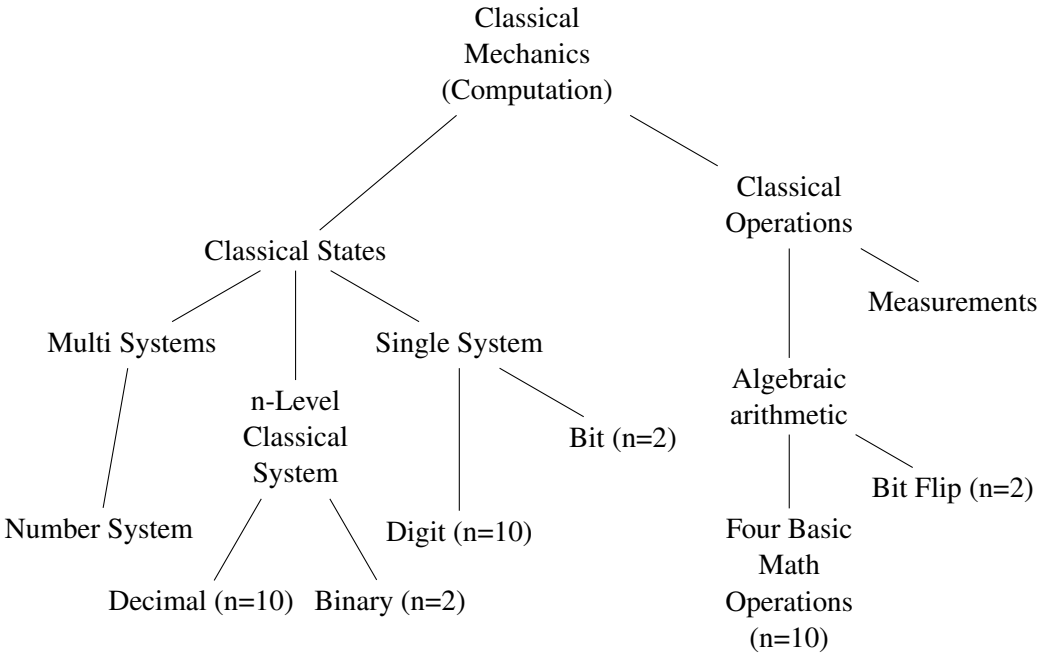

Figure 2.0.1: The basic structure of classical mechanics, in the computational context.

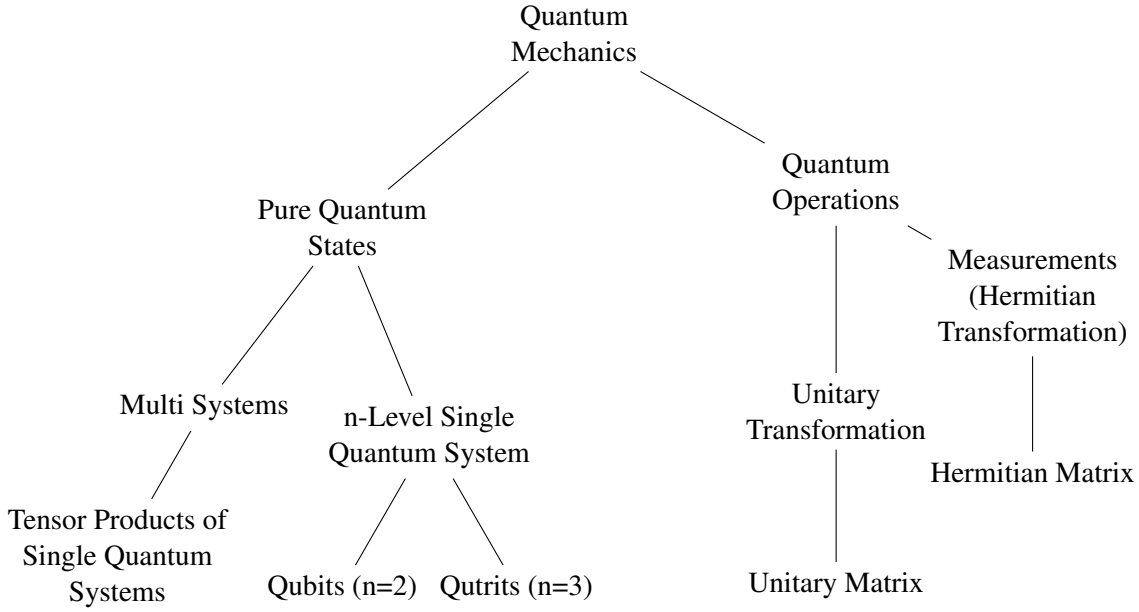

Figure 2.0.2: The basic structure of quantum mechanics, in the computational context.

2.1 Quantum Superposition of Pure Quantum States

We shall only consider isolated quantum systems without any environmental noise interference. The simplest quantum system in quantum mechanics is a two-level quantum system, called a qubit, which is a quantum analogue of a classical bit. A classical bit $\varphi = \{0, 1\}$, upon measurement, will reveal itself to be either 0 or 1. A general qubit $|\varphi\rangle$ is linear complex superposition of up state $|0\rangle$ and down state $|1\rangle$

with some complex coefficients α and β respectively, that is,

$$\begin{aligned} |\varphi\rangle &= \alpha|0\rangle + \beta|1\rangle && (2.1.1) \\ &| \quad \text{In vector notation from linear algebra,} \\ &= \alpha\begin{pmatrix} 1 \\ 0 \end{pmatrix} + \beta\begin{pmatrix} 0 \\ 1 \end{pmatrix} = \begin{pmatrix} \alpha \\ \beta \end{pmatrix} && (2.1.2) \end{aligned}$$

Such a linear complex superposition is called quantum superposition, which allows the qubit to hold a richer set of information, in terms of the complex coefficients α and β. In contrast, a classical bit can only hold one bit of information, either 0 or 1. We may define the hermitian conjugate (dagger †: conjugate transpose) of the qubit as $\langle\varphi| = |\varphi\rangle^\dagger$, that is,

$$\begin{aligned} \langle\varphi| &= \alpha^*\langle 0| + \beta^*\langle 1| && (2.1.3) \\ &= \begin{pmatrix} \alpha^* & \beta^* \end{pmatrix} && (2.1.4) \end{aligned}$$

where $*$ represents complex conjugate, so that we can employ mathematical operations such as matrix multiplication to calculate several useful quantities. $\langle\varphi|$ and $|\varphi\rangle$ physically represent the same qubit, though they are mathematically different. The up state $|0\rangle$ and down state $|1\rangle$ has a special meaning in quantum computing. Both states, when paired as a 2D orthonormal basis set, $\{|0\rangle, |1\rangle\}$, is called the computational basis set. It spans the 2D Hilbert space $\mathscr{H}_2$, that is the space where all possible qubits reside in. As an analogy, a binary bit space contains only 0 and 1 as it is the space where all possible bits reside in. In general, there are infinite number of possible 2D orthonormal basis sets that spans $\mathscr{H}_2$. That is, any set $\{|x\rangle, |y\rangle\}$ can be an orthonormal basis set that spans $\mathscr{H}_2$, if and only if all the basis in the set satisfies the following orthogonality and normalization properties:

$$\begin{aligned} \text{Orthogonality}: \quad \langle x|y\rangle &= 0 \quad | \quad \text{where } |x\rangle \neq |y\rangle. && (2.1.5) \\ &| \quad \text{In vector notation from linear algebra,} \\ &| \quad \text{this usually means a dot product of two vectors.} \\ &| \quad \text{Let } x_i \text{ and } y_i \text{ be the } i^{th} \text{ element of vector } \vec{x} \text{ and } \vec{y} \text{ respectively.} \\ \sum_{i=1}^{2} x_i^* y_i &= 0 && (2.1.6) \end{aligned}$$

$$\begin{aligned} \text{Normalization}: \quad \langle x|x\rangle &= \langle y|y\rangle = 1 \quad | \quad \text{where } |x\rangle \neq |y\rangle. && (2.1.7) \\ &| \quad \text{In vector notation from linear algebra,} \\ \sum_{i=1}^{2} x_i^* x_i &= \sum_{i=1}^{2} y_i^* y_i = 1 && (2.1.8) \end{aligned}$$

Thus, any qubit $|\varphi\rangle$ that resides in $\mathscr{H}_2$, spanned by $\{|x\rangle, |y\rangle\}$, has the following normalization property:

$$\begin{aligned}
\langle\varphi|\varphi\rangle &= [\alpha^* \langle x| + \beta^* \langle y|][\alpha |x\rangle + \beta |y\rangle] && (2.1.9)\\
&= |\alpha|^2 \langle x|x\rangle + \alpha^*\beta \langle x|y\rangle + \beta^*\alpha \langle y|x\rangle + |\beta|^2 \langle y|y\rangle && (2.1.10)\\
&| \quad \text{Using basis orthogonality and normalization properties} \\
&| \quad \text{from equation 2.1.5 and 2.1.7 respectively.} \\
&= |\alpha|^2 + |\beta|^2 = 1 && (2.1.11)
\end{aligned}$$

According to one of the postulates of quantum mechanics, Born's Rule, the squared amplitudes $|\alpha|^2$ and $|\beta|^2$ represent the probability of the qubit being in the $|x\rangle$ and $|y\rangle$ states respectively. That is, $\text{Prob}(|x\rangle) = |\alpha|^2$ and $\text{Prob}(|y\rangle) = |\beta|^2$. As a result of equation 2.1.11, it must be that $\langle\varphi|\varphi\rangle = \text{Prob}(|x\rangle) + \text{Prob}(|y\rangle) = 1$. Therefore, the normalization property of the qubit $|\varphi\rangle$ is interpreted as the unit sum of probabilities that $|\varphi\rangle$ is either state $|x\rangle$ or $|y\rangle$ [SN17].

However, the availability of the infinite choices of 2D orthonormal basis sets might pose a head-scratching problem. Since, the same qubit can be expressed in any 2D orthonormal basis sets and not just computational basis set, how can we enforce which 2D orthonormal basis set a qubit must take, if all 2D orthonormal basis sets are equally preferable? The short answer would be that, any quantum computational operations under any 2D orthonormal basis set are computationally equivalent. As long as we are consistent in the use of an 2D orthonormal basis set throughout the computation, and not switch to other 2D orthonormal basis set unnecessarily, there need not to be any kind of basis set 'enforcement'. In practice, there are times when it required to switch to another basis set from an old set. In that case, all quantum states and operations will have to be translated to the new basis set before any computation. Conventionally, the computational basis set $\{|0\rangle, |1\rangle\}$ is chosen to be basis for quantum computing.

2.2 Unitary Transformation

Classically, manipulating a bit involves a bit flip. This is an example of a classical operation that changes the value of the bit.

$$\varphi = \{0,1\} \quad \overset{\text{Bit Flip}}{\longrightarrow} \quad \{1,0\}$$

Quantum mechanically, manipulating a qubit involves a unitary transformation or operation. It changes the probability of a qubit being in either orthogonal state $|x\rangle, |y\rangle$, while preserving the unit sum of their probabilities. A unitary transformation is physically represented as an unitary operator $\hat{U}$. The defining property of a unitary $\hat{U}$ is that the inverse of $\hat{U}$ must be equal to the hermitian conjugate of $\hat{U}$, that is $\hat{U}^{-1} = \hat{U}^\dagger$. For a general arbitrary 2D unitary operator $\hat{U}$ in the computational basis $\{|0\rangle, |1\rangle\}$, it can be

written as,

$$\begin{aligned}
\hat{U}(\theta,\phi,\lambda,\delta) &= e^{i\delta}\left[\cos\left(\frac{\theta}{2}\right)|0\rangle\langle 0| - e^{i\lambda}\sin\left(\frac{\theta}{2}\right)|0\rangle\langle 1|\right. \\
&\quad \left. + e^{i\phi}\sin\left(\frac{\theta}{2}\right)|1\rangle\langle 0| + e^{i(\phi+\lambda)}\sin\left(\frac{\theta}{2}\right)|1\rangle\langle 1|\right] \qquad (2.2.1)\\
&\quad | \quad \text{In matrix notation from linear algebra,} \\
&\quad | \quad \text{where} \quad \theta,\phi,\lambda,\delta \in [0,2\pi]. \\
&= e^{i\delta}\begin{pmatrix} \cos\left(\frac{\theta}{2}\right) & -e^{i\lambda}\sin\left(\frac{\theta}{2}\right) \\ e^{i\phi}\sin\left(\frac{\theta}{2}\right) & e^{i(\phi+\lambda)}\cos\left(\frac{\theta}{2}\right) \end{pmatrix} \qquad (2.2.2)
\end{aligned}$$

The factor $e^{i\delta}$ of $\hat{U}$ is called a global phase factor that is a non-physical, non-observed property of the transformation. Therefore it is often ignored in calculations. Hence, dropping the phase factor $e^{i\delta}$, we have the general 2D unitary operator up to a global phase $\hat{U}(\theta,\phi,\lambda)$,

$$\hat{U}(\theta,\phi,\lambda) = \begin{pmatrix} \cos\left(\frac{\theta}{2}\right) & -e^{i\lambda}\sin\left(\frac{\theta}{2}\right) \\ e^{i\phi}\sin\left(\frac{\theta}{2}\right) & e^{i(\phi+\lambda)}\cos\left(\frac{\theta}{2}\right) \end{pmatrix} \qquad (2.2.3)$$

When the unitary operator $\hat{U}$ is applied on the qubit $|\varphi\rangle = \alpha|0\rangle + \beta|1\rangle$, the qubit transforms into another unique quantum qubit $|\varphi'\rangle = \gamma|0\rangle + \delta|1\rangle$ with different probabilities $|\gamma|^2$ and $|\delta|^2$, that is $|\varphi\rangle \xrightarrow{\hat{U}} |\varphi'\rangle$. Explicitly, it does the following,

$$\begin{aligned}
\hat{U}|\varphi\rangle &= \left[\cos\left(\frac{\theta}{2}\right)|0\rangle\langle 0| - e^{i\lambda}\sin\left(\frac{\theta}{2}\right)|0\rangle\langle 1|\right. \\
&\quad \left. + e^{i\phi}\sin\left(\frac{\theta}{2}\right)|1\rangle\langle 0| + e^{i(\phi+\lambda)}\sin\left(\frac{\theta}{2}\right)|1\rangle\langle 1|\right][\alpha|0\rangle + \beta|1\rangle] \qquad (2.2.4)\\
&\quad | \quad \text{Using the orthonormalisation properties of the computational basis.} \\
&= \left[\alpha\cos\left(\frac{\theta}{2}\right) - \beta e^{i\lambda}\sin\left(\frac{\theta}{2}\right)\right]|0\rangle + \left[\alpha e^{i\phi}\sin\left(\frac{\theta}{2}\right) + \beta e^{i(\phi+\lambda)}\sin\left(\frac{\theta}{2}\right)\right]|1\rangle \qquad (2.2.5)\\
&\quad | \quad \text{In matrix notation from linear algebra, note the following that } |\gamma| + |\delta|^2 = 1. \\
&= \begin{pmatrix} \alpha\cos\left(\frac{\theta}{2}\right) - \beta e^{i\lambda}\sin\left(\frac{\theta}{2}\right) \\ \alpha e^{i\phi}\sin\left(\frac{\theta}{2}\right) + \beta e^{i(\phi+\lambda)}\sin\left(\frac{\theta}{2}\right) \end{pmatrix} \overset{\text{Let this be}}{=} \begin{pmatrix} \gamma \\ \delta \end{pmatrix} \qquad (2.2.6)\\
&= \gamma|0\rangle + \delta|1\rangle = |\varphi'\rangle \qquad (2.2.7)
\end{aligned}$$

2.3 Measurements and Hermitian Operators

Classical measurement is another classical operation and measuring an unknown classical bit is trivial. Suppose a measurement on an unknown bit φ, that has outcomes 1 and -1 for bit states 0 and 1 respectively, is conducted. Then, two things will happen: the revelation of the measurement outcomes and the final bit state.

Final Bit State	Measurement Outcomes
$\varphi = 0$	1
$\varphi = 1$	-1

Table 2.3.1: Classical post-measurement result of an unknown bit φ.

Similarly, a quantum measurement is another kind of a quantum operation and the measurement of a qubit involves a 2D hermitian operator $\hat{M}$ that has the defining property that the hermitian conjugate of $\hat{M}$ is equal to itself, $\hat{M}^\dagger = \hat{M}$. As a consequence of the hermiticity, the eigenvalues of $\hat{M}$ are always real, called it m, and they are interpreted as the measurement outcomes. However, unlike classical measurements, the post-measured qubit will permanently transform into one of the ortho-normalized eigenstates of $\hat{M}$, called it $|m\rangle$. This quantum transformation is commonly phrased as the *collapse of a measured quantum state*, because the pre-measured qubit cannot be recovered back by any inverse hermitian transformation on the measured qubit.

To see this collapse explicitly, let m_1, m_2 be eigenvalues that corresponds to $|m_1\rangle, |m_2\rangle$ which are ortho-normalized eigenstates of $\hat{M}$, where $m_1 \neq m_2$ and $|m_1\rangle \neq |m_2\rangle$. Decompose the qubit $|\varphi\rangle$ into a linear combination of the ortho-normalized eigenstates $|m_1\rangle, |m_2\rangle$ with corresponding complex coefficients a, b as follows,

$$
\begin{aligned}
|\varphi\rangle &= a|m_1\rangle + b|m_2\rangle && (2.3.1)\\
&| \quad \text{Apply measurement operator } \hat{M}. \\
\hat{M}|\varphi\rangle &= a\hat{M}|m_1\rangle + b\hat{M}|m_2\rangle && (2.3.2)\\
&| \quad \text{Using eigenequation } \hat{M}|m_j\rangle = m_j|m_j\rangle. \\
&= am_1|m_1\rangle + bm_2|m_2\rangle && (2.3.3)
\end{aligned}
$$

Note that since $|am_1|^2 + |bm_2|^2 \neq 1$ in general, $\hat{M}|\varphi\rangle$ is not a valid qubit or a quantum state as it does not satisfy normalization property in equation 2.1.11. By the measurement postulate of quantum mechanics [SN17], such a state $\hat{M}|\varphi\rangle$ will therefore collapse to either eigenstate $|m_1\rangle$ or $|m_2\rangle$, with probability $|a|^2$, $|b|^2$ and with measurement outcomes m_1, m_2 respectively.

Final Qubit State	Measurement Outcomes	Probability
$\|m_1\rangle$	m_1	$\|a\|^2$
$\|m_2\rangle$	m_2	$\|b\|^2$

Table 2.3.2: Quantum post-measurement of a generic qubit $|\varphi\rangle = a|m_1\rangle + b|m_2\rangle$ with measurement operator $\hat{M}$.

This property of quantum measurement has far reaching consequences. Unlike a classical measurement, quantum measurement does not reveal any information about the pre-measured qubit. Therefore, a single measurement on an unknown qubit is insufficient to gain knowledge of the pre-measured qubit. Worse, repeated measurements on the same qubit would not yield any meaningful results, as it would lead to the same outcomes as revealed in the first measurement.

One workaround is to ensemble a collection of equivalent unknown qubits and perform repeated

single measurements on these unknown qubits individually. By doing a statistical count of the measurement outcomes, the probabilities $|a|^2$, $|b|^2$ can be calculated and thus be able to gain some, though not complete, information about the pre-measured qubit using equation 2.3.1.

Often, one is usually interested in finding out the average value of the measurement outcomes given an unknown qubit $|\varphi\rangle$, called expectation value of the measurement operator $\hat{M}$ with respect to the qubit $|\varphi\rangle$, symbolically represented as $\langle\hat{M}\rangle = \langle\varphi|\hat{M}|\varphi\rangle$. We can show this by theoretically calculating the expectation value by applying a hermitian conjugate quantum state $\langle\varphi| = |\varphi\rangle^\dagger$ to $\hat{M}|\varphi\rangle$.

$$\begin{aligned}
\langle\varphi|\hat{M}|\varphi\rangle &= [a^*\langle m_1| + b^*\langle m_2|][am_1|m_1\rangle + bm_2|m_2\rangle] && (2.3.4)\\
&= |a|^2 m_1\langle m_1|m_1\rangle + a^*bm_2\langle m_1|m_2\rangle + b^*am_1\langle m_2|m_1\rangle + |b|^2 m_2\langle m_2|m_2\rangle && (2.3.5)\\
&| \quad \text{Apply orthonormality } \langle m_i|m_j\rangle = \delta_{ij}.\\
&= |a|^2 m_1 + |b|^2 m_2 && (2.3.6)\\
&= \text{Prob}(m_1)\cdot m_1 + \text{Prob}(m_2)\cdot m_2 && (2.3.7)\\
&| \quad \text{By statistics, this is the definition of average using probablities.}\\
&= \langle\hat{M}\rangle && (2.3.8)
\end{aligned}$$

The expectation value is always a value between the measurement outcomes, $m_1 \leq \langle\hat{M}\rangle \leq m_2$, if $m_1 < m_2$. Hence, it is a useful quantity that can be used as a rough gauge to determine how 'close' is the unknown qubit to either of the ortho-normalized eigenvectors.

2.4 Multiple Quantum Systems

To represent more information classically, two or more bits are needed and ordered in a pre-defined way such as a binary system. Quantum mechanically, the act of putting two or more qubits together mathematically represents a linear tensor (Kronecker) product operation $\otimes$, a symbol that is usually omitted for clarity. Consequently, quantum information can be represented as tensor products of multiple qubits. Let $|\varphi_1\rangle$ and $|\varphi_2\rangle$ be two qubits, then,

$$\begin{aligned}
|\varphi_1\rangle\otimes|\varphi_2\rangle &= |\varphi_1\rangle|\varphi_2\rangle \quad | \quad \text{omitted } \otimes \text{ for clarity.} && (2.4.1)\\
&| \quad \text{Using orthonormal basis set } \{|0\rangle, |1\rangle\}.\\
&= [\alpha_1|0_1\rangle + \beta_1|1_1\rangle][\alpha_2|0_2\rangle + \beta_2|1_2\rangle] && (2.4.2)\\
&| \quad \text{Dropping all indices in } |\,\rangle \text{ and combining them.}\\
&= \alpha_1\alpha_2|00\rangle + \alpha_1\beta_2|01\rangle + \beta_1\alpha_2|10\rangle + \beta_1\beta_2|10\rangle && (2.4.3)
\end{aligned}$$

Similarly, multi-qubit unitary transformation and measurements can be constructed from tensor products of the single qubit versions. For example, applying a multi-qubit unitary operation $\hat{A}\otimes\hat{B}$ on $|\varphi_1\rangle\otimes|\varphi_2\rangle$ where $\hat{A}$, $\hat{B}$ are single qubit unitary operators yields,

$$\begin{aligned}
\left(\hat{A}\otimes\hat{B}\right)|\varphi_1\rangle\otimes|\varphi_2\rangle &= \hat{A}|\varphi_1\rangle\hat{B}|\varphi_2\rangle && (2.4.4)\\
&= \alpha_1\alpha_2 A|0\rangle B|0\rangle + \alpha_1\beta_2 A|0\rangle B|1\rangle\\
&\quad + \beta_1\alpha_2 A|1\rangle B|0\rangle + \beta_1\beta_2 A|1\rangle B|1\rangle && (2.4.5)
\end{aligned}$$

However, tensor products of the single qubit quantum operations are just a subset of the possible multi-qubit operations. There are multi-qubits states/operations that cannot be represented using tensor products of single qubit quantum states/operators.

2.5 Quantum Entanglement

When we have an unknown classical binary string, the only way to reveal all classical information of the unknown string is by measuring all of the individual bits. Measuring a unknown bit of an unknown string, trivially and unexpectedly, reveals one bit worth of classical information. However, measuring one unknown qubit of a multi-qubit ensemble, may reveal more than just a qubit worth of quantum information! In fact, it is possible to gain information of all other unknown and unmeasured qubits collectively by just a single measurement of one qubit. This property is commonly called quantum entanglement and the quantum state that exhibits such a property is called an entangled state. This property is crucial as it lies at the heart of many quantum algorithms such as quantum communication, cryptography and teleportation. To demonstrate quantum entanglement concept in an simplified context, consider a two-labelled qubit ensemble $|\varphi_{1,2}\rangle = \alpha|01\rangle + \beta|10\rangle$, that has unknown complex amplitudes α, β such that $|\alpha|^2 + |\beta|^2 = 1$. Note that $|\varphi_{1,2}\rangle$ cannot be expressed in terms of tensor products of individual qubits $|\varphi_1\rangle$ and $|\varphi_2\rangle$. If we were to measure qubit $|\varphi_1\rangle$ in the computational basis, then as a consequence of quantum measurement, $|\varphi_1\rangle$ collapses into either $|0\rangle$ or $|1\rangle$ with probabilities $|\alpha|^2$ or $|\beta|^2$ respectively. Not only, we gain quantum information of the first qubit, we also gain information of the second qubit as we know that the second unmeasured qubit must be $|1\rangle$ or $|0\rangle$ respectively, with absolute certainty. The power of quantum entanglement cannot be overstated as the manipulation of qubit entanglement is definitely one of the things that allows quantum computing to surpass classical computing in certain computational problems. Unfortunately, mastering full control of quantum entanglement is extremely difficult to do experimentally, and is presently an active area of research in quantum computing.

Chapter 3

Quantum Computation

This chapter is also appropriately modified from an earlier work by the same author [Che20]. Classical computing uses a string of bits s and manipulates it by doing an ordered sequence of bit flips before measurement to get an output string s'. Similarly, in quantum computing, a set of qubits $|s\rangle$, called a qubit register, is initialized and unitary transformed by unitary operators to output a quantum state $|s'\rangle$. A measurement is then performed on the output state $|s'\rangle$ by a hermitian operator $\hat{M}$ to get the measurement outcomes m and the collapsed quantum state $|m\rangle$. A simple diagram showing the flow of information for each kind of computing is given in figure 3.0.1.

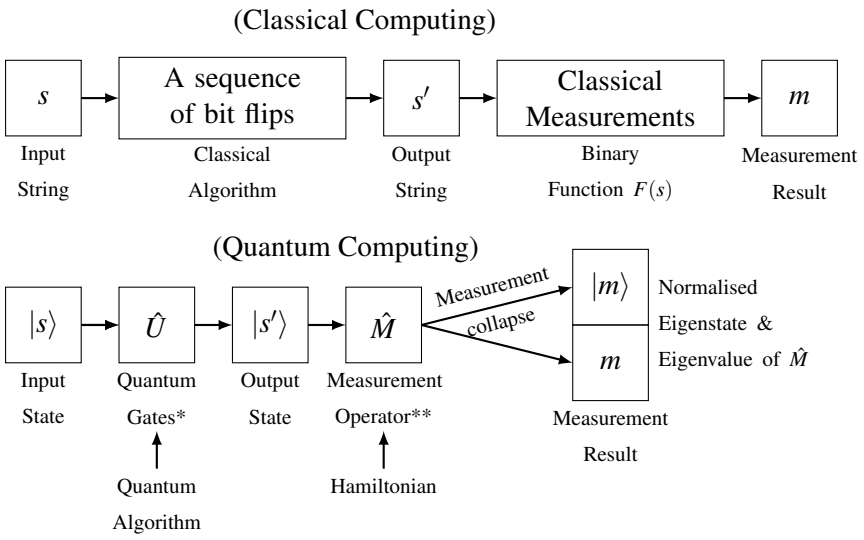

Figure 3.0.1: A basic comparison of the flow of classical and quantum information.

To formalize quantum computations using qubits, models of quantum computations are created to help describe the organization of quantum operations and information so that the performance of a quantum algorithm running on these models can be analysed and evaluated. The standard model of organizing quantum operations is the quantum circuits model as an quantum analogue of classical circuit gate model.

3.1 Quantum Circuits Model

Quantum Circuits is a standard model of quantum computation. Quantum circuits are diagrammatically represented a one way directed set of wires with no loops, cycles, join ins, or fan outs. The wires are laid out horizontally and ordered vertically. Each wire represents a single qubit or a qubit register, depending on context. At the beginning of the quantum circuit, on the left, qubits are prepared and initialized at their respective positions. Quantum and measurement gates, representing unitary operations and measurements, are placed in the middle and at the end of a quantum circuit on the right, respectively. For example, figure 3.1.1 shows a quantum circuit with all qubits initialised in $|0\rangle$, then a series of quantum gates (unitary operators) are applied. Finally, multiple measurements (hermitian operators) are performed, in the computation basis $\{|0\rangle, |1\rangle\}$, on the respective qubits to obtain multiple measurement outcomes.

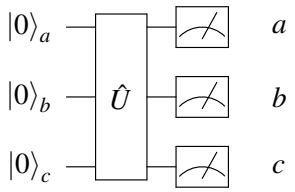

Figure 3.1.1: A generic quantum circuit diagram with 3 initialized qubits $|0\rangle_a |0\rangle_b |0\rangle_c$ on the left, a multi-qubit unitary quantum gate $\hat{U}$ in the middle and a set of measurements on the qubits, represented by a meter symbol on the right.

3.2 Unitary Quantum Gates

Quantum gates are unitary operators in the quantum circuits model. The following subsections will briefly summarise the common set of single, multi-qubit quantum gates and measurement gates. Interested readers may consult various quantum computing textbook such as [NC10] for a more detailed description and elaboration of quantum gates.

3.2.1 Common Gates

There are many single qubit quantum gates which are derivatives of the general arbitrary 2D unitary operator $\hat{U}$ in equation 2.2.3. The common set of single qubit quantum gates are: Pauli-$\hat{Z}$, Pauli-$\hat{X}$, Pauli-$\hat{Y}$, Hadamard $\hat{H}$, Phase $\hat{S}$ and $\frac{\pi}{8}$-gate[1] $\hat{T}$. A summary of operations on a general qubit $|\varphi\rangle$ is given in the equation set 3.2.2 and its symbols are shown in figure 3.2.1.

$$\hat{Z} = \begin{bmatrix} 1 & 0 \\ 0 & -1 \end{bmatrix} \quad , \quad \hat{X} = \begin{bmatrix} 0 & 1 \\ 1 & 0 \end{bmatrix} \quad , \quad \hat{Y} = \begin{bmatrix} 0 & -i \\ i & 0 \end{bmatrix}$$

$$\hat{H} = \tfrac{1}{\sqrt{2}} \begin{bmatrix} 1 & 1 \\ 1 & -1 \end{bmatrix} \quad , \quad \hat{S} = \begin{bmatrix} 1 & 0 \\ 0 & i \end{bmatrix} \quad , \quad \hat{T} = \begin{bmatrix} 1 & 0 \\ 0 & e^{i\pi/4} \end{bmatrix} \tag{3.2.1}$$

[1] An unfortunate naming of the square root of phase gate S [NC10].

$$|\varphi\rangle = \alpha|0\rangle + \beta|1\rangle \begin{cases} \xrightarrow{\hat{Z}} & \alpha|0\rangle - \beta|1\rangle \\ \xrightarrow{\hat{X}} & \beta|0\rangle + \alpha|1\rangle \\ \xrightarrow{\hat{Y}} & i(-\beta|0\rangle + \alpha|1\rangle) \\ \xrightarrow{\hat{H}} & \alpha\frac{|0\rangle+|1\rangle}{\sqrt{2}} + \beta\frac{|0\rangle-|1\rangle}{\sqrt{2}} \\ \xrightarrow{\hat{S}} & \alpha|0\rangle + \beta i|1\rangle \\ \xrightarrow{\hat{T}} & e^{i\pi/8}\left(\alpha e^{-i\pi/8}|0\rangle + \beta e^{i\pi/8}|1\rangle\right) \end{cases} \tag{3.2.2}$$

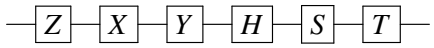

Figure 3.2.1: Common gates symbols, from left to right: Pauli-Z, Pauli-X, Pauli-Y, Hadamard H, Phase S and $\frac{\pi}{8}$ T.

3.2.2 Rotation Gates

Rotation gates are parametrized quantum gates with an angular parameter θ. A summary of these operations on a general qubit $|\varphi\rangle$ is given in the equation set 3.2.3 and its quantum circuit representation are shown in figure 3.2.2. Note that $\mathbb{I}$ represents an identity operation, $\mathbb{I}|\varphi\rangle = |\varphi\rangle$.

$$\begin{aligned} R_z(\theta) &= e^{-i\theta Z/2} = cos(\theta/2)\,\mathbb{I} - isin(\theta/2)\,\hat{Z} = \begin{bmatrix} e^{-i\theta/2} & 0 \\ 0 & e^{i\theta/2} \end{bmatrix} \left(\text{Rotate-}\hat{Z}\right) \\ R_x(\theta) &= e^{-i\theta X/2} = cos(\theta/2)\,\mathbb{I} - isin(\theta/2)\,\hat{X} = \begin{bmatrix} \cos\theta/2 & -i\sin\theta/2 \\ -i\sin\theta/2 & \cos\theta/2 \end{bmatrix} \left(\text{Rotate-}\hat{X}\right) \\ R_y(\theta) &= e^{-i\theta Y/2} = cos(\theta/2)\,\mathbb{I} - isin(\theta/2)\,\hat{Y} = \begin{bmatrix} \cos\theta/2 & -\sin\theta/2 \\ \sin\theta/2 & \cos\theta/2 \end{bmatrix} \left(\text{Rotate-}\hat{Y}\right) \end{aligned} \tag{3.2.3}$$

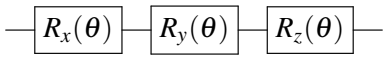

Figure 3.2.2: Rotation gates symbols, from left to right: Rotate-X, $R_x(\theta)$, Rotate-Y, $R_y(\theta)$, Rotate-Z, $R_z(\theta)$.

3.2.3 Swap Gate

Swap gate is a quantum gate that swaps the position of two qubits. Suppose the input qubit register $|x\rangle|y\rangle = |x,y\rangle$, where $x,y = \{0,1\}$, is acted upon by a swap gate S_{wap}, then the resulting qubit register is $|y,x\rangle$. This qubit swap operation and the swap gate symbol are respectively summarised in equation 3.2.4 and figure 3.2.3 below.

$$|x,y\rangle \xrightarrow{S_{wap}} |y,x\rangle \quad , \quad S_{wap} = \begin{bmatrix} 1 & 0 & 0 & 0 \\ 0 & 0 & 1 & 0 \\ 0 & 1 & 0 & 0 \\ 0 & 0 & 0 & 1 \end{bmatrix} \tag{3.2.4}$$

Figure 3.2.3: Two qubit gate: Swap gate S_{wap}.

3.2.4 CNOT and Controlled-Z Gates

Controlled gates are multi-qubit quantum gates that apply a unitary operation on a set of target qubits on the condition of the control qubit. The simplest controlled gates are gates that apply a quantum gate on a single target qubit on the condition of a single control qubit. Two most common controlled gates are CNOT gate C_x and controlled-$\hat{Z}$ gate C_z. CNOT gate applies a Pauli-$\hat{X}$ gate on a single target qubit on the condition of the control qubit being $|1\rangle$. Controlled-$\hat{Z}$ gate is similar to a CNOT, but with a difference that it applies a Pauli-$\hat{Z}$ gate instead. Both controlled operations and the gate symbols are respectively summarised in equations 3.2.5, 3.2.6 and figure 3.2.4 below.

$$|x,y\rangle \xrightarrow{C_x} |x, y\oplus x\rangle \quad , \quad C_x = \begin{bmatrix} 1 & 0 & 0 & 0 \\ 0 & 1 & 0 & 0 \\ 0 & 0 & 0 & 1 \\ 0 & 0 & 1 & 0 \end{bmatrix} \quad (\text{CNOT}) \tag{3.2.5}$$

Note: $\oplus$ modulo 2

$$|x,y\rangle \xrightarrow{C_z} (-1)^{xy}|x,y\rangle \quad , \quad C_z = \begin{bmatrix} 1 & 0 & 0 & 0 \\ 0 & 1 & 0 & 0 \\ 0 & 0 & 1 & 0 \\ 0 & 0 & 0 & -1 \end{bmatrix} \quad \left(\text{Controlled-}\hat{Z}\right) \tag{3.2.6}$$

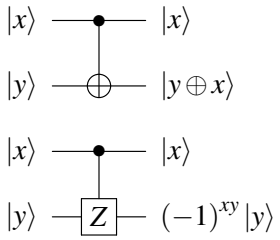

Figure 3.2.4: Single target single control controlled gates, from top to bottom: CNOT, C_x, Controlled-Z, C_z.

3.3 Pauli Measurement Gates

Pauli quantum gates, introduced in earlier subsection 3.2.1, are special gates as they are both unitary and hermitian. Therefore, Pauli gates can act either as unitary gates or measurement gates. The Pauli gates

have the following eigenvectors, eigenbras and eigenvalues.

$$\begin{array}{cccccc} \text{Eigen} & \text{Vectors 1} & \text{Bra 1} & \text{Vectors 2} & \text{Bra 2} \\ \hat{Z} & \begin{pmatrix} 1 \\ 0 \end{pmatrix} & |0\rangle & \begin{pmatrix} 0 \\ 1 \end{pmatrix} & |1\rangle \\ \hat{X} & \frac{1}{\sqrt{2}}\begin{pmatrix} 1 \\ 1 \end{pmatrix} & |+\rangle & \frac{1}{\sqrt{2}}\begin{pmatrix} 1 \\ -1 \end{pmatrix} & |-\rangle \\ \hat{Y} & \frac{1}{\sqrt{2}}\begin{pmatrix} 1 \\ i \end{pmatrix} & |\uparrow_y\rangle & \frac{1}{\sqrt{2}}\begin{pmatrix} 1 \\ -i \end{pmatrix} & |\downarrow_y\rangle \\ \text{Values} & 1 & & -1 & \end{array} \tag{3.3.1}$$

Typically, real quantum computers employ quantum measurements which are done in the computational basis $\{|0\rangle, |1\rangle\}$ that uses Pauli-$\hat{Z}$ gates. To measure qubits other basis such as $\{|+\rangle, |-\rangle\}$ or $\{|\uparrow_y\rangle, |\downarrow_y\rangle\}$, one simply uses an unitary operation to convert these basis into the computation basis for Pauli-$\hat{Z}$ measurements. In other words, to perform Pauli-$\hat{X}$ and Pauli-$\hat{Y}$ measurements using Pauli-$\hat{Z}$ gates, we leverage the following gate decomposition identity, $\hat{X} = HZH$ and $\hat{Y} = SHZHS^\dagger$ respectively, and perform the following Pauli measurement operations as shown in figure 3.3.1 below.

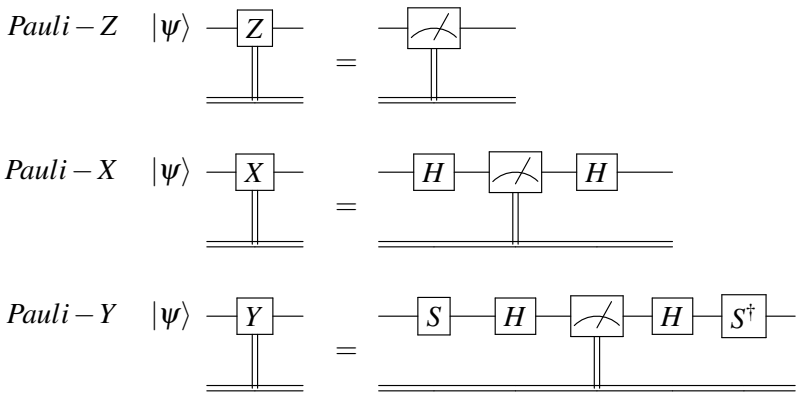

Figure 3.3.1: Pauli measurements circuit decomposition using Pauli-Z gates. Note that the meter symbol denotes a standard Pauli-Z measurement with binary measurement results being $\{0,1\}$ which corresponds to measuring either $\{|0\rangle, |1\rangle\}$ qubit. The double lines represents wires that transmit the classical information in binary.

Suppose if one has an arbitrary measurement operator $\hat{M}$ and wishes to use it on real quantum computers, then, one would probably would need to decompose $\hat{M}$ in terms Pauli operators. Fortunately, it is proven that any 2^nD hermitian operators, which are measurement operators $\hat{M}$, can be expressed as a sum of tensor (Kronecker) product Pauli operators, that is,

$$\hat{M} = \sum_{i,k} \alpha_{ik}\sigma_i^k + \sum_{i_{1,2},k_{1,2}} \alpha_{i_{1,2}k_{1,2}}\sigma_{i_1}^{k_1}\sigma_{i_2}^{k_2} + \sum_{i_{1,2,3},k_{1,2,3}} \alpha_{i_{1,2,3}k_{1,2,3}}\sigma_{i_1}^{k_1}\sigma_{i_2}^{k_2}\sigma_{i_3}^{k_3} + \ldots \tag{3.3.2}$$

where the $\sigma_i^k = \left\{\hat{X}_i, \hat{Y}_i, \hat{Z}_i\right\}$ for $k = 1,2,3$ and on qubit (subspace) i respectively, and α_{ik} is some real

coefficient. Such an expression is called Pauli decomposition and the tensor products of pauli operators are called Pauli Composition. Interested readers may consult any typical quantum group theory or quantum linear algebra mathematical textbooks for proof and more detailed explanation.

3.4 Variational Quantum Algorithm

In physics, we often are interested in measuring the total energy of a given physical system (as the sum of kinetic and potential energies). Under the quantum mechanical framework, the given physical system is treated as a quantum system and the hermitian operator that allows us to measure energy, called Hamiltonian, is applied on it. However, due to quantum measurement collapse, the measured energy would reflect the energy of the collapsed system, instead of the original state. Thus, it is usually preferable to measure the expectation value of the Hamiltonian, which represents the statistical average energy the quantum system.

Sometimes, we may study an unknown physical system by stating its possible energies or the Hamiltonian and we would like to find out what is the ground state of that unknown physical system, which has the lowest energy. This problem is called the Hamiltonian problem and it is significant in physics and chemistry as many interesting physical phenomena happens when a physical system is in a ground state. Consider an elementary Hamiltonian problem:

> Given the electronic Hamiltonian $\hat{H}_e$ of a hydrogen atom, find the electronic ground state of the hydrogen atom.
>
> $$\hat{H}_e = \frac{\hbar^2 \hat{\mathbf{p}}}{2\mu} - \frac{e^2}{4\pi\varepsilon_0 \hat{\mathbf{r}}} \tag{3.4.1}$$
>
> where $\hbar$ is the plank constant, $\mu = \frac{m_e m_p}{m_e + m_p}$ is the reduced mass, with m_e and m_p are the electron and proton masses respectively and ε_0 is the vacuum permittivity.

This problem is a standard physics problem in undergraduate quantum mechanics. We may solve this problem analytically, by using the time-independent Schrödinger equation and the Separation of Variables technique, to obtain the ground state wavefunction $\langle r|\psi_{1,0,0}\rangle$, that is, the positional view of electronic ground quantum state, and ground state energy $E_{1,0,0}$.

$$\langle r|\psi_{1,0,0}\rangle = \frac{1}{\sqrt{\pi a_0^3}} e^{-\frac{r}{a_0}} \tag{3.4.2}$$

$$E_{1,0,0} = -13.6\text{eV} \quad (3\text{s.f.}) \tag{3.4.3}$$

Unfortunately, there are very few examples of Hamiltonian problems with analytical solutions. This is due to the fact that the analytical method of using the Schrödinger equation is difficult and often complicated as it is akin to solving a linear partial differential equation, with no general analytical solution. Although, there exist analytical approximation techniques, such as perturbation theory or Wentzel–Kramers–Brillouin (WKB) method that involves simplifying the Schrödinger equation down to a manageable one with known analytical solutions, such approximations that relies on mathematical tricks or non-physical assumptions cannot be generalised to solve for Hamiltonians with complicated systems such as electron states in a large molecule.

The variational quantum algorithm (VQA) is a type of the quantum algorithm that attempts to solve this problem approximately using quantum computing. VQA is basically a computational extension of the variational method used in quantum mechanics to find approximated solutions to the Hamiltonian problem with complicated systems. The variational method starts with a parametrised quantum state, which contains parameters that one could adjust, that best represents the unknown quantum system. Then, one may substitute some trial parameters and measure the expectation value of the Hamiltonian to find the statistical average energy of the parametrised quantum state. By the variational principle, if the minimum expectation value of the Hamiltonian is measured to be exactly the ground state energy, then the parametrised quantum state must be the ground state of the quantum system. Otherwise, it is inconclusive and the method repeats with new trial parameters until the ground state is found. Conventionally, classical computers are employed to run the variational method numerically. However, representing quantum states using classical information and processing them take vast amounts of classical computing resources. Quantum computers resolves these resource limitations by allowing users to prepare and process multiple qubits easily, which represent the parametrised quantum states naturally, and take energy measurements directly, while leaving the parameter optimisation to classical computers. This is the essence of Hybrid Quantum-Classical Parameter Optimisation Strategy [Per+13; McC+15]. The following pseudocode is an outline of the VQA:

Variational Quantum Algorithm

Inputs:

- A pure initial quantum state $|\Psi_0\rangle$.
- A problem Hamiltonian $\hat{H}$.
- A desired precision threshold ε.

Outputs:

- An approximated quantum ground state of $\hat{H}$, $|\Psi_g\rangle$.
- An approximated ground state energy E.

Algorithm Steps:

1. (Parametrised State Preparation) Starting with the input initial quantum state $|\Psi_0\rangle$, output a parametrised quantum state $\left|\Psi\left(\vec{\theta}\right)\right\rangle$, where $\vec{\theta}$ is an adjustable set of real parameters, using a quantum computer.
2. (Hamiltonian Expectation Measurement) Measure the expectation value of the Hamiltonian $\left\langle\Psi\left(\vec{\theta}\right)|\hat{H}|\Psi\left(\vec{\theta}\right)\right\rangle$.
3. (Classical Optimization Subroutine) Use a classical optimizer to determine and adjust new parameters $\vec{\theta}$ such that it will minimise $\left\langle\Psi\left(\vec{\theta}\right)|\hat{H}|\Psi\left(\vec{\theta}\right)\right\rangle$ at the end of the algorithm.
4. Repeat the above step 1 to 3 until $\left\langle\Psi\left(\vec{\theta}\right)|\hat{H}|\Psi\left(\vec{\theta}\right)\right\rangle$ converges to a minimum, that is, the algorithm will terminate when the experimental error is below the desired threshold ε.

Part II

Apprenticeship Project

Chapter 4

Quantum Approximate Optimisation Algorithm

Quantum Approximate Optimisation Algorithm (QAOA) is a type of variational quantum algorithm (VQA) that aims to solve combinatorial problems approximately. A combinatorial problem ask for a solution binary string x^* that solves a binary function $f(x) = c$, for some integer c. QAOA attempts to find such a solution binary string x^* by outputting a candidate quantum state $|\phi_p\rangle$ that has a high probability of collapsing to a solution state $|x^*\rangle$. To generate the candidate state $|\phi_P\rangle$, an initial state $|\psi\rangle$ is prepared and fed as input into QAOA, where it will apply two parametrised unitary operators, $\hat{U}_C(\gamma_p)$ and $\hat{U}_B(\beta_p)$ consecutively, in a finite P number of times as shown in figure 4.0.1 below.

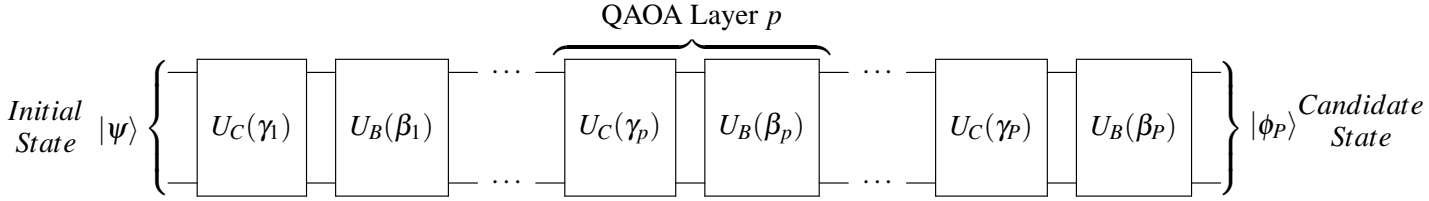

Figure 4.0.1: Quantum circuit decomposition of QAOA of depth P.

As a result, the candidate state $|\phi_p\rangle$ may be expressed as

$$|\phi_P\rangle \quad = \quad \left[\prod_{p=1}^{P} \hat{U}_B(\beta_p)\hat{U}_C(\gamma_p)\right]|\psi\rangle \tag{4.0.1}$$

where the unitary $\hat{U}_C(\gamma_p)\hat{U}_B(\beta_p)$ is called the QAOA operator of layer p. The parametrised operators $\hat{U}_C(\gamma_p)$ and $\hat{U}_B(\beta_p)$ are given as,

$$\hat{U}_C(\gamma_p) = \exp\left(-i\gamma_p\hat{C}\right) \quad , \quad \hat{U}_B(\beta_p) = \exp\left(-i\beta_p\hat{B}\right) \tag{4.0.2}$$

which are driven by two different Hamiltonians $\hat{C}$ and $\hat{B}$ respectively, parametrised by two real angular variables γ_p and β_p respectively. $\hat{C}$ is a hermitian operator that encodes the binary function $f(x)$. By treating $f(x)$ as an energy function, $\hat{C}$ is also typically called as the problem Hamiltonian. $\hat{B}$ is a hermitian operator responsible for manipulating qubit entanglement, it is called a mixer Hamiltonian. We may represent the QAOA parameters as two vectors, $\vec{\gamma}_P = (\gamma_1, \ldots, \gamma_P)$ and $\vec{\beta}_P = (\beta_1, \ldots, \beta_P)$. If the QAOA parameters are optimal, such that it maximises the probability of solution state $|x^*\rangle$ in the

candidate state $|\phi_P\rangle$, then QAOA has successfully solve the combinatorial problem approximately. However, since the solution state $|x^*\rangle$ is usually unknown, we may indirectly maximise the probability by optimising the expectation value of problem Hamiltonian $\langle\phi_P|\hat{C}|\phi_P\rangle$.

4.1 MaxCut Problem

The combinatorial problem of interest is the MaxCut problem. This problem presents an unweighted graph $G = \{V, E\}$, with a set of vertices V and a set of edges E, and ask one to find out what is the maximum number of edges (MaxCut value) that a single line cut could dissect, given that the line cut must start and end outside of the graph and it is only allowed to cut an edge no more than once, without intersecting itself. The MaxCut problem can be extended to weighted graphs with weighted edges by asking one, what is the maximum sum of edge weights that a single line cut could dissect, given the same set of restrictions. Solving this computationally requires one to reformulate the problem in binary. To do so, notice that any cut will split the vertices into two cut sets and we may assign a binary bit, either 0 or 1, to one of the cut sets and the other bit to the other set. If we label the vertices using integers, then we may use it create a binary string x that represents the cut. Thus, the MaxCut problem is a combinatorial problem, in an another way, ask for a solution binary string x^* that maximises the binary MaxCut function,

$$f(x) = \sum_{(i,j)\in E} \frac{1}{2}(1 - x_i x_j) \tag{4.1.1}$$

To solve the MaxCut problem using quantum algorithms, the problem must be reformulated quantum mechanically. We can treat each labelled vertex in the graph as a qubit. In this way, a graph cut state can be quantum mechanically represented as a quantum state $|x\rangle$. To count the number of cut edges of the quantum state $|x\rangle$, a measurement operator $\hat{C}$, called the MaxCut Hamiltonian, is used to measure the *negative* of number of cut edges of a cut x. Explicitly,

$$\hat{C}_{\text{unweighted}} = \sum_{(i,j)\in E} -\frac{1}{2}\left(\mathbb{I} - \hat{Z}_i\hat{Z}_j\right) \tag{4.1.2}$$

$$\hat{C}_{\text{weighted}} = \sum_{(i,j)\in E} -\frac{w_{ij}}{2}\left(\mathbb{I} - \hat{Z}_i\hat{Z}_j\right) \tag{4.1.3}$$

where $\hat{C}_{\text{unweighted}}$ and $\hat{C}_{\text{weighted}}$ represent the MaxCut Hamiltonian for unweighted and weighted graph respectively. As we will be solving MaxCut for the unweighted case, we will use $\hat{C} = \hat{C}_{\text{unweighted}}$ throughout this project, unless otherwise stated. Note that the ground quantum state of MaxCut Hamiltonian $\hat{C}$ is the desired solution state $|x^*\rangle$ that would solve MaxCut problem, as it corresponds to the smallest energy or the maximum number of cut edges. With the quantum formulation of the MaxCut problem, it possible to implement any VQA to solve it. In this project, we will use QAOA to generate a candidate state candidate state $|\phi_P\rangle$ that has the highest possible probability in collapsing to the solution $|x^*\rangle$ by optimising expectation value of MaxCut Hamiltonian $\langle\phi_P|\hat{C}|\phi_P\rangle$ as shown in figure 4.1.1.

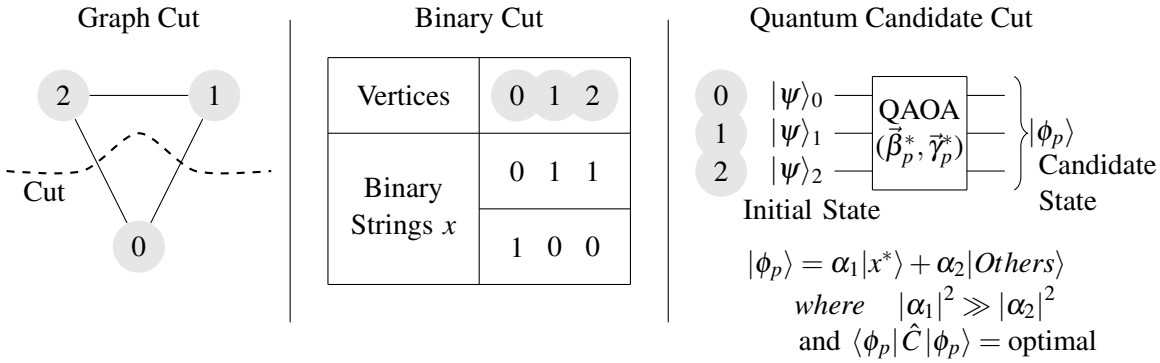

Figure 4.1.1: Quantum mechanical attempt to solve the MaxCut problem using the Quantum Approximate Optimisation Algorithm (QAOA).

Currently, Goemans and Williamson MaxCut Algorithm and its variants are the best known classical algorithms to find an high quality approximated MaxCut value, by employing semidefinite programming and randomized rounding subroutines, in polynomial time with respect to the problem size [WG94]. It is unfortunate that there is no known quantum algorithm that trumps Goemans and Williamson's algorithm, and QAOA is no exception has it has an inferior approximated MaxCut values. However, the speed that it achieves its results may be potentially faster, using a quantum computer.

4.2 Hybrid Quantum-Classical Optimisation

In addition to defining the MaxCut Hamiltonian $\hat{C}$ for the QAOA, it is necessary to specify the mixer Hamiltonian $\hat{B}$ that is responsible for manipulating the qubit entanglement. The original authors, who first proposed QAOA to solve the MaxCut, used the transverse field Hamiltonian as their mixer, that is,

$$\hat{B} \quad = \quad \sum_{i=1}^{|V|} \hat{X}_i \tag{4.2.1}$$

which has become the de-facto standard mixer Hamiltonian for QAOA due to its relative ease of implementation. Therefore, the transverse field Hamiltonian will be used throughout this project as our mixer Hamiltonian for our QAOA.

To obtain a good candidate state $|\phi_P\rangle$ using QAOA$_P$, there is a need to adjust the parameters $\vec{\beta}_P$ and $\vec{\gamma}_P$ such that it optimises the expectation of MaxCut Hamiltonian $\langle\phi_P|\hat{C}|\phi_P\rangle$. We shall implement a simple hybrid quantum-classical optimisation strategy framework to do such a parameter adjustment, as shown in figure 4.2.1 below. Starting at the quantum computer, the initial state $|\psi\rangle$ and initial parameters are supplied to QAOA$_P$ and the quantum algorithm is executed to generate an output candidate state $|\phi_P\rangle$. Then, a quantum measurement is applied to measure the MaxCut value of the collapsed candidate state. This measurement process is repeated several times in a measurement loop, to obtain a statistical average of the MaxCut value, which is the expectation value of the MaxCut Hamiltonian $\langle\phi_P|\hat{C}|\phi_P\rangle$. The expectation value $\langle\phi_P|\hat{C}|\phi_P\rangle$ is fed as an input to the classical computer that executes the classical optimiser, which will output a new set(s) of parameters $\vec{\beta}_P$ and $\vec{\gamma}_P$ which may, hopefully, generate a better candidate state $|\phi_P\rangle$. With this framework, its performance depends heavily on the type of the classical optimiser or the hybrid strategy used.

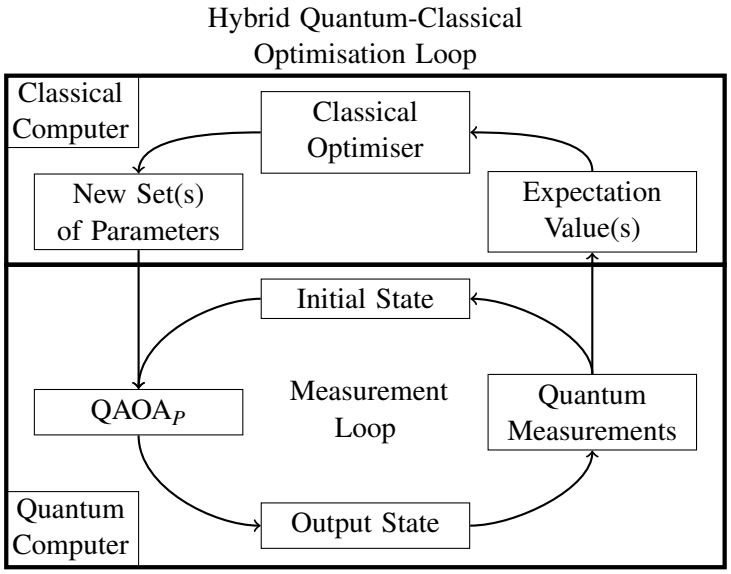

Figure 4.2.1: Hybrid Quantum Classical Optimisation Strategy Framework.

In this project, we shall focus on the greedy-based hybrid strategies, where greedy heuristic refers to the optimisation of the QAOA local parameters (β_p, γ_p) layer by layer as shown in figure 4.2.2.

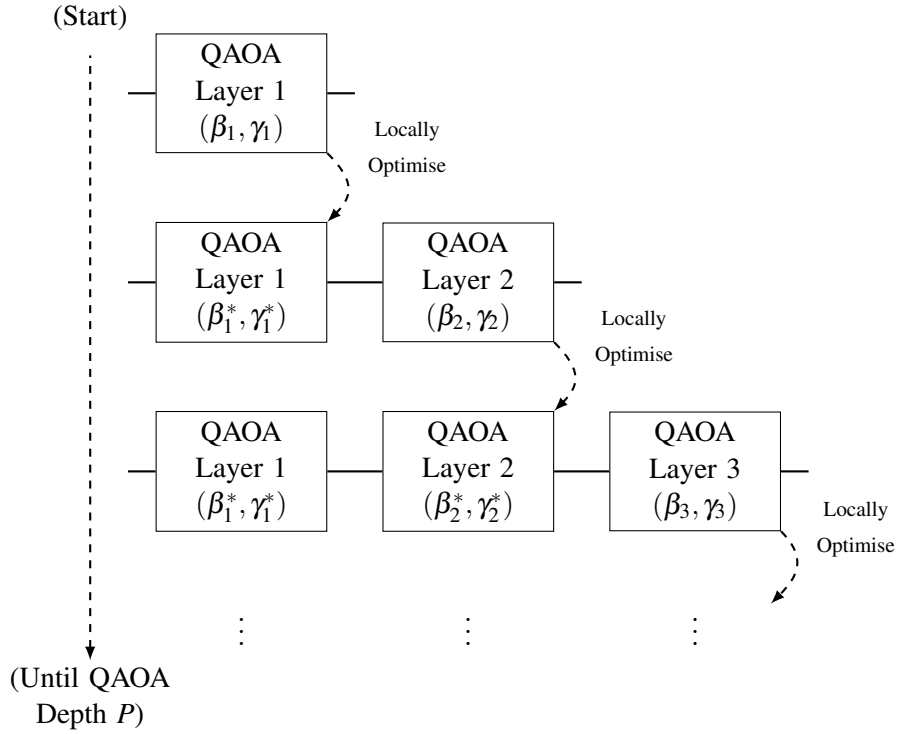

Figure 4.2.2: A general greedy-based strategy.

We shall also evaluate performance of the greedy strategies based on three key performance indicators (KPIs) as shown in table 4.2.1. These three KPIs are chosen specifically for commercial interest, that is the solving duration, quantum usage cost, product (solution) quality. The relevant KPIs are therefore the total simulated computational time, total quantum computer calls and the approximation ratio. The total simulated computational time is simply total overall time to solve the

MaxCut problem. The total quantum computer calls is the total number of independent executions of quantum algorithm (QAOA) required by the hybrid strategy. The approximation ratio is a ratio of the approximated MaxCut value to MaxCut solution value.

Commercial Attribute	KPIs	Actual Measurement
Solving Duration	Total Simulated Computation Time	Overall time to solve the MaxCut problem.
Quantum Usage Cost	Total Quantum Computer Calls	The number of independent executions of QAOA.
Product (Solution) Quality	Approximation Ratio	The ratio of the approximated to the actual MaxCut value.

Table 4.2.1: Key Performance Indicators (KPIs) for Hybrid Quantum-Classical Optimisation Strategies.

There are three types of greedy-based hybrid strategies to be analysed: Standard Greedy Search, Greedy Subsearch and Greedy Newton. Standard Greedy Search is a well-known hybrid strategy that is reliable and consistent in producing reasonable solutions, but it is potentially slow in its implementation. Greedy Subsearch is a modified variant of the Standard Greedy Search, it is fast but produces slightly worse solutions. Greedy Newton is a modified hybrid strategy that adapts Greedy Subsearch and combines with the Newton's method of optimisation in an attempt to produce solutions that are as good as the Standard Greedy Search and run as fast as the Greedy Subsearch.

4.2.1 Standard Greedy Search

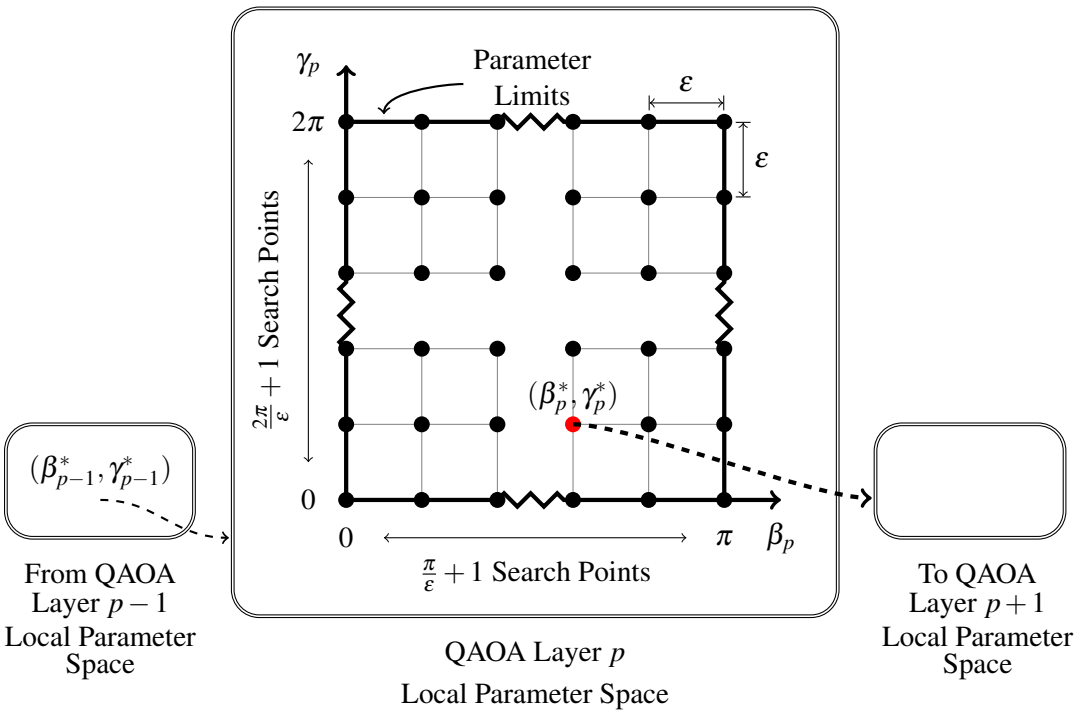

Figure 4.2.3: Standard Greedy Search hybrid strategy optimizer for QAOA parameter optimisation.

The figure 4.2.3 summarises the optimizer of the Standard Greedy Search hybrid strategy. A Standard Greedy Search is simply an exhaustive local discrete search of the locally optimised parameters (β_p^*, γ_p^*) point of QAOA layer p, such that it locally optimises the expectation value of the MaxCut Hamiltonian $\langle\phi_p|\hat{C}|\phi_p\rangle$ at layer p. The search runs successively for all depths from $p = 1$ to P.

Suppose each QAOA parameter of layer p has a fixed domain interval of $\beta_p \in [0, \pi]$, $\gamma_p \in [0, 2\pi]$, which are domains recommended by the original QAOA inventors due to periodicity. Let ε be the desired division size between each neighbouring points. Also, let M be the desired number of quantum measurements needed for each expectation. Then, the instructions for Standard Greedy Search hybrid strategy are:

1. Start from depth $p = 1$.
2. Prepare the all QAOA operators from layer 1 to p, with all QAOA parameters of layer $p-1$ and below, fixed to the latest known optimised value.
3. Adjust the free QAOA parameters of layer p to one of the unsearched points in the local discrete parameter space.
4. Run the QAOA of depth p on a quantum computer, starting from a fixed initial state $|\psi\rangle$, and obtain the output candidate state $|\phi_p\rangle$.
5. Measure the MaxCut value of the collapsed candidate state $|\phi_p\rangle$ of using the MaxCut Hamiltonian $\hat{C}$.
6. Repeat step 4 to 5 for M times to measure the expectation value of the MaxCut Hamiltonian and save the results in the database.
7. Repeat step 2 to 6 till all points in the local discrete parameter space are searched.
8. From the database of results, find the optimal (minimum) expectation value and the corresponding optimal parameter values (β_p^*, γ_p^*) on the classical computer.
9. Increase the depth by 1 to $p+1$ and repeat step 2 to 9, up to a fixed desired depth P.

4.2.2 Greedy Subsearch

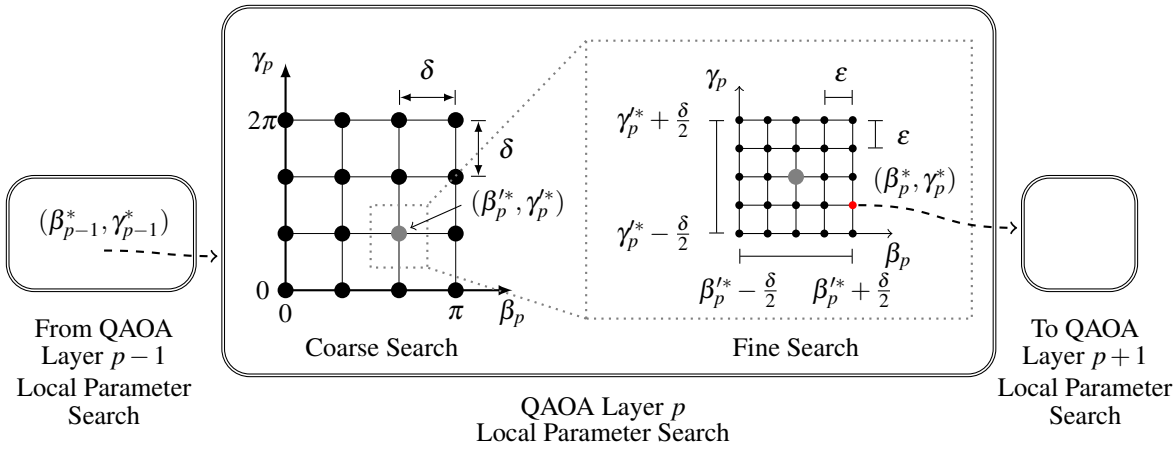

Figure 4.2.4: Greedy Subsearch hybrid strategy optimizer for a faster QAOA parameter optimisation.

The figure 4.2.4 summarises the optimizer of the Greedy Subsearch hybrid strategy. A Greedy Subsearch is a modified variant of the Standard Greedy Search, whereby it reduces number of search points to speedup the optimisation process. A coarse search of a larger division size δ is used to discretise the search space first. When the suboptimal parameter point $\left(\beta_p'^*, \gamma_p'^*\right)$ is found from the coarse search, the search space is restricted to a square neighbourhood around of point $\left(\beta_p'^*, \gamma_p'^*\right)$ of length δ. This means that the domain interval is reduced to $\gamma_p \in \left[\gamma_p'^* - \frac{\delta}{2}, \gamma_p'^* + \frac{\delta}{2}\right]$, $\beta_p \in \left[\beta_p'^* - \frac{\delta}{2}, \beta_p'^* + \frac{\delta}{2}\right]$. Then, a fine search of a smaller division size ε is then employed on a restricted search space, where it will find the locally optimised parameter point $\left(\beta_p^*, \gamma_p^*\right)$ of layer p. Compared to Standard Greedy Search, the instructions for Greedy Subsearch hybrid strategy almost similar, as only difference lies in the how the parameter space is discretised, and thus the instructions will not be given.

4.3 Greedy Newton Hybrid Strategy

4.3.1 Newton's Method

Before introducing Greedy Newton, it it worthwhile to review Newton's Method. It is an extremely well-known approximation algorithm where its original use was to find a root of real-valued twice-differentiable function f, upon given an initial guess point x_0, by iteratively applying the recursive function,

$$x_{n+1} = x_n - \frac{f(x_n)}{f'(x_n)} \tag{4.3.1}$$

When it is applied to an high dimensional optimisation problem, where one is required to find an extremal point of multiple parameters $\vec{x}^*$ and an extremal value $F(\vec{x}^*)$ of an twice-differential objective function F, starting from an initial guess point $\vec{x}_0$, the recursive function is adapted to be,

$$\vec{x}_{n+1} = \vec{x}_n - \alpha \left[\nabla F(\vec{x}_n)\right] \left[\nabla^2 F(\vec{x}_n)\right]^{-1} \tag{4.3.2}$$

where $\nabla F(\vec{x}_n)$, $\nabla^2 F(\vec{x}_n)$ are known as the gradient and the Hessian of function F respectively and α is known as the Newton step size. The main advantage of this optimisation method is that under certain conditions, if satisfied, provides a guarantee quadratic rate of convergence. However, if conditions are unmet, it will not work as one of the necessary condition is that $\left|\nabla^2 F(\vec{x}_n)\right| > 0$, so that $\left[\nabla^2 F(\vec{x}_n)\right]^{-1}$ exist. For a more detailed explanation and elaboration, interested readers are advised to consult vast resources available online as Newton's Method is a famous and well-documented classical optimiser. Greedy Newton uses Newton's method to find the local optimal QAOA parameter point $\left(\beta_p^*, \gamma_p^*\right)$ of layer p to optimise the expectation $\langle \phi_p | \hat{C} | \phi_p \rangle$.

4.3.2 Greedy Newton

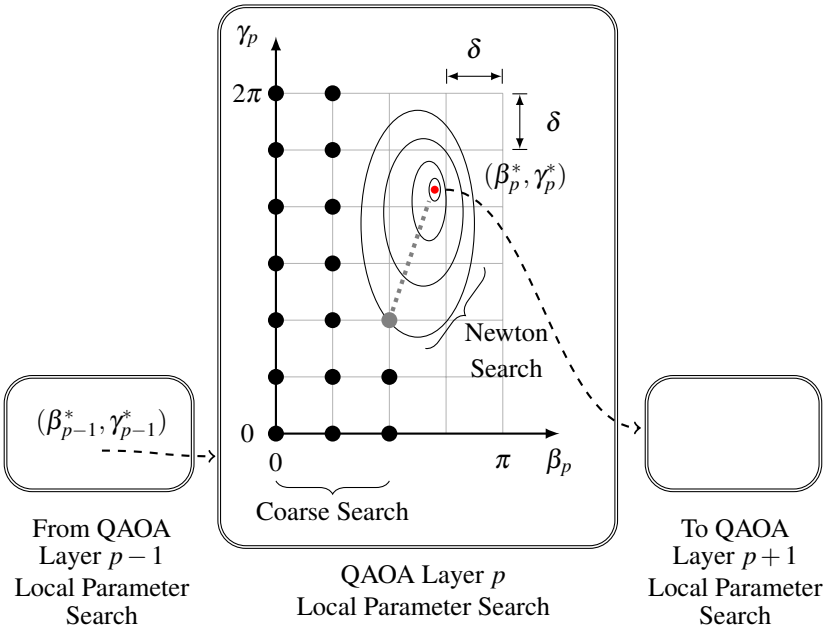

Figure 4.3.1: Greedy Newton hybrid strategy optimizer for a better and faster QAOA parameter optimisation.

The figure 4.3.1 summarises the optimizer of the Greedy Newton hybrid strategy. In the basic sense, Greedy Newton adapts the Greedy Subsearch hybrid strategy by replacing the fine search component with Newton's method to find locally optimised parameters point $\left(\beta_p^*, \gamma_p^*\right)$ of layer p. In coarse search, each parameter point is tested separately and in succession, to check if the Newton's conditions are satisfied. If so, then Newton's Method will be applied starting from that satisfied parameter point until convergence is reached. If the Newton's Method fails to reach a satisfactory convergence or if the parameter point does not satisfy the Newton's conditions, then coarse search will continue to return the next untested point in the coarse search space. In the worst case scenario, if all parameter points in the coarse search either fails in satisfying Newton's conditions or fails to converge in Newton's Method, a fail-safe optimisation is implemented. The fail-safe optimisation is a basic exhaustive search of the optimal (minimum) expectation value and the corresponding optimal parameter point $\left(\beta_p^*, \gamma_p^*\right)$ from a database of searched points.

However, there is a major problem which such an implementation. There is a difficulty in the experimental measurement of the gradient $\nabla\left\langle\hat{C}\right\rangle$ and the Hessian $\nabla^2\left\langle\hat{C}\right\rangle$ of expectation value of the MaxCut Hamiltonian with respect to the local parameters β_p and γ_p. Prior work in developing solution to resolve this problem were found to be too complicated. There were novel quantum algorithms developed specifically to find the derivatives which were cumbersome in its implementation [Jor04; Bul05; Reb+16]. Also, there were attempts to approximate the derivatives using the finite difference method in the Quasi-Newton's Method, that requires even more search points which may potentially slow the optimisation [GS17; Zho+18]. My solution to resolve this major problem is simply by differentiating the Pauli decomposition of $\langle\phi_p|\hat{C}\,|\phi_p\rangle$ with respect to β_p and γ_p. The major problem will be deconstructed and tackled in the following chapter 5. After resolving this problem, the explicit instructions for implementing the Greedy Newton Strategy will be given in chapter 6.

Chapter 5

Expectation of the MaxCut Hamiltonian

This chapter focuses on problem of experimentally measuring the gradient and Hessian of the expectation value of the MaxCut Hamiltonian $\hat{C}$ with respect to the local parameters β_p and γ_p using quantum computers. My solution to resolve this major problem is simply by differentiating the Pauli decomposition of $\langle\phi_p|\hat{C}|\phi_p\rangle$ with respect to β_p and γ_p.

5.1 Naive Differentiation

The MaxCut Hamiltonian $\hat{C}$ is a composition of Pauli-Z operators and Identities. Thus, the expectation of $\hat{C}$ can be measured easily using the standard Pauli-Z measurements. However, directly differentiating the expectation of $\hat{C}$, respect to the local parameters β_p and γ_p, will change $\hat{C}$ to a different measurement operator. To find out what and how does it change the composition, we do a naive decomposition on the expectation value of $\hat{C}$. Let us define our current problem:

> For a given set of QAOA parameters up to layer p, $\vec{\beta}_p = (\beta_1, \ldots, \beta_p)$ and $\vec{\gamma}_p = (\gamma_1, \ldots, \gamma_p)$ and the initial state $|\psi\rangle$, what is the expectation value of the MaxCut Hamiltonian, its gradient and Hessian, that is $\nabla^{0,1,2}\langle\phi_p|\hat{C}|\phi_p\rangle$ at QAOA depth p, with respect to the local parameters β_p and γ_p?

Suppose we implement QAOA of depth p, with QAOA parameters $\vec{\beta}_p = (\beta_1, \ldots, \beta_p)$ and $\vec{\gamma}_p = (\gamma_1, \ldots, \gamma_p)$, where $\beta_1, \ldots, \beta_{p-1}$ and $\gamma_1, \ldots, \gamma_{p-1}$ are fixed constants, whereas β_p, γ_p are real variables. Then, from equation 4.0.1, QAOA will output a candidate state $|\phi_p\rangle$, given as,

$$\begin{aligned} |\phi_p\rangle &= \left[\prod_{l=1}^{p} U_B(\beta_l)\, U_C(\gamma_l)\right]|\psi\rangle \\ &| \quad \text{where } U_B(\beta_l) = \exp\left(-i\beta_l\hat{B}\right) \\ &| \quad \text{and } U_C(\gamma_l) = \exp\left(-i\gamma_l\hat{C}\right) \end{aligned} \tag{5.1.1}$$

The corresponding expectation value of the MaxCut Hamiltonian is therefore written as $\left\langle\hat{C}\right\rangle_p = \langle\phi_p|\hat{C}|\phi_p\rangle$ where $\hat{C} = \sum_{(i,j)\in E} -\frac{1}{2}\left(\mathbb{I} - \hat{Z}_i\hat{Z}_j\right)$. Experimentally, $\left\langle\hat{C}\right\rangle_p$ can be easily measured using standard Pauli-Z measurements at QAOA depth p, on a typical quantum computer. To find the

gradient, that is,

$$\nabla \left\langle \hat{C} \right\rangle_p = \left(\frac{\partial \left\langle \hat{C} \right\rangle_p}{\partial \gamma_p}, \frac{\partial \left\langle \hat{C} \right\rangle_p}{\partial \beta_p} \right) \tag{5.1.2}$$

we first express $\left\langle \hat{C} \right\rangle_p$ in terms local parameters β_p, γ_p and the QAOA output state $|\phi_{p-1}\rangle$ at depth $p-1$. After that, we differentiate it with respect to β_p and γ_p which yield,

$$\begin{aligned}
\left\langle \hat{C} \right\rangle_p &= \langle \phi_{p-1} | \exp\left(i\gamma_p \hat{C}\right) \exp\left(i\beta_p \hat{B}\right) \hat{C} \exp\left(-i\beta_p \hat{B}\right) \exp\left(-i\gamma_p \hat{C}\right) |\phi_{p-1}\rangle && (5.1.3) \\
&| \quad \text{using } \frac{\partial U_B(\beta_p)}{\partial \beta_p} = -i\hat{B} \exp\left(-i\beta_p \hat{B}\right) \\
&| \quad \text{and } \frac{\partial U_C(\gamma)}{\partial \gamma_p} = -i\hat{C} \exp\left(-i\gamma_p \hat{C}\right) \\
\frac{\partial \left\langle \hat{C} \right\rangle_p}{\partial \beta_p} &= i \langle \phi_{p-1} | \exp\left(i\gamma_p \hat{C}\right) \exp\left(i\beta_p \hat{B}\right) \left[\hat{B}, \hat{C}\right] \exp\left(-i\beta_p \hat{B}\right) \exp\left(-i\gamma_p \hat{C}\right) |\phi_{p-1}\rangle && (5.1.4) \\
\frac{\partial \left\langle \hat{C} \right\rangle_p}{\partial \gamma_p} &= i \langle \phi_{p-1} | \exp\left(i\gamma_p \hat{C}\right) \left[\hat{C}, \exp\left(i\beta_p \hat{B}\right) \hat{C} \exp\left(-i\beta_p \hat{B}\right)\right] \exp\left(-i\gamma_p \hat{C}\right) |\phi_{p-1}\rangle && (5.1.5)
\end{aligned}$$

We may repeat the same steps to obtain the hessian, that is,

$$\nabla^2 \left\langle \hat{C} \right\rangle_p = \begin{pmatrix} \frac{\partial^2 \left\langle \hat{C} \right\rangle_p}{\partial \beta_p^2} & \frac{\partial^2 \left\langle \hat{C} \right\rangle_p}{\partial \beta_p \partial \gamma_p} \\ \frac{\partial^2 \left\langle \hat{C} \right\rangle_p}{\partial \beta_p \partial \gamma_p} & \frac{\partial^2 \left\langle \hat{C} \right\rangle_p}{\partial \gamma_p^2} \end{pmatrix} \tag{5.1.6}$$

which will yield,

$$\begin{aligned}
\frac{\partial^2 \left\langle \hat{C} \right\rangle_p}{\partial \beta_p^2} &= \left\langle \phi_{p-1} \right| \exp\left(i\gamma_p \hat{C}\right) \exp\left(i\beta_p \hat{B}\right) \left[\left[\hat{B}, \hat{C}\right], \hat{B}\right] \exp\left(-i\beta_p \hat{B}\right) \exp\left(-i\gamma_p \hat{C}\right) \left| \phi_{p-1} \right\rangle && (5.1.7) \\
\frac{\partial^2 \left\langle \hat{C} \right\rangle_p}{\partial \gamma_p^2} &= \left\langle \phi_{p-1} \right| \exp\left(i\gamma_p \hat{C}\right) \left[\left[\hat{C}, \exp\left(i\beta_p \hat{B}\right) \hat{C} \exp\left(-i\beta_p \hat{B}\right)\right], \hat{C}\right] \exp\left(-i\gamma_p \hat{C}\right) \left| \phi_{p-1} \right\rangle && (5.1.8) \\
\frac{\partial^2 \left\langle \hat{C} \right\rangle_p}{\partial \beta_p \partial \gamma_p} &= \left\langle \phi_{p-1} \right| \left[\exp\left(i\gamma_p \hat{C}\right) \exp\left(i\beta_p \hat{B}\right) \left[\hat{B}, \hat{C}\right] \exp\left(-i\beta_p \hat{B}\right) \exp\left(-i\gamma_p \hat{C}\right), \hat{C}\right] \left| \phi_{p-1} \right\rangle && (5.1.9)
\end{aligned}$$

From the equations above, we observe that to measure the expectation value $\left\langle \hat{C} \right\rangle_p$, the gradient $\nabla \left\langle \hat{C} \right\rangle_p$ and the Hessian $\nabla^2 \left\langle \hat{C} \right\rangle_p$, one has find a way to translate those complicated measurement operators into standard Pauli-Z measurements at QAOA depth $p-1$, which is difficult. To resolve this, it is necessary to decompose these complicated measurement operators even further using Pauli decomposition, that is to re-express the above forms using Pauli operators, which will be easier to translate to standard Pauli-Z measurements at QAOA depth $p-1$ and to differentiate.

5.2 Pauli Decomposition

In this section, we consider the Pauli decomposition of expectation value of the MaxCut Hamiltonian $\left\langle \hat{C} \right\rangle_p$, the gradient $\nabla \left\langle \hat{C} \right\rangle_p$ and the Hessian $\nabla^2 \left\langle \hat{C} \right\rangle_p$. Interested readers may consult the appendix 8.6 for the other case of the weighted MaxCut Hamiltonian. Let us start by restating the problem:

For a given set of QAOA parameters up to layer p, $\vec{\beta} = (\beta_1, \ldots, \beta_p)$ and $\vec{\gamma} = (\gamma_1, \ldots, \gamma_p)$ and

the initial state $|\psi\rangle$, what is the expectation value of the MaxCut Hamiltonian, its gradient and Hessian at QAOA depth p, with respect to the local parameters β_p and γ_p, in terms of Pauli operators? Suppose given a MaxCut problem graph $G = \{V, E\}$ of set of labelled vertices V and labelled unweighted edges $E = \{(i, j) \mid i, j \in V\}$.

Without the loss of generality and to reduce cumbersome writing, we drop the arbitrary index p from the QAOA output state $|\phi_p\rangle = |\phi\rangle$ and the local parameters $\beta_p = \beta$ and $\gamma_p = \gamma$. Explicitly, quantum states that will be frequently used in this section are given in table 5.2.1 below.

State	Description
$\|\psi\rangle$	QAOA Initial State
$\left\|\psi'_{p-1}\right\rangle$	QAOA Intermediary State of Depth $p-1$
$\|\phi_{p-1}\rangle$	QAOA Output State of Depth $p-1$
$\|\psi'\rangle$	$= e^{-i\gamma\hat{C}}\|\phi_{p-1}\rangle$ QAOA Intermediary State of Depth p
$\|\phi\rangle$	$= e^{-i\beta\hat{B}}\|\psi'\rangle$ QAOA Output State of Depth p

Table 5.2.1: Various QAOA Quantum States.

Let us denote $\hat{C}_{ij} = -\frac{1}{2}\mathbb{I} + \frac{1}{2}\hat{Z}_i\hat{Z}_j$ as the MaxCut Hamiltonian of an unweighted edge (i, j). Then, we express the expectation of unweighted MaxCut Hamiltonian $\langle\phi|\hat{C}|\phi\rangle$ as a summation, indexed by edges,

$$\langle\phi|\hat{C}|\phi\rangle = \sum_{(i,j)\in \mathrm{E}} \langle\phi|\hat{C}_{ij}|\phi\rangle \tag{5.2.1}$$

where the expectation value of MaxCut Hamiltonian of an unweighted edge (i, j), $\langle\phi|\hat{C}_{ij}|\phi\rangle$ is given as,

$$\langle\phi|\hat{C}_{ij}|\phi\rangle \quad = \quad \frac{1}{2}\left(-1 + \langle\phi|\hat{Z}_i\hat{Z}_j|\phi\rangle\right) \tag{5.2.2}$$

We observe that $\frac{1}{2}$ is our expectation scaling prefactor, and -1 is our expectation offset of the observable $\hat{Z}_i\hat{Z}_j$. Before decomposing $\langle\phi|\hat{Z}_i\hat{Z}_j|\phi\rangle$, it would be wise to recall some algebraic properties of Pauli operators given in the figure 5.2.1 below. Then, we may express QAOA operators of depth p, $e^{-i\beta\hat{B}}e^{-i\gamma\hat{C}}$ as,

$$e^{-i\beta\hat{B}} \quad = \quad \prod_{k=1}^{|V|} e^{-i\beta\hat{X}_k} \tag{5.2.3}$$

$$e^{-i\gamma\hat{C}} \quad = \quad e^{\frac{i\gamma}{2}|E|\mathbb{I}} \prod_{(u,v)\in E} e^{-\frac{i\gamma}{2}\hat{Z}_u\hat{Z}_v} \tag{5.2.4}$$

Using the algebraic properties of Pauli Operators, $\langle\phi|\hat{Z}_i\hat{Z}_j|\phi\rangle$ is expressed in terms of local parameter

β and the QAOA intermediary state $|\psi'\rangle$ as,

$$\langle\phi|\hat{Z}_i\hat{Z}_j|\phi\rangle = \cos^2 2\beta \langle\psi'|\hat{Z}_i\hat{Z}_j|\psi'\rangle + \frac{1}{2}\sin 4\beta \langle\psi'|\hat{Y}_i\hat{Z}_j + \hat{Z}_i\hat{Y}_j|\psi'\rangle + \sin^2 2\beta \langle\psi'|\hat{Y}_i\hat{Y}_j|\psi'\rangle \tag{5.2.5}$$

The explicit derivation of equation 5.2.5 is given in figure 5.2.2 below.

Algebraic Properties of Pauli Operators

Recall the Pauli commutation and anti-commutation rules and its derived properties. Let σ_j^1, σ_j^2, σ_j^3 refer to $\hat{X}_j$, $\hat{Y}_j$, $\hat{Z}_j$ of the same vertex j, then,

$$\left[\sigma_j^a, \sigma_j^b\right] = 2i\varepsilon_{abc}\sigma_j^c, \quad \left\{\sigma_j^a, \sigma_j^b\right\} = 2\delta_{ab}I, \quad \forall a,b,c = \{1,2,3\} \tag{5.2.6}$$

$$\sigma_j^a\sigma_j^b = \delta_{ab}I + i\varepsilon_{abc}\sigma_j^c, \quad \forall a,b,c = \{1,2,3\} \tag{5.2.7}$$

where ε_{abc} is the Levi-Civita symbol, δ_{ab} is the kronecker delta. Note that any Pauli operators that each belong to a different separate subspace or vertex, will commute.

$$\left[\sigma_j^a, \sigma_k^b\right] = 0, \quad j \neq k, \quad \forall a,b = \{1,2,3\} \tag{5.2.8}$$

From the above properties, we can obtain a useful the commutation relation between Pauli operators and its exponential,

$$e^{i\theta\sigma_j^a}\sigma_j^b = \sigma_j^b e^{(-1)^{\delta_{ab}} i\theta\sigma_j^b}, \quad \forall a,b = \{1,2,3\} \tag{5.2.9}$$

$$e^{i\theta\sigma_j^a}\sigma_k^b = \sigma_k^b e^{i\theta\sigma_j^b}, \quad j \neq k, \quad \forall a,b = \{1,2,3\} \tag{5.2.10}$$

Note that we can express the exponential of any complex composite Pauli operators $f\left(\sigma_j^a\right)$ (regardless of its subspace) in trigonometry by a generalisation of Euler's formula,

$$e^{i\theta f(\sigma_j^a)} = \cos\theta I + i\sin\theta f\left(\sigma_j^a\right) \tag{5.2.11}$$

Figure 5.2.1: Summarised algebraic properties of Pauli operators.

$$\langle\phi|\hat{Z}_i\hat{Z}_j|\phi\rangle \tag{5.2.12}$$

$$= \langle\psi'|e^{i\beta\hat{B}}\hat{Z}_i\hat{Z}_j e^{-i\beta\hat{B}}|\psi'\rangle \tag{5.2.13}$$

$$= \langle\psi'|\left(\prod_{k=1}^{|V|} e^{i\beta\hat{X}_k}\right)\hat{Z}_i\hat{Z}_j\left(\prod_{k=1}^{|V|} e^{-i\beta\hat{X}_k}\right)|\psi'\rangle \tag{5.2.14}$$

$$= \langle\psi'|e^{i\beta\hat{X}_i}e^{i\beta\hat{X}_j}\hat{Z}_i\hat{Z}_j e^{-i\beta\hat{X}_i}e^{-i\beta\hat{X}_j}|\psi'\rangle \tag{5.2.15}$$

$$= \langle\psi'|\hat{Z}_i\hat{Z}_j e^{-i2\beta\hat{X}_i}e^{-i2\beta\hat{X}_j}|\psi'\rangle \tag{5.2.16}$$

$$= \langle\psi'|\hat{Z}_i\hat{Z}_j\left[(\cos 2\beta)I - (i\sin 2\beta)\hat{X}_i\right]\left[(\cos 2\beta)I - (i\sin 2\beta)\hat{X}_j\right]|\psi'\rangle \tag{5.2.17}$$

$$= \cos^2 2\beta \langle\psi'|\hat{Z}_i\hat{Z}_j|\psi'\rangle + \frac{1}{2}\sin 4\beta \langle\psi'|\left(\hat{Y}_i\hat{Z}_j + \hat{Z}_i\hat{Y}_j\right)|\psi'\rangle + \sin^2 2\beta \langle\psi'|\hat{Y}_i\hat{Y}_j|\psi'\rangle \tag{5.2.18}$$

Figure 5.2.2: The explicit derivation of the result of $\langle\phi|\hat{Z}_i\hat{Z}_j|\phi\rangle$.

To express $\langle\phi|\hat{Z}_i\hat{Z}_j|\phi\rangle$ in terms of local parameter γ, it required of us to re-express three terms

$\langle\psi'|\hat{Z}_i\hat{Z}_j|\psi'\rangle$, $\langle\psi'|\hat{Y}_i\hat{Z}_j+\hat{Z}_i\hat{Y}_j|\psi'\rangle$ and $\langle\psi'|\hat{Y}_i\hat{Y}_j|\psi'\rangle$ separately, in terms of QAOA output state $|\phi_{p-1}\rangle$. The first term $\langle\psi'|\hat{Z}_i\hat{Z}_j|\psi'\rangle$ is found to be independent of local parameter γ, that is,

$$\left\langle\psi'\right|\hat{Z}_i\hat{Z}_j\left|\psi'\right\rangle = \langle\phi_{p-1}|\hat{Z}_i\hat{Z}_j|\phi_{p-1}\rangle \tag{5.2.19}$$

The second term $\langle\psi'|\hat{Y}_i\hat{Z}_j|\psi'\rangle$ is found to yield a product sequence of Pauli operators,

$$\left\langle\psi'\right|\hat{Y}_i\hat{Z}_j\left|\psi'\right\rangle = \langle\phi_{p-1}|\left(\cos\gamma\hat{Y}_i\hat{Z}_j+\sin\gamma\hat{X}_i\right)\left[\prod_{(i,v)\in E_{\{i\}}/ij}\left(\cos\gamma I - i\sin\gamma\hat{Z}_i\hat{Z}_v\right)\right]|\phi_{p-1}\rangle \tag{5.2.20}$$

where $E_{\{i\}}$ refers to the set of all edges that the includes vertex i and $E_{\{i\}}/ij$ refers to the same set $E_{\{i\}}$, excluding edge (i,j). The explicit derivation of equation 5.2.20 is given in figure 5.2.3 below.

$$\langle\psi'|\hat{Y}_i\hat{Z}_j|\psi'\rangle \tag{5.2.21}$$
$$= \langle\psi'|e^{i\gamma\hat{C}}\hat{Y}_i\hat{Z}_j e^{-i\gamma\hat{C}}|\psi'\rangle \tag{5.2.22}$$
$$= \langle\phi_{p-1}|\left(\prod_{(u,v)\in E} e^{\frac{i\gamma}{2}\hat{Z}_u\hat{Z}_v}\right)\hat{Y}_i\hat{Z}_j\left(\prod_{(u,v)\in E} e^{-\frac{i\gamma}{2}\hat{Z}_u\hat{Z}_v}\right)|\phi_{p-1}\rangle \tag{5.2.23}$$
$$= \langle\phi_{p-1}|\left(\prod_{(u,v)\in E_{\{i\}}} e^{\frac{i\gamma}{2}\hat{Z}_u\hat{Z}_v}\right)\hat{Y}_i\hat{Z}_j\left(\prod_{(u,v)\in E_{\{i\}}} e^{-\frac{i\gamma}{2}\hat{Z}_u\hat{Z}_v}\right)|\phi_{p-1}\rangle \tag{5.2.24}$$
$$= \langle\phi_{p-1}|\hat{Y}_i\hat{Z}_j\prod_{(i,v)\in E_{\{i\}}} e^{-i\gamma\hat{Z}_i\hat{Z}_v}|\phi_{p-1}\rangle \tag{5.2.25}$$
$$= \langle\phi_{p-1}|\hat{Y}_i\hat{Z}_j\left[\prod_{(i,v)\in E_{\{i\}}}\left(\cos\gamma I - i\sin\gamma\hat{Z}_i\hat{Z}_v\right)\right]|\phi_{p-1}\rangle \tag{5.2.26}$$
$$= \langle\phi_{p-1}|\hat{Y}_i\hat{Z}_j\left(\cos\gamma I - i\sin\gamma\hat{Z}_i\hat{Z}_j\right)\left[\prod_{(i,v)\in E_{\{i\}}/ij}\left(\cos\gamma I - i\sin\gamma\hat{Z}_i\hat{Z}_v\right)\right]|\phi_{p-1}\rangle \tag{5.2.27}$$
$$= \langle\phi_{p-1}|\left(\cos\gamma\hat{Y}_i\hat{Z}_j+\sin\gamma\hat{X}_i\right)\left[\prod_{(i,v)\in E_{\{i\}}/ij}\left(\cos\gamma I - i\sin\gamma\hat{Z}_i\hat{Z}_v\right)\right]|\phi_{p-1}\rangle \tag{5.2.28}$$

Figure 5.2.3: The explicit derivation of the result of $\langle\psi'|\hat{Y}_i\hat{Z}_j|\psi'\rangle$.

By symmetry, switching and relabelling indexes i,j should not affect the derivation and thus, the overall result. Therefore, without explicit derivation, $\langle\psi'|\hat{Z}_i\hat{Y}_j|\psi'\rangle$ is conjectured to be,

$$\left\langle\psi'\right|\hat{Z}_i\hat{Y}_j\left|\psi'\right\rangle = \langle\phi_{p-1}|\left(\cos\gamma\hat{Z}_i\hat{Y}_j+\sin\gamma\hat{X}_j\right)\left[\prod_{(j,v)\in E_{\{j\}}/ij}\left(\cos\gamma I - i\sin\gamma\hat{Z}_j\hat{Z}_v\right)\right]|\phi_{p-1}\rangle \tag{5.2.29}$$

where $E_{\{j\}}/ij$ refers to the set of all edges that includes the vertex j, excluding edge (i,j). Lastly, the third term $\langle\psi'|\hat{Y}_i\hat{Y}_j|\psi'\rangle$ is found to be,

$$\left\langle\psi'\right|\hat{Y}_i\hat{Y}_j\left|\psi'\right\rangle = \langle\phi_{p-1}|\hat{Y}_i\hat{Y}_j\left(\prod_{(u,v)\in E_{\{i,j\}}/ij}\left(\cos\gamma I - i\sin\gamma\hat{Z}_u\hat{Z}_v\right)\right)|\phi_{p-1}\rangle \tag{5.2.30}$$

where $E_{\{i,j\}}/ij$ refers to the set of all edges that includes the vertex i or j, excluding edge (i,j). The

explicit derivation of equation 5.2.30 is given in figure 5.2.4 below.

$$\langle \psi' | \hat{Y}_i \hat{Y}_j | \psi' \rangle \tag{5.2.31}$$

$$= \langle \phi_{p-1} | \left(\prod_{(u,v)\in E_{\{i,j\}}} e^{\frac{i\gamma}{2}\hat{Z}_u\hat{Z}_v} \right) \hat{Y}_i\hat{Y}_j \left(\prod_{(u,v)\in E_{\{i,j\}}} e^{-\frac{i\gamma}{2}\hat{Z}_u\hat{Z}_v} \right) | \phi_{p-1} \rangle \tag{5.2.32}$$

$$= \langle \phi_{p-1} | \left(\prod_{(u,v)\in E_{\{i,j\}/ij}} e^{\frac{i\gamma}{2}\hat{Z}_u\hat{Z}_v} \right) \left(e^{\frac{i\gamma}{2}\hat{Z}_i\hat{Z}_j} \right) \hat{Y}_i\hat{Y}_j \left(e^{-\frac{i\gamma}{2}\hat{Z}_i\hat{Z}_j} \right) \left(\prod_{(u,v)\in E_{\{i,j\}/ij}} e^{-\frac{i\gamma}{2}\hat{Z}_u\hat{Z}_v} \right) | \phi_{p-1} \rangle \tag{5.2.33}$$

$$= \langle \phi_{p-1} | \left(\prod_{(u,v)\in E_{\{i,j\}/ij}} e^{\frac{i\gamma}{2}\hat{Z}_u\hat{Z}_v} \right) \hat{Y}_i\hat{Y}_j \left(\prod_{(u,v)\in E_{\{i,j\}/ij}} e^{-\frac{i\gamma}{2}\hat{Z}_u\hat{Z}_v} \right) | \phi_{p-1} \rangle \tag{5.2.34}$$

$$= \langle \phi_{p-1} | \hat{Y}_i\hat{Y}_j \left(\prod_{(u,v)\in E_{\{i,j\}/ij}} e^{-i\gamma\hat{Z}_u\hat{Z}_v} \right) | \phi_{p-1} \rangle \tag{5.2.35}$$

$$= \langle \phi_{p-1} | \hat{Y}_i\hat{Y}_j \left(\prod_{(u,v)\in E_{\{i,j\}/ij}} \left(\cos\gamma I - i\sin\gamma\hat{Z}_u\hat{Z}_v\right) \right) | \phi_{p-1} \rangle \tag{5.2.36}$$

Figure 5.2.4: The explicit derivation of the result of $\langle \psi' | \hat{Y}_i\hat{Y}_j | \psi' \rangle$.

By a simple substitution of newly found expressions of three terms $\langle \psi' | \hat{Z}_i\hat{Z}_j | \psi' \rangle$, $\langle \psi' | \hat{Y}_i\hat{Z}_j + \hat{Z}_i\hat{Y}_j | \psi' \rangle$ and $\langle \psi' | \hat{Y}_i\hat{Y}_j | \psi' \rangle$, we have successfully re-expressed the expectation of unweighted MaxCut Hamiltonian $\langle \phi | \hat{C} | \phi \rangle$ in terms of Pauli operators and the QAOA parameters β ,γ of depth p. However, newly found expression are difficult to differentiate as the parameters, especially gamma, are coupled to Pauli operators whose composition are dependent on the problem graph structure, that resides in the product sequence. In other words, there is no simple way of directly differentiating the expressions without complicating it as using product rule of differentiation which will introduce more unwanted Pauli operators. Therefore, it is required of us to expand the following product sequences as summation, such that the differentiation will not complicate the expressions any further.

$$\prod_{(i,v)\in E_{\{i\}}/ij} \left(\cos\gamma I - i\sin\gamma\hat{Z}_i\hat{Z}_v\right), \quad \prod_{(j,v)\in E_{\{j\}}/ij} \left(\cos\gamma I - i\sin\gamma\hat{Z}_j\hat{Z}_v\right), \quad \prod_{(u,v)\in E_{\{i,j\}/ij}} \left(\cos\gamma I - i\sin\gamma\hat{Z}_u\hat{Z}_v\right)$$

Of course, expanding any of these terms is significantly more difficult as it requires a great deal of mathematical visualisation and intuition. Fortunately, such an product expansion, which we are about to attempt, is closely related to the generalised binomial expansion. Interested readers may wish to consult a standard mathematical textbook in elementary algebra for a refresher on binomial expansion. To reduce the difficultly further, notice that the expression forms of these three terms are the same, expanding one will resolve the other two.

Let us consider the first product sequence. If we refer all the edges (i,v), which consist of vertex i, as the left edges, then there are ℓ_{ij} number of such left edges, excluding edge (i,j). Next, we denote the other vertex $v \to l_a$, where index a ranges from 1 to ℓ_{ij} , then the first product sequence can be written

as an summation, iterating through index k, as,

$$\prod_{(i,v)\in E_{\{i\}}/ij}\left(\cos\gamma I - i\sin\gamma\hat{Z}_i\hat{Z}_v\right) = \sum_{k=0}^{\ell_{ij}}\left[\left(\cos\gamma I\right)^{\ell_{ij}-k}\left(-i\sin\gamma\hat{Z}_i\right)^k \sum_{\lambda\in\Lambda_k^{\ell_{ij}}}\left(I\prod_{a\in\lambda}\hat{Z}_{l_a}\right)\right] \tag{5.2.37}$$

where $\Lambda_k^{\ell_{ij}}$ is a set of all possible k-combinations of elements λ of the index set $\Theta_{\ell_{ij}} = \left\{a \mid 1 \le a \le \ell_{ij},\, a \in \mathbb{Z}\right\}$. Note the index usage of k as an integer for the element combination and index usage of a as an integer for labelling the other vertex $v \to l_a$ on the left edges. The explicit derivation of equation 5.2.37 is given in figure 5.2.5 below, while an example of calculation $\sum_{\lambda\in\Lambda_k^{\ell_{ij}}}\left(I\prod_{a\in\lambda}\hat{Z}_{l_a}\right)$ is given in the figure 5.2.6 below.

$$\begin{aligned}
\prod_{(i,v)\in E_{\{i\}}/ij}\left(\cos\gamma I - i\sin\gamma\hat{Z}_i\hat{Z}_v\right) &= \prod_{k=1}^{\ell_{ij}}\left(\cos\gamma I - i\sin\gamma\hat{Z}_i\hat{Z}_{l_k}\right) && (5.2.38)\\
&= \left[\cos\gamma I + \left(-i\sin\gamma\hat{Z}_i\right)\hat{Z}_{l_1}\right]\ldots\left(\cos\gamma I + \left(-i\sin\gamma\hat{Z}_i\right)\hat{Z}_{l_\ell}\right) && (5.2.39)\\
&= \Big[\cos^2\gamma I + \cos\gamma\left(-i\sin\gamma\hat{Z}_i\right)\left(\hat{Z}_{l_1}+\hat{Z}_{l_2}\right)\\
&\qquad + \left(-i\sin\gamma\hat{Z}_i\right)^2\hat{Z}_{l_1}\hat{Z}_{l_2}\Big]\ldots\left(\cos\gamma I + \left(-i\sin\gamma\hat{Z}_i\right)\hat{Z}_{l_\ell}\right) && (5.2.40)\\
&= \Big[\cos^3\gamma I + \cos^2\gamma\left(-i\sin\gamma\hat{Z}_i\right)\left(\hat{Z}_{l_1}+\hat{Z}_{l_2}+\hat{Z}_{l_3}\right)\\
&\qquad + \cos\gamma\left(-i\sin\gamma\hat{Z}_i\right)^2\left(\hat{Z}_{l_1}\hat{Z}_{l_2}+\hat{Z}_{l_2}\hat{Z}_{l_3}+\hat{Z}_{l_1}\hat{Z}_{l_3}\right)\\
&\qquad + \left(-i\sin\gamma\hat{Z}_i\right)^3\hat{Z}_{l_1}\hat{Z}_{l_2}\hat{Z}_{l_3}\Big]\ldots\left(\cos\gamma I + \left(-i\sin\gamma\hat{Z}_i\right)\hat{Z}_{l_\ell}\right) && (5.2.41)\\
&\quad \mid \text{ Invoke binomial formula for operators}\\
&= \sum_{k=0}^{\ell_{ij}}\left[\left(\cos\gamma I\right)^{\ell_{ij}-k}\left(-i\sin\gamma\hat{Z}_i\right)^k \sum_{\lambda\in\Lambda_k^{\ell_{ij}}}\left(I\prod_{a\in\lambda}\hat{Z}_{l_a}\right)\right] && (5.2.42)
\end{aligned}$$

Figure 5.2.5: The explicit derivation of the result of the first product sequence $\prod_{(i,v)\in E_{\{i\}}/ij}\left(\cos\gamma I - i\sin\gamma\hat{Z}_i\hat{Z}_v\right)$.

Example: If $\ell_{ij}=3$, then $\Theta_3=\{1,2,3\}$ and $\sum_{\lambda\in\Lambda_k^{\ell_{ij}}} I\left(\prod_{a\in\lambda}\hat{Z}_{l_a}\right)$ generates the following terms for $0\le k\le 3$, $k\in\mathbb{Z}$,

$$\begin{aligned} k=0, \qquad & \Lambda_0^3=\emptyset \\ \sum_{\lambda\in\Lambda_0^3}\left(I\prod_{a\in\lambda}\hat{Z}_{l_a}\right) &= I \end{aligned} \tag{5.2.43}$$

$$\begin{aligned} k=1, \qquad & \Lambda_1^3=\{\{1\},\{2\},\{3\}\} \\ \sum_{\lambda\in\Lambda_1^3}\left(I\prod_{a\in\lambda}\hat{Z}_{l_a}\right) &= \left(I\prod_{a\in\{1\}}\hat{Z}_{l_a}\right)+\left(I\prod_{a\in\{2\}}\hat{Z}_{l_a}\right)+\left(I\prod_{a\in\{3\}}\hat{Z}_{l_a}\right) \\ &= \hat{Z}_{l_1}+\hat{Z}_{l_2}+\hat{Z}_{l_3} \end{aligned} \tag{5.2.44}$$

$$\begin{aligned} k=2, \qquad & \Lambda_2^3=\{\{2,3\},\{1,3\},\{1,2\}\} \\ \sum_{\lambda\in\Lambda_2^3}\left(I\prod_{a\in\lambda}\hat{Z}_{l_a}\right) &= \left(I\prod_{a\in\{1,2\}}\hat{Z}_{l_a}\right)+\left(I\prod_{a\in\{2,3\}}\hat{Z}_{l_a}\right)+\left(I\prod_{a\in\{3,1\}}\hat{Z}_{l_a}\right) \\ &= \hat{Z}_{l_1}\hat{Z}_{l_2}+\hat{Z}_{l_2}\hat{Z}_{l_3}+\hat{Z}_{l_1}\hat{Z}_{l_3} \end{aligned} \tag{5.2.45}$$

$$\begin{aligned} k=3, \qquad & \Lambda_3^3=\{\{1,2,3\}\} \\ \sum_{\lambda\in\Lambda_3^3}\left(I\prod_{a\in\lambda}\hat{Z}_{l_a}\right) &= \left(I\prod_{a\in\{1,2,3\}}\hat{Z}_{l_a}\right) \\ &= \hat{Z}_{l_1}\hat{Z}_{l_2}\hat{Z}_{l_3} \end{aligned} \tag{5.2.46}$$

Figure 5.2.6: An example of calculating $\sum_{\lambda\in\Lambda_k^3}\left(I\prod_{a\in\lambda}\hat{Z}_{l_a}\right)$.

Similarly, if we refer to the edges (j,v) , which consist of vertex j, as the right edges, then there are ξ_{ij} number of right edges, excluding edge (i,j). Afterwards, we denote the other vertex $v\to r_b$, where index b ranges from 1 to ξ_{ij}. Using the symmetry argument and without explicit derivation, the second product sequence can be written as an summation, iterating through index k, as,

$$\prod_{(j,v)\in E_{\{j\}}/ij}\left(\cos\gamma I-i\sin\gamma\hat{Z}_j\hat{Z}_v\right)=\sum_{k=0}^{\xi_{ij}}\left[(\cos\gamma I)^{\xi_{ij}-k}\left(-i\sin\gamma\hat{Z}_j\right)^k\sum_{\lambda\in\Lambda_k^{\xi_{ij}}}\left(I\prod_{b\in\lambda}\hat{Z}_{r_b}\right)\right] \tag{5.2.47}$$

where $\Lambda_k^{\xi_{ij}}$ is a set of all possible k-combinations of elements λ of the index set $\Theta_{\xi_{ij}}=\left\{b\mid 1\le b\le\xi_{ij},\ b\in\mathbb{Z}\right\}$.

Consider the third product sequence, we may split the edge set $E_{\{i,j\}/ij}$ into two mutually exclusive edge sets, $E_{\{i\}/ij}$ and $E_{\{j\}/ij}$. $E_{\{i\}/ij}$ is the set of all left edges that contain vertex i, but not edge (i,j). $E_{\{j\}/ij}$ is the set of all right edges that contain vertex j, but not edge (i,j). That is,

$$E_{\{i,j\}/ij} = E_{\{i\}/ij}\cup E_{\{j\}/ij} \tag{5.2.48}$$

$$\emptyset = E_{\{i\}/ij}\cap E_{\{j\}/ij} \tag{5.2.49}$$

Using index l_a and r_b to denote other vertex of the left and right edges respectively, the third product

sequence can be expanded as,

$$\prod_{(u,v)\in E_{\{i,j\}/ij}} \left(\cos\gamma I - i\sin\gamma \hat{Z}_u\hat{Z}_v\right) =$$
$$\sum_{n=0}^{\xi_{ij}}\sum_{m=0}^{\ell_{ij}} \left(\cos\gamma I\right)^{\ell_{ij}+\xi_{ij}-m-n}\left(-i\sin\gamma\right)^{m+n}\left(\hat{Z}_i\right)^m\left(\hat{Z}_j\right)^n \left[\sum_{\lambda_1\in\Lambda_m^{\ell_{ij}}}\sum_{\lambda_2\in\Lambda_n^{\xi_{ij}}}\left(I\prod_{a\in\lambda_1}\hat{Z}_{l_a}\right)\left(\prod_{b\in\lambda_2}\hat{Z}_{r_b}\right)\right] \tag{5.2.50}$$

The explicit derivation of equation 5.2.50 is given in figure 5.2.7 below.

$$\prod_{(u,v)\in E_{\{i,j\}/ij}} \left(\cos\gamma I - i\sin\gamma \hat{Z}_u\hat{Z}_v\right) \tag{5.2.51}$$
$$= \left[\prod_{m=1}^{\ell_{ij}}\left(\cos\gamma I - i\sin\gamma\hat{Z}_i\hat{Z}_{l_m}\right)\right]\left[\prod_{n=1}^{\xi_{ij}}\left(\cos\gamma I - i\sin\gamma\hat{Z}_j\hat{Z}_{r_n}\right)\right] \tag{5.2.52}$$
$$= \left\{\sum_{m=0}^{\ell_{ij}}\left[\left(\cos\gamma I\right)^{\ell_{ij}-m}\left(-i\sin\gamma\hat{Z}_i\right)^m\sum_{\lambda_1\in\Lambda_m^{\ell_{ij}}}\left(I\prod_{a\in\lambda_1}\hat{Z}_{l_a}\right)\right]\right\}\left\{\sum_{n=0}^{\xi_{ij}}\left[\left(\cos\gamma I\right)^{\xi_{ij}-n}\left(-i\sin\gamma\hat{Z}_j\right)^n\sum_{\lambda_2\in\Lambda_n^{\xi_{ij}}}\left(I\prod_{b\in\lambda_2}\hat{Z}_{r_b}\right)\right]\right\} \tag{5.2.53}$$
$$= \sum_{n=0}^{\xi_{ij}}\sum_{m=0}^{\ell_{ij}}\left(\cos\gamma I\right)^{\ell_{ij}+\xi_{ij}-m-n}\left(-i\sin\gamma\right)^{m+n}\left(\hat{Z}_i\right)^m\left(\hat{Z}_j\right)^n\left[\sum_{\lambda_1\in\Lambda_m^{\ell_{ij}}}\sum_{\lambda_2\in\Lambda_n^{\xi_{ij}}}\left(I\prod_{a\in\lambda_1}\hat{Z}_{l_a}\right)\left(\prod_{b\in\lambda_2}\hat{Z}_{r_b}\right)\right] \tag{5.2.54}$$

Figure 5.2.7: The explicit derivation of the result of of the third product sequence $\prod_{(u,v)\in E_{\{i,j\}/ij}}\left(\cos\gamma I - i\sin\gamma\hat{Z}_u\hat{Z}_v\right)$.

Finally, substituting the results back into the expectation value of MaxCut Hamiltonian $\langle\phi|\hat{C}|\phi\rangle$, we will have our desired expressions. To avoid cumbersome writing, the following expressions of expectation values of the Pauli compositions given in figure 5.2.8 shall be used. From this point onwards, it is straightforward to calculate all the required higher order derivatives as the QAOA parameters β ,γ of depth p are decoupled from the Pauli operators. Thus, the explicit derivation of the higher order derivatives will not be given. The final Pauli decomposition of the expressions of the expectation value of the MaxCut Hamiltonian $\left\langle\hat{C}\right\rangle_p$, the gradient $\nabla\left\langle\hat{C}\right\rangle_p$ and the Hessian $\nabla^2\left\langle\hat{C}\right\rangle_p$ are given the following three boxes.

$$\left\langle y_i z_j z_i^k\right\rangle_\lambda = \langle\phi_{p-1}|\hat{Y}_i\hat{Z}_j\left(\hat{Z}_i\right)^k\left(I\prod_{a\in\lambda}\hat{Z}_{l_a}\right)|\phi_{p-1}\rangle \tag{5.2.55}$$
$$\left\langle x_i z_i^k\right\rangle_\lambda = \langle\phi_{p-1}|\hat{X}_i\left(\hat{Z}_i\right)^k\left(I\prod_{a\in\lambda}\hat{Z}_{l_a}\right)|\phi_{p-1}\rangle \tag{5.2.56}$$
$$\left\langle z_i y_j z_j^k\right\rangle_\lambda = \langle\phi_{p-1}|\hat{Z}_i\hat{Y}_j\left(\hat{Z}_j\right)^k\left(I\prod_{b\in\lambda}\hat{Z}_{r_b}\right)|\phi_{p-1}\rangle \tag{5.2.57}$$
$$\left\langle x_j z_j^k\right\rangle_\lambda = \langle\phi_{p-1}|\hat{X}_j\left(\hat{Z}_j\right)^k\left(I\prod_{b\in\lambda}\hat{Z}_{r_b}\right)|\phi_{p-1}\rangle \tag{5.2.58}$$
$$\left\langle y_i y_j z_i^k z_j^k\right\rangle_{\lambda_1,\lambda_2} = \langle\phi_{p-1}|\hat{Y}_i\hat{Y}_j\left(\hat{Z}_i\right)^m\left(\hat{Z}_j\right)^n\left(I\prod_{a\in\lambda_1}\hat{Z}_{l_a}\right)\left(\prod_{b\in\lambda_2}\hat{Z}_{r_b}\right)|\phi_{p-1}\rangle \tag{5.2.59}$$

Figure 5.2.8: Denotion to simplify cumbersome writing.

Pauli Decomposition of the QAOA Expectation Value of Unweighted MaxCut Hamiltonian

$$\langle\phi|\hat{C}|\phi\rangle =$$

$$\sum_{(i,j)\in \mathrm{E}} \frac{1}{2}\left(\cos^2 2\beta \left\langle\psi'\right|\hat{Z}_i\hat{Z}_j\left|\psi'\right\rangle + \frac{1}{2}\sin 4\beta \left\langle\psi'\right|\hat{Y}_i\hat{Z}_j + \hat{Z}_i\hat{Y}_j\left|\psi'\right\rangle + \sin^2 2\beta \left\langle\psi'\right|\hat{Y}_i\hat{Y}_j\left|\psi'\right\rangle - 1\right) \tag{5.2.60}$$

where,

$$\left\langle\psi'\right|\hat{Z}_i\hat{Z}_j\left|\psi'\right\rangle \quad = \quad \left\langle\phi_{p-1}\right|\hat{Z}_i\hat{Z}_j\left|\phi_{p-1}\right\rangle \tag{5.2.61}$$

$$\left\langle\psi'\right|\hat{Y}_i\hat{Z}_j\left|\psi'\right\rangle =$$

$$\sum_{k=0}^{\ell_{ij}}\left[(\cos\gamma I)^{\ell_{ij}-k}(-i\sin\gamma)^k\left(\cos\gamma\sum_{\lambda\in\Lambda_k^{\ell_{ij}}}\left\langle y_i z_j z_i^k\right\rangle_\lambda + \sin\gamma\sum_{\lambda\in\Lambda_k^{\ell_{ij}}}\left\langle x_i z_i^k\right\rangle_\lambda\right)\right] \tag{5.2.62}$$

$$\left\langle\psi'\right|\hat{Z}_i\hat{Y}_j\left|\psi'\right\rangle =$$

$$\sum_{k=0}^{\xi_{ij}}\left[(\cos\gamma I)^{\xi_{ij}-k}(-i\sin\gamma)^k\left(\cos\gamma\sum_{\lambda\in\Lambda_k^{\xi_{ij}}}\left\langle z_i y_j z_j^k\right\rangle_\lambda + \sin\gamma\sum_{\lambda\in\Lambda_k^{\xi_{ij}}}\left\langle x_j z_j^k\right\rangle_\lambda\right)\right] \tag{5.2.63}$$

$$\left\langle\psi'\right|\hat{Y}_i\hat{Y}_j\left|\psi'\right\rangle =$$

$$\sum_{n=0}^{\xi_{ij}}\sum_{m=0}^{\ell_{ij}}\left[(\cos\gamma I)^{\ell_{ij}+\xi_{ij}-m-n}(-i\sin\gamma)^{m+n}\sum_{\lambda_1\in\Lambda_m^{\ell_{ij}}}\sum_{\lambda_2\in\Lambda_n^{\xi_{ij}}}\left\langle y_i y_j z_i^m z_j^n\right\rangle_{\lambda_1,\lambda_2}\right] \tag{5.2.64}$$

Pauli Decomposition of the Gradient of the Expectation Value

$$\nabla \langle \phi | \hat{C} | \phi \rangle = \sum_{(i,j)\in \mathrm{E}} \frac{1}{2} \begin{pmatrix} \frac{\partial}{\partial \beta} \\ \frac{\partial}{\partial \gamma} \end{pmatrix} \langle \phi | \hat{Z}_i \hat{Z}_j | \phi \rangle \tag{5.2.65}$$

where,

$$\frac{\partial}{\partial \beta} \langle \phi | \hat{Z}_i \hat{Z}_j | \phi \rangle = 2\cos 4\beta \left\langle \psi' \middle| \hat{Y}_i \hat{Z}_j + \hat{Z}_i \hat{Y}_j \middle| \psi' \right\rangle + 2\sin 4\beta \left\langle \psi' \middle| \hat{Y}_i \hat{Y}_j - \hat{Z}_i \hat{Z}_j \middle| \psi' \right\rangle \tag{5.2.66}$$

$$\frac{\partial}{\partial \gamma} \langle \phi | \hat{Z}_i \hat{Z}_j | \phi \rangle = \frac{1}{2} \sin 4\beta \frac{\partial}{\partial \gamma} \left\langle \psi' \middle| \hat{Y}_i \hat{Z}_j + \hat{Z}_i \hat{Y}_j \middle| \psi' \right\rangle + \sin^2 2\beta \frac{\partial}{\partial \gamma} \left\langle \psi' \middle| \hat{Y}_i \hat{Y}_j \middle| \psi' \right\rangle \tag{5.2.67}$$

and,

$$\frac{\partial}{\partial \gamma} \left\langle \psi' \middle| \hat{Y}_i \hat{Z}_j \middle| \psi' \right\rangle =$$

$$\sum_{k=0}^{\ell_{ij}} (\cos \gamma I)^{\ell_{ij}-k} (-i \sin \gamma)^k$$

$$\times \left\{ \left[\left(k-\ell_{ij}\right) \tan\gamma + k\cot\gamma - \tan\gamma \right] \cos\gamma \sum_{\lambda \in \Lambda_k^{\ell_{ij}}} \left\langle y_i z_j z_i^k \right\rangle_\lambda \right.$$

$$\left. + \left[\left(k-\ell_{ij}\right) \tan\gamma + k\cot\gamma + \cot\gamma \right] \sin \sum_{\lambda \in \Lambda_k^{\ell_{ij}}} \left\langle x_i z_i^k \right\rangle_\lambda \right\} \tag{5.2.68}$$

$$\frac{\partial}{\partial \gamma} \left\langle \psi' \middle| \hat{Z}_i \hat{Y}_j \middle| \psi' \right\rangle =$$

$$\sum_{k=0}^{\xi_{ij}} (\cos \gamma I)^{\xi_{ij}-k} (-i \sin \gamma)^k$$

$$\times \left\{ \left[\left(k-\xi_{ij}\right) \tan\gamma + k\cot\gamma - \tan\gamma \right] \cos\gamma \sum_{\lambda \in \Lambda_k^{\xi_{ij}}} \left\langle z_i y_j z_j^k \right\rangle_\lambda \right.$$

$$\left. + \left[\left(k-\xi_{ij}\right) \tan\gamma + k\cot\gamma + \cot\gamma \right] \sin\gamma \sum_{\lambda \in \Lambda_k^{\xi_{ij}}} \left\langle x_j z_j^k \right\rangle_\lambda \right\} \tag{5.2.69}$$

$$\frac{\partial}{\partial \gamma} \left\langle \psi' \middle| \hat{Y}_i \hat{Y}_j \middle| \psi' \right\rangle =$$

$$\sum_{n=0}^{\xi_{ij}} \sum_{m=0}^{\ell_{ij}} (\cos \gamma I)^{\ell_{ij}+\xi_{ij}-m-n} (-i \sin \gamma)^{m+n} \left(\sum_{\lambda_1 \in \Lambda_m^{\ell_{ij}}} \sum_{\lambda_2 \in \Lambda_n^{\xi_{ij}}} \left\langle y_i y_j z_i^m z_j^n \right\rangle_{\lambda_1,\lambda_2} \right)$$

$$\times \left[\left(-\ell_{ij} - \xi_{ij} + m + n\right) (\tan\gamma) + (m+n)\cot\gamma \right] \tag{5.2.70}$$

Pauli Decomposition of the Hessian of the Expectation Value

$$\nabla^2 \langle\phi|\hat{C}|\phi\rangle = \sum_{(i,j)\in \mathrm{E}} \frac{1}{2} \begin{pmatrix} \frac{\partial^2}{\partial\beta^2} & \frac{\partial^2}{\partial\gamma\partial\beta} \\ \frac{\partial^2}{\partial\beta\partial\gamma} & \frac{\partial^2}{\partial\gamma^2} \end{pmatrix} \langle\phi|\hat{Z}_i\hat{Z}_j|\phi\rangle \tag{5.2.71}$$

where,

$$\frac{\partial^2}{\partial\beta^2}\langle\phi|\hat{Z}_i\hat{Z}_j|\phi\rangle = -8\sin 4\beta \left\langle\psi'\middle|\hat{Y}_i\hat{Z}_j+\hat{Z}_i\hat{Y}_j\middle|\psi'\right\rangle + 8\cos 4\beta \left\langle\psi'\middle|\hat{Y}_i\hat{Y}_j-\hat{Z}_i\hat{Z}_j\middle|\psi'\right\rangle \tag{5.2.72}$$

$$\frac{\partial^2}{\partial\gamma^2}\langle\phi|\hat{Z}_i\hat{Z}_j|\phi\rangle = \frac{1}{2}\sin 4\beta \frac{\partial^2}{\partial\gamma^2}\left\langle\psi'\middle|\hat{Y}_i\hat{Z}_j+\hat{Z}_i\hat{Y}_j\middle|\psi'\right\rangle + \sin^2 2\beta \frac{\partial^2}{\partial\gamma^2}\left\langle\psi'\middle|\hat{Y}_i\hat{Y}_j\middle|\psi'\right\rangle \tag{5.2.73}$$

$$\frac{\partial^2}{\partial\beta\partial\gamma}\langle\phi|\hat{Z}_i\hat{Z}_j|\phi\rangle = 2\cos 4\beta \frac{\partial}{\partial\gamma}\left\langle\psi'\middle|\hat{Y}_i\hat{Z}_j+\hat{Z}_i\hat{Y}_j\middle|\psi'\right\rangle + 2\sin 4\beta \frac{\partial}{\partial\gamma}\left\langle\psi'\middle|\hat{Y}_i\hat{Y}_j\middle|\psi'\right\rangle \tag{5.2.74}$$

$$= \frac{\partial^2}{\partial\gamma\partial\beta}\langle\phi|\hat{Z}_i\hat{Z}_j|\phi\rangle \tag{5.2.75}$$

and,

$$\frac{\partial^2}{\partial\gamma^2}\left\langle\psi'\middle|\hat{Y}_i\hat{Z}_j\middle|\psi'\right\rangle =$$

$$\sum_{k=0}^{\ell_{ij}} (\cos\gamma I)^{\ell_{ij}-k}(-i\sin\gamma)^k$$

$$\times\Bigg\{\Big[(k-\ell_{ij}-1)(k-\ell_{ij})\tan^2\gamma+\left(k^2-k\right)\cot^2\gamma+(2k+1)(k-\ell_{ij}-1)-k\Big]\cos\gamma\sum_{\lambda\in\Lambda_k^{\ell_{ij}}}\left\langle y_i z_j z_i^k\right\rangle_\lambda$$

$$+\Big[(k-\ell_{ij}+1)(k-\ell_{ij})\tan^2\gamma+\left(k^2+k\right)\cot^2\gamma+(2k+3)(k-\ell_{ij})-(k+1)\Big]\sin\gamma\sum_{\lambda\in\Lambda_k^{\ell_{ij}}}\left\langle x_i z_i^k\right\rangle_\lambda\Bigg\} \tag{5.2.76}$$

$$\frac{\partial^2}{\partial\gamma^2}\left\langle\psi'\middle|\hat{Z}_i\hat{Y}_j\middle|\psi'\right\rangle =$$

$$\sum_{k=0}^{\xi_{ij}} (\cos\gamma I)^{\xi_{ij}-k}(-i\sin\gamma)^k$$

$$\times\Bigg\{\Big[(k-\xi_{ij}-1)(k-\xi_{ij})\tan^2\gamma+\left(k^2-k\right)\cot^2\gamma+(2k+1)(k-\xi_{ij}-1)-k\Big]\cos\gamma\sum_{\lambda\in\Lambda_k^{\xi_{ij}}}\left\langle z_i y_j z_j^k\right\rangle_\lambda$$

$$+\Big[(k-\xi_{ij}+1)(k-\xi_{ij})\tan^2\gamma+\left(k^2+k\right)\cot^2\gamma+(2k+3)(k-\xi_{ij})-(k+1)\Big]\sin\gamma\sum_{\lambda\in\Lambda_k^{\xi_{ij}}}\left\langle x_j z_j^k\right\rangle_\lambda\Bigg\} \tag{5.2.77}$$

$$\frac{\partial^2}{\partial\gamma^2}\left\langle\psi'\middle|\left(\hat{Y}_i\hat{Y}_j\right)\middle|\psi'\right\rangle =$$

$$\sum_{n=0}^{\xi_{ij}}\sum_{m=0}^{\ell_{ij}} (\cos\gamma I)^{\ell_{ij}+\xi_{ij}-m-n}(-i\sin\gamma)^{m+n}\left(\sum_{\lambda_1\in\Lambda_m^{\ell_{ij}}}\sum_{\lambda_2\in\Lambda_n^{\xi_{ij}}}\left\langle y_i y_j z_i^m z_j^n\right\rangle_{\lambda_1,\lambda_2}\right)$$

$$\times\Big\{\left[(-\ell_{ij}-\xi_{ij}+m+n)(\tan\gamma)+(m+n)\cot\gamma\right]^2+\Big[(-\ell_{ij}-\xi_{ij}+m+n)\left(\sec^2\gamma\right)-(m+n)\csc^2\gamma\Big]\Big\} \tag{5.2.78}$$

5.3 Computing Expectation Value and its Derivatives

At first, it may seem that the results obtained from the Pauli Decomposition are too tedious to be useful for anything, due to its lengthy expressions. On the contrary, our results suggest that the expectation $\left\langle \hat{C} \right\rangle_p$ can be calculated in a different way. We can actually calculate the gradient $\nabla \left\langle \hat{C} \right\rangle_p$ and the Hessian $\nabla^2 \left\langle \hat{C} \right\rangle_p$ easily and directly from classical computing, instead from quantum computing! The reason is that our new expressions are simply a linear combination of the various expectations of the observables or Pauli compositions σ, which are independent of the local parameters β, γ as shown in figure 5.3.1. If one has the estimates of all the expectations of Pauli compositions $\langle \sigma \rangle_{p-1} = \langle \phi_{p-1} | \sigma | \phi_{p-1} \rangle$, then it will only take a simple substitution of local parameters β, γ to find the quantities $\nabla^{0,1,2} \left\langle \hat{C} \right\rangle_p$. The cardinality of set of the expectation of Pauli compositions $\langle \sigma \rangle_{p-1}$ is heavily dependent on the graph structure. If the structure of the graph is sparse with low regularity g, then the set will have fewer number of expectations. Conversely, if the structure of the graph is dense with high regularity g, then the set will have a larger number of expectations.

We will exploit this result, by proposing a new way of calculating the expectation value of the MaxCut Hamiltonian $\left\langle \hat{C} \right\rangle_p$, the gradient $\nabla \left\langle \hat{C} \right\rangle_p$ and the Hessian $\nabla^2 \left\langle \hat{C} \right\rangle_p$ as shown the flowchart in figure 5.3.2. Conventionally in Standard Greedy Search and Greedy Subsearch, to measure $\left\langle \hat{C} \right\rangle_p$, the set of locally optimal QAOA parameters $\left(\vec{\beta}^*_{p-1}, \vec{\gamma}^*_{p-1} \right)$ up to layer $p-1$ and the QAOA search parameter point (β_p, γ_p) of layer p are used to prepare QAOA_p of depth p in the quantum computer (QC). Then, the MaxCut Hamiltonian $\hat{C}$ is supplied in the quantum measurement loop process to estimate $\left\langle \hat{C} \right\rangle_p$. In the proposed method which will be employed in the Greedy Newton strategy, only the set of locally optimal QAOA parameters $\left(\vec{\beta}^*_{p-1}, \vec{\gamma}^*_{p-1} \right)$ up to depth $p-1$ used to prepare QAOA_{p-1} of layer $p-1$ in the quantum computer (QC). Afterwards, the various Pauli compositions σ are supplied in the quantum measurement loop process to estimate its expectation value $\langle \sigma \rangle_{p-1}$. These expectation values $\langle \sigma \rangle_{p-1}$ loaded into the classical computer (CC), which has the Pauli decomposition equations, ready to be used for calculating $\nabla^{0,1,2} \left\langle \hat{C} \right\rangle_p$ upon substitution of the QAOA search parameters $\left(\vec{\beta}_p, \vec{\gamma}_p \right)$. Detailed instructions for Greedy Newton hybrid strategy will be given in the following chapter 6.

$$\sigma = \left\{ \langle \phi_{p-1} | \hat{Z}_i \hat{Z}_j | \phi_{p-1} \rangle, \left\{ \sum_{\lambda \in \Lambda_k^{\ell_{ij}}} \left\langle y_i z_j z_i^k \right\rangle_\lambda, 0 \le k \le \ell_{ij} \right\}, \left\{ \sum_{\lambda \in \Lambda_k^{\ell_{ij}}} \left\langle x_i z_i^k \right\rangle_\lambda, 0 \le k \le \ell_{ij} \right\}, \right.$$
$$\left\{ \sum_{\lambda \in \Lambda_k^{\xi_{ij}}} \left\langle z_i y_j z_j^k \right\rangle_\lambda, 0 \le k \le \xi_{ij} \right\}, \left\{ \sum_{\lambda \in \Lambda_k^{\xi_{ij}}} \left\langle x_j z_j^k \right\rangle_\lambda, 0 \le k \le \xi_{ij} \right\},$$
$$\left. \left\{ \sum_{\lambda_1 \in \Lambda_m^{\ell_{ij}}} \sum_{\lambda_2 \in \Lambda_n^{\xi_{ij}}} \langle y_i y_j z_i^m z_j^n \rangle_{\lambda_1, \lambda_2}, 0 \le n \le \xi_{ij}, 0 \le m \le \ell_{ij} \right\} \right\} \tag{5.3.1}$$

Figure 5.3.1: The set of the various observables (Pauli compositions) σ, whose expectation, with respect to the QAOA output state $|\phi_{p-1}\rangle$ of depth $p-1$, needed to calculated an expectation value of unweighted MaxCut Hamiltonian of an edge (i, j).

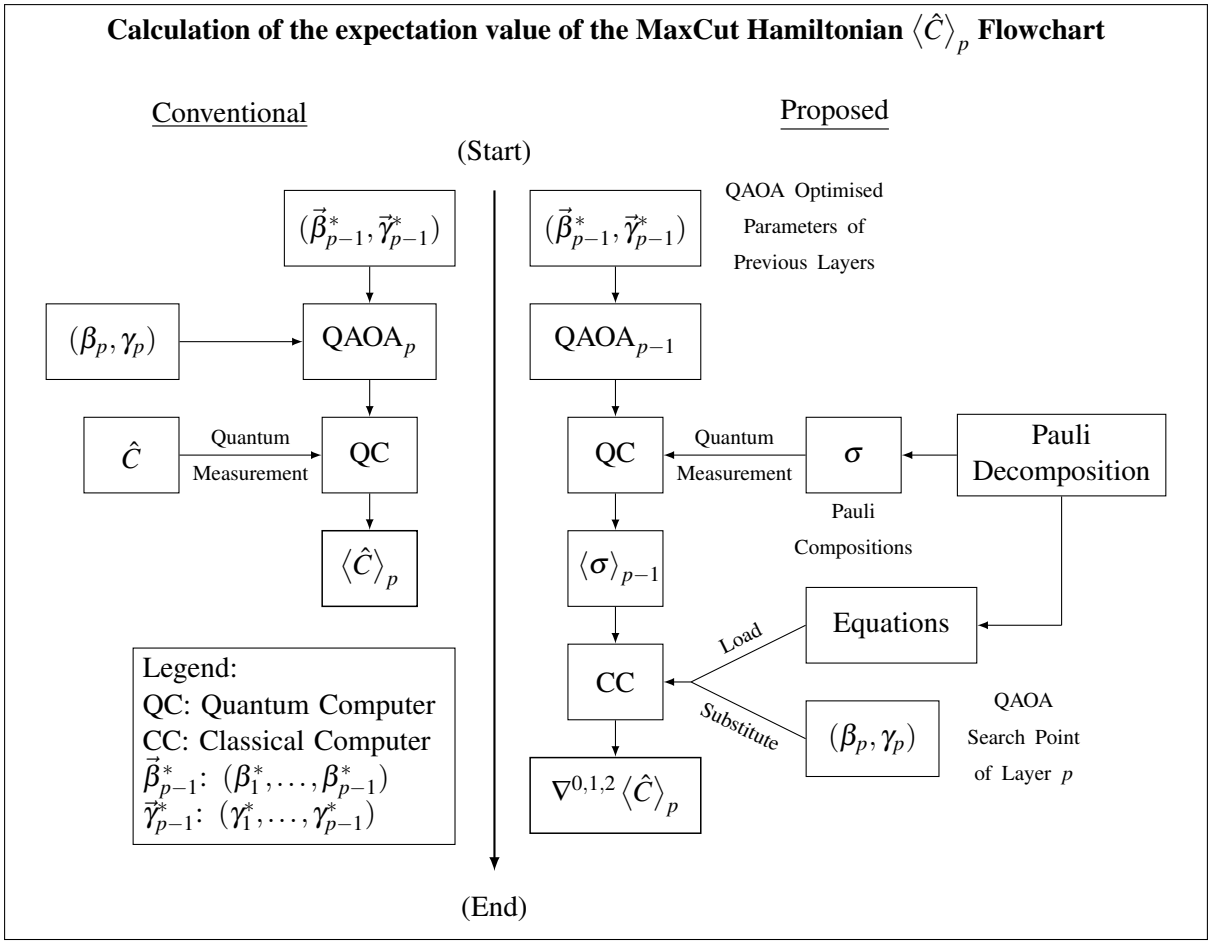

Figure 5.3.2: Comparison of between the conventional and the proposed way of calculating the expectation value of the MaxCut Hamiltonian and its derivatives. Not shown in this flowchart is the quantum measurement loop process.

Chapter 6

Greedy Newton Implementation

The results of the Pauli decomposition of the expectation value of the MaxCut Hamiltonian $\left\langle \hat{C} \right\rangle_p$ in previous section 5.2 suggests another an alternative method of calculation of $\nabla^{0,1,2} \left\langle \hat{C} \right\rangle_p$. As a result this new method, the instructions for the Greedy Newton strategy differs significantly from the other two conventional Greedy strategies. Explicitly, the instructions are summarised below as:

1. Start from depth $p = 1$.
2. From the problem graph given, determine the necessary Pauli compositions σ.
3. Translate the Pauli compositions into Pauli-Z measurements.
4. Prepare all QAOA operators from layer 1 to $p-1$, with all QAOA parameters of layer $p-1$ and below, fixed to the latest known optimised value.
5. Run the QAOA of depth $p-1$ on a quantum computer, starting from a fixed initial state $|\psi\rangle$, and obtain the output candidate state $|\phi_{p-1}\rangle$.
6. Measure the various expectation values of the Pauli compositions $\langle \sigma \rangle_{p-1}$ by applying the corresponding Pauli-Z measurements for M times each on newly generated output candidate state $|\phi_{p-1}\rangle$ individually.
7. Load the measured expectation values of the Pauli compositions $\langle \sigma \rangle_{p-1}$ into a classical computer that has the equations of the Pauli decomposition of $\nabla^{0,1,2} \left\langle \hat{C} \right\rangle_p$.
8. From the coarse search, substitute the one of the unsearched points (β_p, γ_p) in the local discrete parameter space, into the classical computer to calculate $\nabla^{0,1,2} \left\langle \hat{C} \right\rangle_p$. Save the calculation results in the database.
9. Check for Newton's conditions:
   (a) If satisfied, run Newton's method to obtain the next trial Newton's point (β_p, γ_p). Repeat step 9 until the parameter differences between two consecutive Newton iterations are below a certain threshold, which indicates Newton's Method is successful.
   (b) If unsatisfied, repeat step 8 and 9. If all points in the local discrete parameter space are searched, then Newton's Method is unsuccessful.

10. Find Optimal point:

    (a) If Newton's method is successful, then set the latest point found by the Newton's method as the optimal parameter values $\left(\beta_p^*, \gamma_p^*\right)$ for depth p.

    (b) If Newton's method is unsuccessful, then from the database of search points, including all points generated by Newton's Method, find the optimal parameter values $\left(\beta_p^*, \gamma_p^*\right)$ that has the optimal (minimum) corresponding $\left\langle \hat{C} \right\rangle_p$.

11. Increase the depth p by 1 to $p+1$ and repeat step 5 to 11, up to a fixed desired depth P.

6.1 Theoretical Results

6.1.1 Quantum Computation Calls

We analyse the quantum computational usage cost in terms of the total number of quantum calls needed for solving the MaxCut problem. Ideally, fewer quantum calls are desirable as it would potentially translate to cheaper quantum usage cost. Before counting, suppose we fix a few variables first. Let the total QAOA layer be an integer P. Each parameter β_p, γ_p of layer p has a fixed domain interval of $\beta_p \in [0, \pi]$, $\gamma_p \in [0, 2\pi]$, with the desired division size of ε. Also, let M be a number of quantum measurements for each expectation.

For the Standard Greedy Search, the total number of quantum calls needed is about,

$$= MP\left(\frac{2\pi}{\varepsilon} + 1\right)\left(\frac{\pi}{\varepsilon} + 1\right) \tag{6.1.1}$$

which has a number scaling linear in MP and a number scaling quadratic in the inverse division size $\frac{1}{\varepsilon}$.

For the Greedy Subsearch, ignoring boundary corrections, the total number of quantum calls needed is

$$= MP\left(\left(\frac{2\pi}{\delta} + 1\right)\left(\frac{\pi}{\delta} + 1\right) + \left(\frac{\delta}{\varepsilon} + 1\right)^2\right) \tag{6.1.2}$$

which as also has a number scaling linear in MP. In this project, we will chose $\delta^2 = \pi\varepsilon$, such that the number scaling is linear with respect to the inverse division size $\frac{1}{\varepsilon}$.

Finally, for Greedy Newton, the number of quantum computation calls is equal to MP multiplied by the total number of expectations of Pauli compositions needed. That is,

$$= MP \sum_{(i,j)\in E} \left[1 + 2^{\ell_{ij}+1} + 2^{\xi_{ij}+1} + 2^{\ell_{ij}+\xi_{ij}}\right] \tag{6.1.3}$$

which is dependent only on the structure of the problem graph, that is edges set E. For g-regular graph, the number expression can be simplified by substituting $\ell_{ij} = \xi_{ij} = g - 1$ and replacing the summation sign with multiplication the number of edges of a regular graph $|E|$. A summary of the calculated results is shown in table 6.1.1. For a fixed regularity g, the number scaling is linear in number of vertices n. However, for fixed n, the number scaling is linear-exponential in g, the regularity of the graph. Complete graph or $g = n - 1$ regular has the worst number scaling as it is quadratic-exponential in number of vertices n.

g-Regular	Total number of Quantum Computation Calls
1	$3nMP$
2	$13nMP$
3	$\frac{99}{2}nMP$
g	$\frac{ng}{2}\left[\frac{1}{4}\left(2^g+4\right)^2-3\right]MP$
$n-1$	$\frac{n(n-1)}{2}\left[\frac{1}{4}\left(2^{n-1}+4\right)^2-3\right]MP$

Table 6.1.1: A list of the number of quantum computational calls needed for a g-regular graph using the Pauli Decompostion in Greedy Newton. Note that we have used the number of edges in a regular graph, by the Handshake lemma, $|E|=\frac{ng}{2}$ and a quadratic identity $\frac{1}{4}\left(2^g+4\right)^2-3=1+2^{g+1}+2^{2g-2}$ in the calculations.

6.2 Numerical Experiment

6.2.1 Numerical Code

The numerical code is programmed based on python 3.7 language supported by standard python packages such as random, numpy, math, time, networkx, itertools and csv. The code is written in a object-oriented way such that it empower the user to perform high level numerical experiments without verbose programming. This does not mean that the code allows the user to perform the experiment as few of lines of code as possible, rather, it should permit the user to prepare or setup the experiment intuitively. Two python files are created for the numerical experiment: *my_quantum_simulator_objects.py* and *my_quantum_simulator_helper_functions.py*. The main python file *my_quantum_simulator_objects.py* contains python classes with built-in pre-defined methods (class functions) that represents quantum objects such as quantum state, Hamiltonian, algorithm, simulator and strategy. A high level summary of this file is given in figure 6.2.1. The supporting file *my_quantum_simulator_helper_functions.py* contains common functions that are frequently used by two or more python classes. The file may also contain helper functions that externalises complicated code which helps to improve code readability in the main file. Please refer to appendix 8.1 for an example code that implements the numerical experiment.

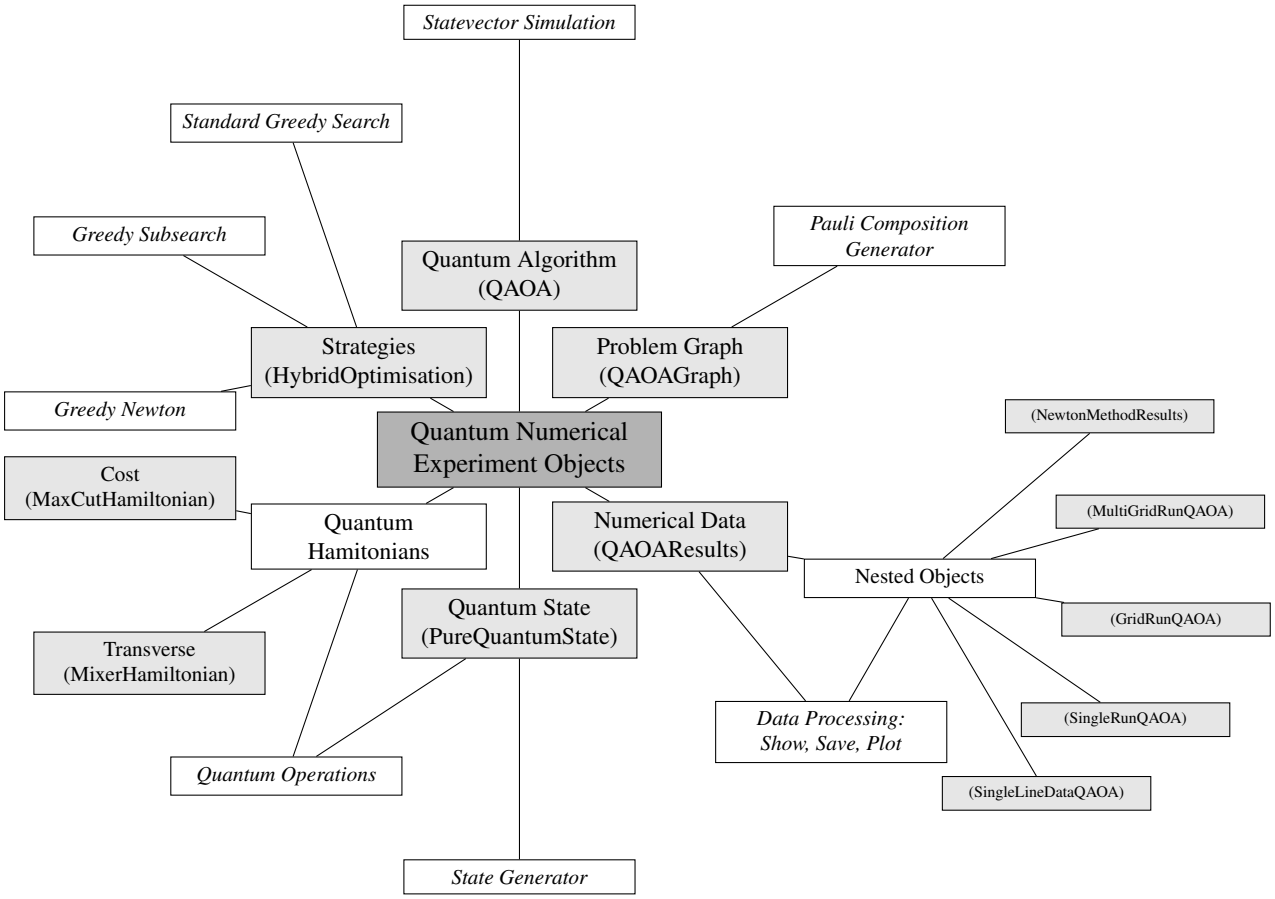

Figure 6.2.1: The outline the numerical experiment code in file *my_quantum_simulator_objects.py*. The words in brackets, highlighted in a light grey box, are actual names of python classes used. The word in italics are high level descriptive words that describes the collection of methods (class functions) available for each class.

6.2.2 Implementation

All the three greedy-based hybrid strategy are implemented in the numerical code and tested against each other. The numerical experiment is implemented on a desktop computer equipped with an Intel Core i5-6500 CPU, with four cores and four threads that has a base clock of 3.20 GHz and 32 GB DDR4 RAM with a clock speed of 2133 MHz. The quantum computer, that will be used in this project, is classically simulated using a custom built quantum statevector simulator, that is simply, matrix multiplication. For each greedy-based hybrid strategy implementation, the input will be a problem graph generated by networkx and the output is an approximated MaxCut value. Three KPIs will be measured, as given in table 4.2.1, which are the total computational time, total quantum computer calls and the approximation ratio. The total QAOA depth is fixed at $P = 10$. Each parameter β_p, γ_p of layer p has a fixed domain interval of $\beta_p \in [0, \pi]$, $\gamma_p \in [0, 2\pi]$, with a fixed division sizes $\varepsilon = \frac{\pi}{64}$ and $\delta = \sqrt{\pi\varepsilon} = \frac{\pi}{8}$. The QAOA initial state is prepared as the all plus state $|+\rangle$. The number of quantum measurements for each expectation M is not needed in this numerical simulation, therefore it is set to $M = 1$ for consistency sake. For Greedy Newton, the Newton conditions are set to be,

$$\text{Det}\left(\nabla^2 \left\langle \hat{C} \right\rangle_p\right) > 10^{-9} \tag{6.2.1}$$

$$\frac{\partial \left\langle \hat{C} \right\rangle_p}{\partial \gamma_p} \text{ or } \frac{\partial \left\langle \hat{C} \right\rangle_p}{\partial \beta_p} > 10^{-9} \tag{6.2.2}$$

The maximum number of Newton iteration is set to 100 and the successful condition is set to be when parameters differences between each consecutive Newton iterations are both less than 0.001 rad. After much testing of the Newton Method, it was found that a Newton step size of $\gamma = 0.35$ has a good rate of convergence, with a low number of iteration needed and a low risk of overshooting the optimal point. Five types of unweighted graphs: 1-Regular, Path, Cycle, Complete and 3-Regular, up to 8 labelled vertices, will be used as a problem graph for the MaxCut problem. Example of these graphs are shown in figures 6.3.1, 6.3.3, 6.3.5, 6.3.7 and 6.3.9 respectively.

6.3 Numerical Results

6.3.1 Overall Results: General Trends

For the total number of computer computer calls, in all cases, under Standard Greedy Search, it is found to be a fixed number, 83850 calls, while under Greedy Subsearch, it varies about an average of 1900 ± 200 calls. Under Greedy Newton, the number of calls follows a formula, given in equation 6.1.3, that is dependent on the graph structure. For the total simulated computational time, due to the use of the quantum statevector simulation, all plots are found to increase exponentially in the number of vertices. Unlike the Standard Greedy Search and the Greedy Subsearch strategies where both have a generally smooth increasing trend, the Greedy Newton has a generally uneven increasing trend. For the approximate ratio, the trends varies greatly across the types of problem graphs and strategies used. The average performance results, from the perspective of Greedy Newton, are shown in table 6.3.1 below. The probability distribution of the binary cut string for the various problem graphs are given in the appendix 8.2.

	Average Order Improvement in Calls $lg(calls)$		Average Order Improvement in Time $lg(sec)$		Average Percentage Improvement %	
Graph	G Standard	G Sub	G Standard	G Sub	G Standard	G Sub
1 Regular	2.8	1.2	3.0	1.3	0.0	0.0
Path	2.4	0.8	2.5	1.0	−2.1	2.4
Cycle	2.1	0.5	2.3	0.8	−0.8	−0.6
Complete	1.0	−0.7	1.1	−0.4	0.2	1.2
3 Regular	1.4	−0.2	1.9	0.2	−1.3	1.6

Table 6.3.1: The averaged performance results, when compared from the perspective of Greedy Newton. All values are given in 1 decimal place. Note: 'Order Improvement' refers to the reduction of the orders of magnitude.

6.3.2 1 Regular

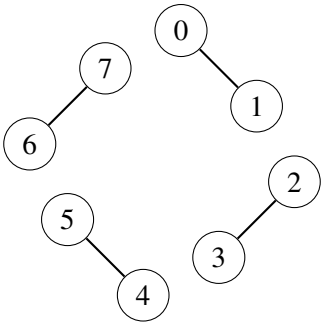

Figure 6.3.1: A 1-Regular graph with 8 vertices.

The various measurement quantities are plotted against the number of vertices as shown in figure 6.3.2 below. The results show that has an overall better performance in terms of the number of quantum computer calls and total computational time. On average, it has a positive 2.8 $lg(calls)$ and positive 3.0 $lg(sec)$ order improvement respectively against Standard Greedy Search. Also, it has a positive 1.2 $lg(calls)$ and positive 1.3 $lg(sec)$ order improvement respectively against Greedy Subsearch. All three strategies saturates the approximation ratio, which tells us that the solution quality of the candidate state produced by these three strategies are equal and optimal.

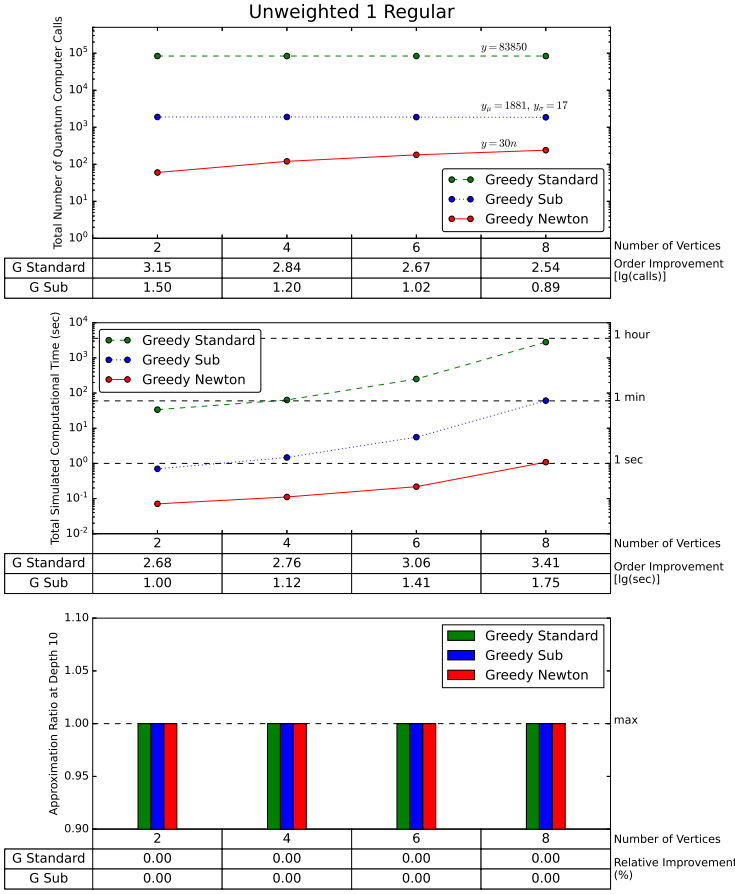

Figure 6.3.2: Numerical results for unweighted 1 Regular graphs up to 8 vertices.

6.3.3 Path

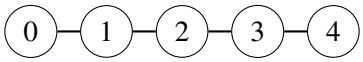

Figure 6.3.3: A path graph with 5 vertices.

The various measurement quantities are plotted against the number of vertices as shown in figure 6.3.4 below. The results show that Greedy Newton has an overall better performance in terms of the number of quantum computer calls and total computational time. On average, it has a positive 2.4 $lg(calls)$ and positive 2.5 $lg(sec)$ order improvement respectively against Standard Greedy Search. Also, it has a positive 0.8 $lg(calls)$ and positive 1.0 $lg(sec)$ order improvement respectively against Greedy Subsearch. However, Greedy Newton performed worse in terms of solution quality with a negative 2.1% improvement in approximation ratio against Standard Greedy Search, but perform better with a positive 2.4% improvement against Greedy Subsearch. Overall, the approximation ratio plot showed a general decreasing trend across all strategies used.

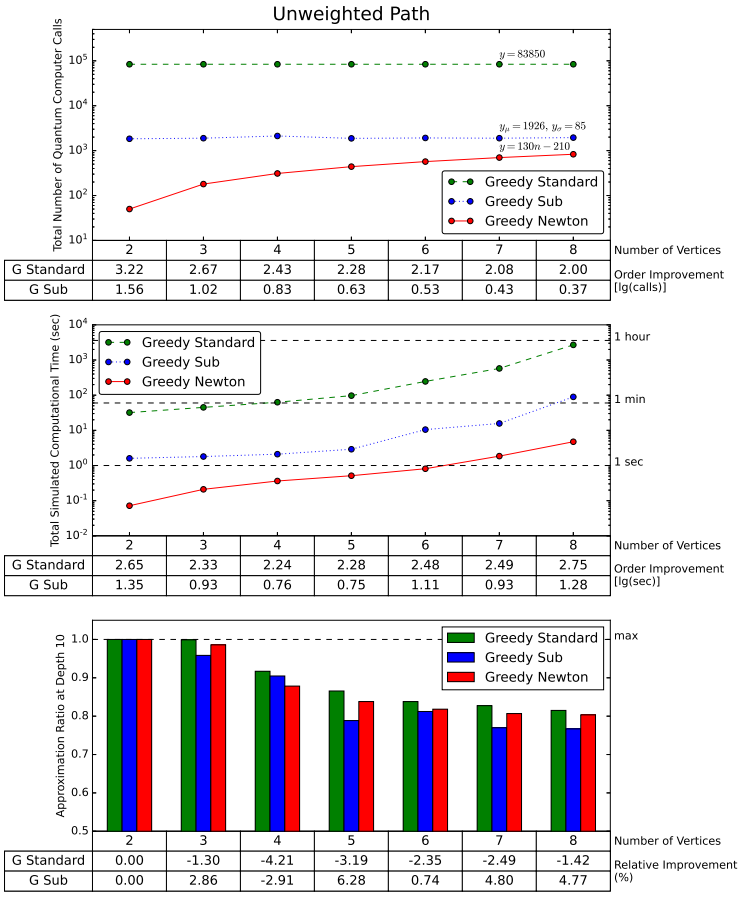

	2	3	4	5	6	7	8	
G Standard	3.22	2.67	2.43	2.28	2.17	2.08	2.00	Order Improvement [lg(calls)]
G Sub	1.56	1.02	0.83	0.63	0.53	0.43	0.37	

	2	3	4	5	6	7	8	
G Standard	2.65	2.33	2.24	2.28	2.48	2.49	2.75	Order Improvement [lg(sec)]
G Sub	1.35	0.93	0.76	0.75	1.11	0.93	1.28	

	2	3	4	5	6	7	8	
G Standard	0.00	-1.30	-4.21	-3.19	-2.35	-2.49	-1.42	Relative Improvement (%)
G Sub	0.00	2.86	-2.91	6.28	0.74	4.80	4.77	

Figure 6.3.4: Numerical results for unweighted path graphs up to 8 vertices.

6.3.4 Cycle

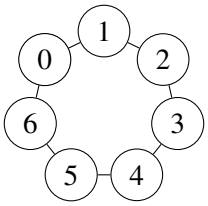

Figure 6.3.5: A cycle graph with 7 vertices.

The various measurement quantities are plotted against the number of vertices as shown in figure 6.3.6 below. The results show that Greedy Newton has an overall better performance in terms of the number of quantum computer calls and total computational time. On average, it has a positive 2.1 $lg(calls)$ and positive 2.3 $lg(sec)$ order improvement respectively against Standard Greedy Search. Also, it has a positive 0.5 $lg(calls)$ and positive 0.8 $lg(sec)$ order improvement respectively against Greedy Subsearch. However, Greedy Newton performed marginally worse in terms of the solution quality with a negative 0.76% and negative 0.60% improvement in approximation ratio against Standard Greedy Search and Greedy Subsearch respectively. Generally, approximation ratio plot for all strategies show that it fluctuates significantly about a decreasing trend.

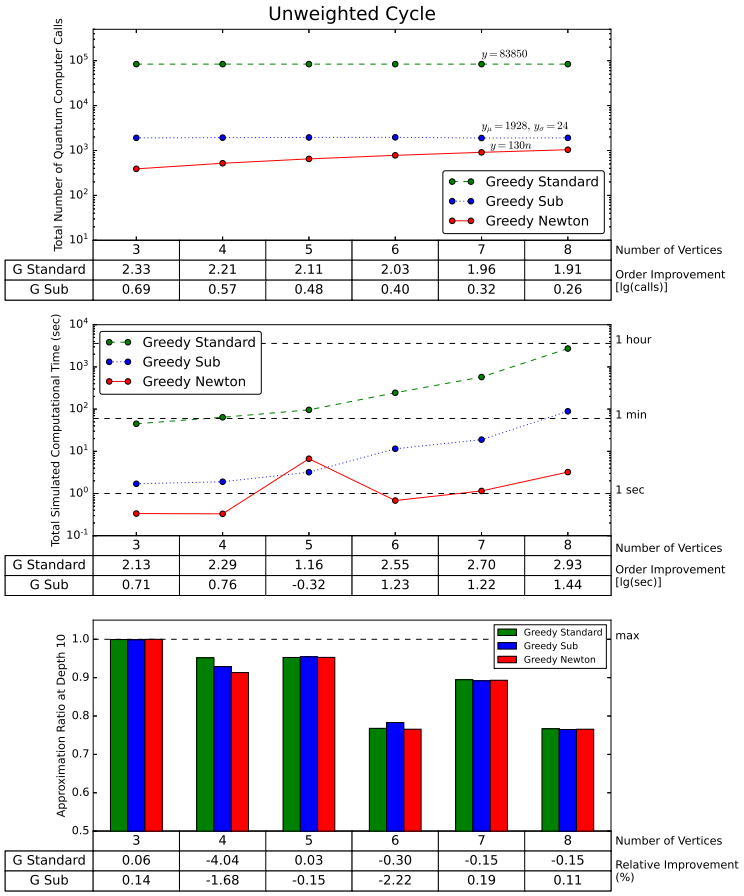

	3	4	5	6	7	8
G Standard	2.33	2.21	2.11	2.03	1.96	1.91
G Sub	0.69	0.57	0.48	0.40	0.32	0.26

	3	4	5	6	7	8
G Standard	2.13	2.29	1.16	2.55	2.70	2.93
G Sub	0.71	0.76	-0.32	1.23	1.22	1.44

	3	4	5	6	7	8
G Standard	0.06	-4.04	0.03	-0.30	-0.15	-0.15
G Sub	0.14	-1.68	-0.15	-2.22	0.19	0.11

Figure 6.3.6: Numerical results for unweighted cycle graphs up to 8 vertices. Note the anomalous point, under Greedy Newton, in the total simulated computational time at 5 number of vertices, which is reproducible.

6.3.5 Complete

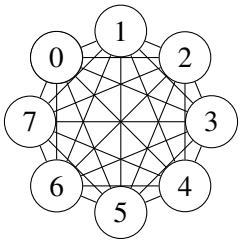

Figure 6.3.7: Complete graph with 8 vertices.

The various measurement quantities are plotted against the number of vertices as shown in figure 6.3.8 below. The results show that Greedy Newton has a mixed set of performance in terms of the number of quantum computer calls and total computational time. On average, it has better performance with positive 1.0 $lg(calls)$ and positive 1.1 $lg(sec)$ order improvement respectively against Standard Greedy Search, but has worse performance with negative 0.7 $lg(calls)$ and negative 0.4 $lg(sec)$ order improvement respectively against Greedy Subsearch. Surprisingly, Greedy Newton performed slightly better in terms of the solution quality with a positive 0.18% and positive 1.2% improvement in approximation ratio against Standard Greedy Search and Greedy Subsearch respectively. Generally, for Standard Greedy Search and Greedy Newton, its approximation ratio plot showed an slight decreasing trend while for Greedy Subsearch, its fluctuates significantly about an decreasing trend.

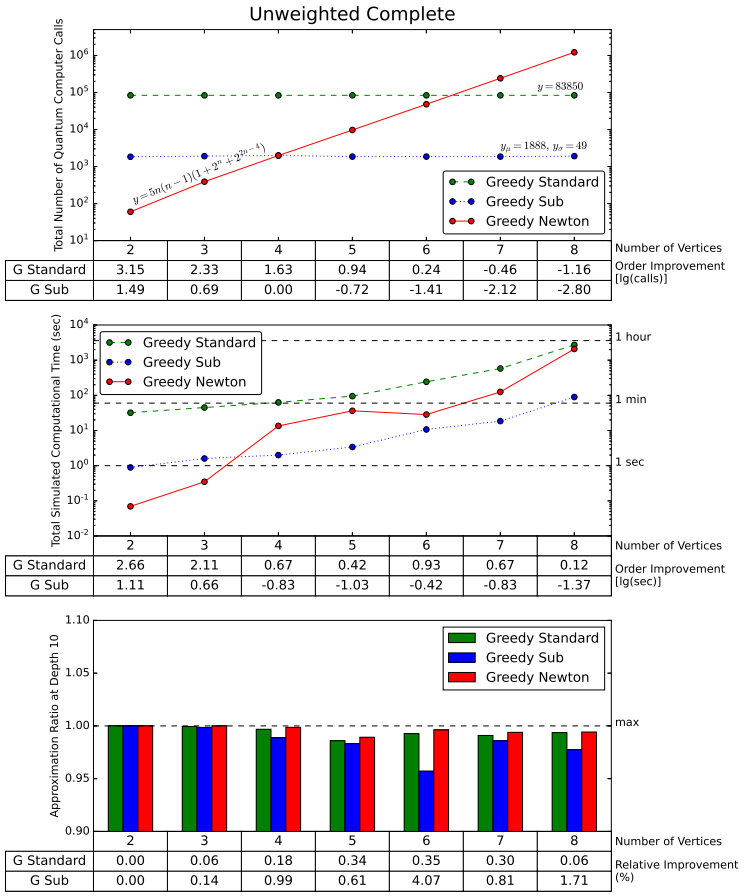

	2	3	4	5	6	7	8
G Standard	3.15	2.33	1.63	0.94	0.24	-0.46	-1.16
G Sub	1.49	0.69	0.00	-0.72	-1.41	-2.12	-2.80

	2	3	4	5	6	7	8
G Standard	2.66	2.11	0.67	0.42	0.93	0.67	0.12
G Sub	1.11	0.66	-0.83	-1.03	-0.42	-0.83	-1.37

	2	3	4	5	6	7	8
G Standard	0.00	0.06	0.18	0.34	0.35	0.30	0.06
G Sub	0.00	0.14	0.99	0.61	4.07	0.81	1.71

Figure 6.3.8: Numerical results for unweighted complete graphs up to 8 vertices.

6.3.6 3 Regular

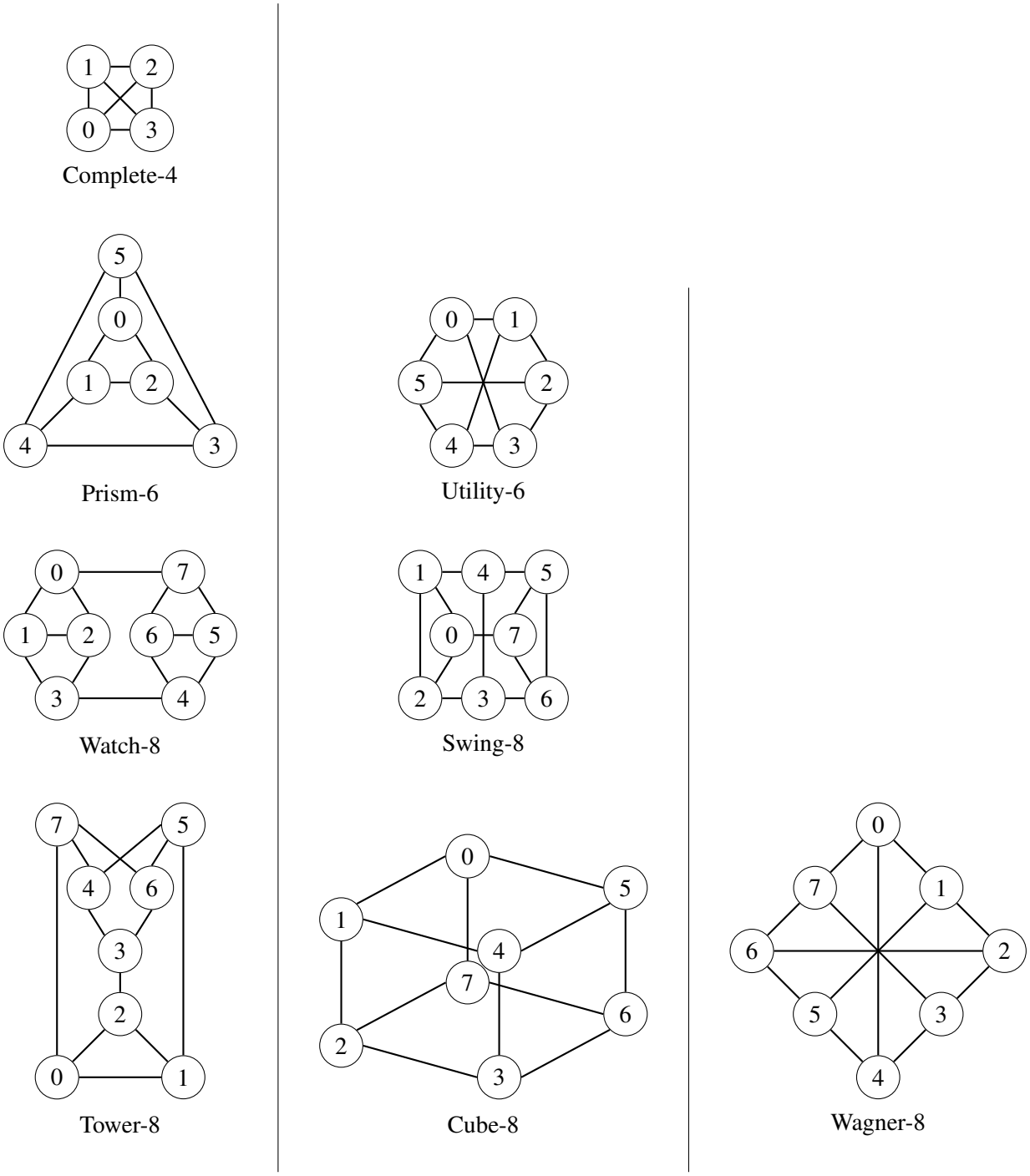

Figure 6.3.9: All unique 3-Regular graphs up to 8 vertices.

The various measurement quantities are plotted against each unique 3-regular graph up to 8 vertices as shown in figure 6.3.10. The results show that Greedy Newton has mixed set of performance in terms of the number of computational calls and total computational time. On average, it has a positive 1.4 $lg(calls)$ and positive 1.9 $lg(sec)$ order improvement respectively against Standard Greedy Search. However, it perform comparably with a negative 0.2 $lg(calls)$ and positive 0.2 $lg(sec)$ order improvement respectively against Greedy Subsearch. Interestingly, Greedy Newton is generally faster

than Greedy Subsearch despite requiring more quantum calls. In terms of the solution quality Greedy Newton performed marginally worse with a negative 1.3% improvement in approximation ratio against Standard Greedy Search, but perform somewhat better with a positive 1.6% improvement against Greedy Subsearch. In the approximation ratio plots, shows significant fluctuations across all unique graphs. Note that a typical trend analysis could not be conducted by obvious reasons.

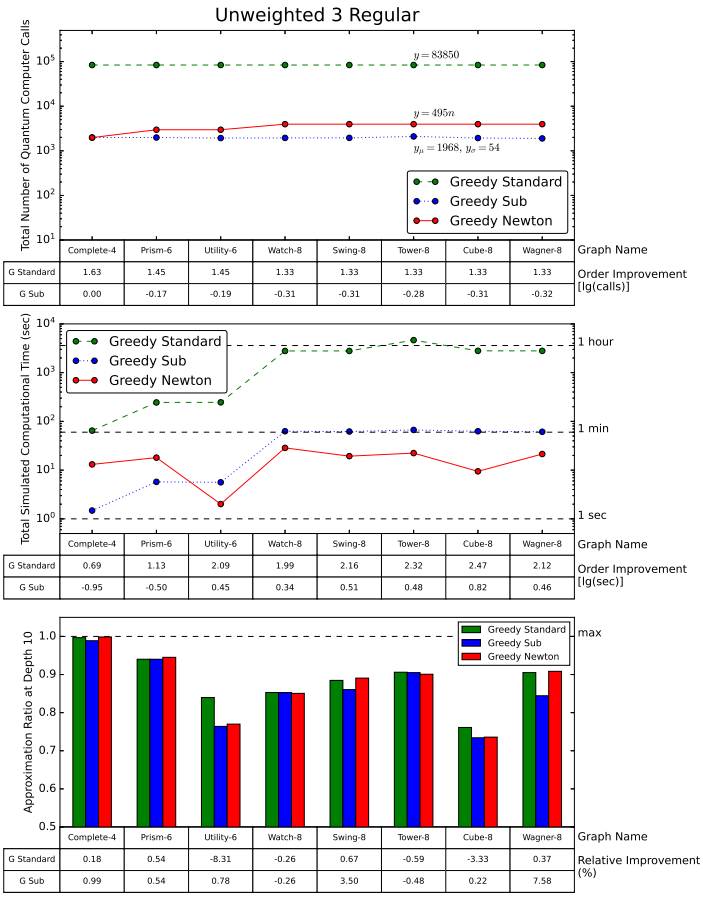

	Complete-4	Prism-6	Utility-6	Watch-8	Swing-8	Tower-8	Cube-8	Wagner-8
G Standard	1.63	1.45	1.45	1.33	1.33	1.33	1.33	1.33
G Sub	0.00	-0.17	-0.19	-0.31	-0.31	-0.28	-0.31	-0.32

	Complete-4	Prism-6	Utility-6	Watch-8	Swing-8	Tower-8	Cube-8	Wagner-8
G Standard	0.69	1.13	2.09	1.99	2.16	2.32	2.47	2.12
G Sub	-0.95	-0.50	0.45	0.34	0.51	0.48	0.82	0.46

	Complete-4	Prism-6	Utility-6	Watch-8	Swing-8	Tower-8	Cube-8	Wagner-8
G Standard	0.18	0.54	-8.31	-0.26	0.67	-0.59	-3.33	0.37
G Sub	0.99	0.54	0.78	-0.26	3.50	-0.48	0.22	7.58

Figure 6.3.10: Numerical results for unweighted 3 Regular graphs up to 8 vertices.

6.4 Discussion

6.4.1 On the Total Quantum Computer Calls

In all cases, the Standard Greedy Search strategy employs a fixed number of quantum computer calls, which matches the theoretical value. For Greedy Subsearch, the number of quantum computer calls fluctuates within a band of values, even though, the parameter precision was fixed. This was due to a active global parameter boundary restriction imposed in the actual algorithm. The coarse search may unpredictably return a valid optimal search point that is on the boundary. This resulted in the unwanted generation of the area of fine search parameter space which is outside of the global parameter boundaries. The actual algorithm is programmed to detect this unwanted generation and remove it from the fine search, leading to a systematically fewer fine search points. As a result, the overall number of calls fluctuates within a fixed range. In Greedy Newton, the number of quantum computer call corresponds to the total number of expectations of observables or Pauli composition needed to calculate $\langle \hat{C} \rangle$.

6.4.2 On the Total Computational Time

In general, there is strong correlation between the total number of quantum computer calls and the total computation time. This is because a majority of the computing power is used to calculate the output state of the QAOA which uses quantum statevector simulation that scales exponentially in the number of vertices. Therefore, a higher number of quantum computer calls means a higher amount of computation time. This general relationship can be observed in problem graphs such as 1 Regular, Path, Cycle and Complete.

However, this relationship does not strictly hold in some cases. The opposite relationship can be observed in the reproducible anomalous data point in 5-Cycle graph case and in the 3 Regular graphs case when comparing between Greedy Newton and Greedy Subsearch strategy. In the case of the reproducible anomalous point in 5-cycle graph, the computational time needed in Greedy Newton is more than that in Greedy Subsearch, even when the computational calls is significantly fewer. This is because, for that particular 5-cycle graph, Greedy Newton search was a total failure in the last 7 QAOA layers, with a total about 332 failed Newton descent attempts, each having about 2.5 Newton iterations. An example of a failed Greedy Newton parameter search at QAOA layer 4 for 5-Cycle is shown in figure 6.4.1. This forced Greedy Newton to employ its worse case scenario fail-safe optimization, that is to exhaustively check the database of searched points for the most optimal point, resulting in a huge amount of computational time spent.

These a majority of failures are directly attributed to the failure in satisfying the Newton's conditions during descent while a minority portion failed due to the generation of new Newton points that are outside of the global parameter boundary. After much deeper investigation, it is revealed that the Newton descent had indeed identified the correct direction to reach the optimal point, but the optimal point lies in a neighbourhood of space whose gradient is almost flat along the gamma direction, yet the hessian is almost singular around it, which make it impossible for Newton to descent properly along the beta direction.

In the case of 3 Regular graphs, Newton Method was extremely successful with minimal failure attempts, without having to resort to worse case scenario. Although the search spaces in both cases has a similar landscape, but the hessian is not singular around the flat line of optimal points, which allowed Newton to descent quadratically fast, reducing the amount of computational time needed for optimisation, resulting in an overall low amount of time spent, despite having a larger portion of time devoted to quantum statevector simulation when compared to Greedy Subsearch.

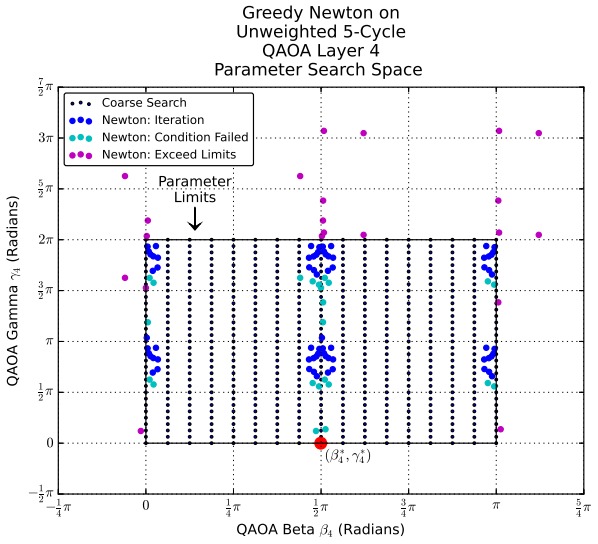

Figure 6.4.1: QAOA layer 4 local parameter search space on unweighted 5-Cycle under Greedy Newton hybrid strategy. Note: The optimal local parameter (β_4^*, γ_4^*) was found by exhaustive database search as a fail-safe optimisation.

6.4.3 On the Approximate Ratio

It is curious to note that for every problem graphs, the approximation ratio differs slightly across the three greedy strategies. There are several possible speculative factors that qualitatively explain such differences. One, is that the Standard Greedy Search can be considered as a global optimiser in a local context, that is, it will search for absolute optimum search point within its entire discretised search space. On the other hand, Greedy Subsearch and Greedy Newton are considered local optimisers, that is, it will search for the a local optimum within a neighbourhood of a small segment of the search space. Thus, it is expected that the Standard Greedy Search would perform generally better than the other two in terms of approximation ratio.

Second, the differences in the precision of the parameters used might have affected the approximation ratios. In the Standard Greedy Search and Greedy Subsearch, the smallest division size is $\varepsilon = \frac{\pi}{64} \approx 0.05$ rad, a rational fraction of π, while the maximum parameter precision used in Greedy Newton is 0.001 rad, but the Newton' iteration will always generate parameters where its difference will be an irrational fraction of π that is less than 0.001 rad. Although, a higher precision is always desired, however, one must be aware that the expectation value, in essence, is simply a trigonometric polynomial of some order N. Finding the optimal point is akin to finding the roots of trigonometric polynomial, where its roots are periodic within any domain interval of size 2π, therefore the roots must be some unknown rational fraction of π. Hence, it is likely that the irrational π fraction of optimal parameter generated by Greedy Newton have resulted in the built up 'errors' at increasing depth, which negatively impacted its approximation ratio at the end.

It is difficult to definitively pinpoint all the actual factors that affects the approximation ratio due to the lack of relevant quantitative data processing in the numerical experiment. There are multiple quantities that are whose intertwined relationship which are hard to identify, isolate and process. For example, one would wish to know the explicit relationship between the approximation ratio and depth so that one may exploit it to minimise QAOA depth to reduce computation cost. However, such a

relationship is not a clear cut one as there multiple factors, such the graph structure, optimisation strategy, noise and errors which are all hard to quantify.

6.4.4 Performance Summary

A performance comparison of all three greedy based strategies is shown in table 6.4.1 below. On the number of quantum calls, the Standard Greedy Search has an inverse quadratic scaling in the division size ε, while Greedy Subsearch has an inverse linear scaling. Greedy Newton has a linear scaling in the number of vertices n, if regularity g is fixed. Otherwise, if $g = n-1$ on the complete graph case, then it would have an exponential scaling in n. On the simulated computational time, all strategies has an exponential scaling in the number of vertices n due to quantum statevector simulation. However, based on absolute time, for $g \leq 3$ and $n \leq 8$, Standard Greedy Search took the longest time to complete, followed by Greedy Subsearch and Greedy Newton. For $g = n-1$ and $n \leq 8$ on the complete graph case, Standard Greedy Search still took the longest time to complete but Greedy Newton took longer than Greedy Subsearch. In all cases and strategies, the approximation ratio never dipped below 0.73. Taking results from the Cube-8 case, which has the average lowest approximation ratio, Greedy Subsearch produces a 'Good' candidate state solution that solve MaxCut with at least 73.4% probability of success. However, Greedy Newton and Standard Greedy Search produces 'Better' and 'Best' candidate states with at least 73.6% and 76.1% probability of success.

Greedy Strategies	Quantum Calls Scaling	Simulated Computational Time (Exponential in n)	Candidate State Solution Quality
Standard Greedy Search	Quadratic in $\frac{1}{\varepsilon}$	Longest	Best
Greedy Subsearch	Linear in $\frac{1}{\varepsilon}$	Short	Good
Greedy Newton	Linear in n (Fixed g regularity) Exponential in n (For $g = n-1$)	Shortest* (For small $n \leq 8,\ g \leq 3$) Long ** (For $g = n-1$)	Better

Table 6.4.1: Performance comparison of all three greedy based strategies. * only if Newton's Method is successful, or ** if otherwise.

Part III

Project Conclusion

Chapter 7

Conclusion and Summary

7.1 Future Research

There are many potential extensions and improvements that this project can take. An obvious extension would be an implementation of Greedy Newton on a real world NISQ quantum computer to validate its robustness and reliability. Another possible extension would be to use Greedy Newton to solve the weighted MaxCut problem by leveraging the extended results of weighted case as given in appendix 8.6. A crucial extension of the project would probably require a performance comparison between Greedy Newton and other non-greedy based strategies. To improve the numerical experiment, we may consider the use of Tensor Contraction simulation [Fri+17] to replace the statevector simulator for a much efficient quantum simulation, so that problems graphs more vertices can be simulated.

7.2 Closing Thoughts

We have investigated three greedy-based Hybrid Quantum Classical Parameter Optimisation strategy on optimising the QAOA parameters to solve the unweighted MaxCut Problem: Standard Greedy Search, Greedy Subsearch and Greedy Newton. We have also analysed and discussed the relative performance between strategies in terms the total number of quantum computer calls, total simulated computational time and the approximation ratio. To implement Greedy Newton effectively, using the results of Pauli decomposition of $\left\langle \hat{C} \right\rangle_p$, an unconventional method of calculating the expectation value of the MaxCut Hamiltonian and its derivatives $\nabla^{0,1,2} \left\langle \hat{C} \right\rangle_p$ was proposed for Newton's Descent. By the numerical results of problem graphs with low regularity $g \leq 3$ and number of vertices $n \leq 8$, it was found that Greedy Newton performed better than the other two by at most 2 orders of magnitude in terms of the number of quantum calls and the amount of computational time, with comparable approximation ratio. For complete problem graphs $g = n - 1$, Greedy Newton was found to be the worst among the three, due to the exponential scaling in calls and time needed with respect to n. It shall be emphasised that these conclusions cannot be extrapolated for other types of problem graphs with regularity $g \geq 4$.

In conclusion, Greedy Newton is designed to be a *better-than-average* greedy strategy. Given the right conditions, Greedy Newton should be competitive with other non-greedy strategies. However, Greedy Newton itself cannot overcome the inherent limitations of its greedy nature. Nonetheless, I believe its practicality and ease of implementation will confidently trumps over such inconvenient limitations.

Bibliography

[Ans+18] Eric R Anschuetz et al. “Variational Quantum Factoring”. In: (2018), pp. 1–18. arXiv: 1808.08927. URL: http://arxiv.org/abs/1808.08927.

[Ben+19] Andreas Bengtsson et al. “Quantum approximate optimization of the exact-cover problem on a superconducting quantum processor”. In: 1.3 (2019), pp. 1–8. arXiv: 1912.10495. URL: http://arxiv.org/abs/1912.10495.

[Bul05] David Bulger. “Quantum computational gradient estimation”. In: (2005). arXiv: 0507109 [quant-ph]. URL: http://arxiv.org/abs/quant-ph/0507109.

[Che20] Chong Hian Chee. “The quantum linear problem and its quantum algorithmic solutions”. In: (2020). URL: https://hdl.handle.net/10356/138662.

[Cro18] Gavin E Crooks. “Performance of the Quantum Approximate Optimization Algorithm on the Maximum Cut Problem”. In: (2018), pp. 15–17. arXiv: 1811.08419. URL: http://arxiv.org/abs/1811.08419.

[FGG14a] Edward Farhi, Jeffrey Goldstone and Sam Gutmann. “A Quantum Approximate Optimization Algorithm Applied to a Bounded Occurrence Constraint Problem”. In: (2014), pp. 1–13. arXiv: 1412.6062. URL: http://arxiv.org/abs/1412.6062.

[FGG14b] Edward Farhi, Jeffrey Goldstone and Sam Gutmann. “A Quantum Approximate Optimization Algorithm”. In: (2014). arXiv: 1411.4028. URL: http://arxiv.org/abs/1411.4028.

[Fri+17] E Schuyler Fried et al. “qTorch: The Quantum Tensor Contraction Handler”. In: (2017). DOI: 10.1371/journal.pone.0208510. arXiv: 1709.03636. URL: http://arxiv.org/abs/1709.03636.

[GM18] G G Guerreschi and A Y Matsuura. “QAOA for Max-Cut requires hundreds of qubits for quantum speed-up”. In: (2018), pp. 1–14. DOI: 10.1038/s41598-019-43176-9. arXiv: 1812.07589. URL: http://arxiv.org/abs/1812.07589.

[GPRA18] Sevag Gharibian, Ojas D. Parekh and Ciaran Ryan-Anderson. “Approximate Constraint Satisfaction in the Quantum Setting”. In: *Symposium on Discrete Algorithms 2018*. New Orleans, LA: USDOE National Nuclear Security Administration (NNSA), 2018, pp. 1–26. URL: https://www.osti.gov/servlets/purl/1468312.

[Gro96] Lov K. Grover. “A fast quantum mechanical algorithm for database search”. In: *Proceedings 28th Annual ACM Symposium on the Theory of Computing* (1996), pp. 212–219. arXiv: 9605043 [quant-ph]. URL: http://arxiv.org/abs/quant-ph/9605043.

[GS17] Gian Giacomo Guerreschi and Mikhail Smelyanskiy. “Practical optimization for hybrid quantum-classical algorithms”. In: (2017), pp. 1–25. arXiv: 1701.01450. URL: http://arxiv.org/abs/1701.01450.

[GSR19] Artur Garcia-Saez and Jordi Riu. “Quantum Observables for continuous control of the Quantum Approximate Optimization Algorithm via Reinforcement Learning”. In: (2019). arXiv: 1911.09682. URL: http://arxiv.org/abs/1911.09682.

[Had18] Stuart Hadfield. “Quantum Algorithms for Scientific Computing and Approximate Optimization”. In: (2018). arXiv: 1805.03265. URL: http://arxiv.org/abs/1805.03265.

[Jor04] Stephen P Jordan. “Fast quantum algorithm for numerical gradient estimation”. In: 02139 (2004), pp. 1–4. DOI: 10.1103/PhysRevLett.95.050501. arXiv: 0405146 [quant-ph]. URL: http://arxiv.org/abs/quant-ph/0405146.

[Kha+19a] Sami Khairy et al. “Learning to Optimize Variational Quantum Circuits to Solve Combinatorial Problems”. In: (2019). arXiv: 1911.11071. URL: http://arxiv.org/abs/1911.11071.

[Kha+19b] Sami Khairy et al. “Reinforcement-Learning-Based Variational Quantum Circuits Optimization for Combinatorial Problems”. In: NeurIPS (2019), pp. 1–7. arXiv: 1911.04574. URL: http://arxiv.org/abs/1911.04574.

[Li+19] Li Li et al. “Quantum Optimization with a Novel Gibbs Objective Function and Ansatz Architecture Search”. In: 1 (2019), pp. 1–12. DOI: 10.1103/PhysRevResearch.2.023074. arXiv: 1909.07621. URL: http://arxiv.org/abs/1909.07621.

[LZ16] Cedric Yen-yu Lin and Yechao Zhu. “Performance of QAOA on Typical Instances of Constraint Satisfaction Problems with Bounded Degree”. In: January 2016 (2016). arXiv: 1601.01744. URL: http://arxiv.org/abs/1601.01744.

[McC+15] Jarrod R. McClean et al. “The theory of variational hybrid quantum-classical algorithms”. In: (2015), pp. 1–20. DOI: 10.1088/1367-2630/18/2/023023. arXiv: 1509.04279. URL: http://arxiv.org/abs/1509.04279.

[McC+18] Jarrod R. McClean et al. “Barren plateaus in quantum neural network training landscapes”. In: (2018), pp. 1–7. DOI: 10.1038/s41467-018-07090-4. arXiv: 1803.11173. URL: http://arxiv.org/abs/1803.11173.

[MCD20] Charles Moussa, Henri Calandra and Vedran Dunjko. “To quantum or not to quantum: towards algorithm selection in near-term quantum optimization”. In: (2020), pp. 1–11. arXiv: 2001.08271. URL: http://arxiv.org/abs/2001.08271.

[McK+19] Keri A. McKiernan et al. “Automated quantum programming via reinforcement learning for combinatorial optimization”. In: (2019). arXiv: 1908.08054. URL: http://arxiv.org/abs/1908.08054.

[NC10] Michael a. Nielsen and Isaac L. Chuang. *Quantum Computation and Quantum Information*. Cambridge: Cambridge University Press, 2010, p. 702. ISBN: 9780511976667. DOI: 10.1017/CBO9780511976667. arXiv: arXiv:1011.1669v3. URL: http://ebooks.cambridge.org/ref/id/CBO9780511976667.

[Oh+19] Young-Hyun Oh et al. “Solving Multi-Coloring Combinatorial Optimization Problems Using Hybrid Quantum Algorithms”. In: (2019). arXiv: 1911 . 00595. URL: http://arxiv.org/abs/1911.00595.

[Pag+19] G. Pagano et al. “Quantum Approximate Optimization of the Long-Range Ising Model with a Trapped-Ion Quantum Simulator”. In: 1.1 (2019), pp. 1–17. arXiv: 1906 . 02700. URL: http://arxiv.org/abs/1906.02700.

[Per+13] Alberto Peruzzo et al. “A variational eigenvalue solver on a quantum processor”. In: 1.2 (2013), pp. 1–10. DOI: 10.1038/ncomms5213. arXiv: 1304.3061. URL: http://arxiv.org/abs/1304.3061.

[Pre18] John Preskill. “Quantum Computing in the NISQ era and beyond”. In: *Quantum* 2.July (2018), p. 79. ISSN: 2521-327X. DOI: 10 . 22331 / q - 2018 - 08 - 06 - 79. arXiv: 1801 . 00862. URL: http://arxiv.org/abs/1801.00862.

[Reb+16] Patrick Rebentrost et al. “Quantum gradient descent and Newton’s method for constrained polynomial optimization”. In: (2016). arXiv: 1612 . 01789. URL: http://arxiv.org/abs/1612.01789.

[Sho94] P.W. Shor. “Algorithms for quantum computation: discrete logarithms and factoring”. In: *Proceedings 35th Annual Symposium on Foundations of Computer Science*. IEEE Comput. Soc. Press, 1994, pp. 124–134. ISBN: 0-8186-6580-7. DOI: 10.1109/SFCS.1994.365700. URL: http://ieeexplore.ieee.org/document/365700/.

[SN17] Jun John Sakurai and Jim Napolitano. *Modern Quantum Mechanics*. Cambridge University Press, 2017. ISBN: 9781108499996. DOI: 10 . 1017 / 9781108499996. URL: https://doi.org/10.1017/9781108499996.

[Swe+19] Ryan Sweke et al. “Stochastic gradient descent for hybrid quantum-classical optimization”. In: (2019), pp. 1–23. arXiv: 1910.01155. URL: http://arxiv.org/abs/1910.01155.

[Sze19] Mario Szegedy. “What do QAOA energies reveal about graphs?” In: (2019), pp. 1–31. arXiv: 1912.12277. URL: http://arxiv.org/abs/1912.12277.

[Tom+20] Teague Tomesh et al. “Coreset Clustering on Small Quantum Computers”. In: (2020), pp. 1–16. arXiv: 2004.14970. URL: http://arxiv.org/abs/2004.14970.

[UBP20] Utkarsh, Bikash K Behera and Prasanta K Panigrahi. “Solving Vehicle Routing Problem Using Quantum Approximate Optimization Algorithm”. In: (2020), pp. 1–7. arXiv: 2002.01351. URL: http://arxiv.org/abs/2002.01351.

[Ver+19] Guillaume Verdon et al. “Learning to learn with quantum neural networks via classical neural networks”. In: (2019), pp. 1–12. arXiv: 1907.05415. URL: http://arxiv.org/abs/1907.05415.

[Vik+19] Pontus Vikstål et al. “Applying the Quantum Approximate Optimization Algorithm to the Tail Assignment Problem”. In: (2019), pp. 1–9. arXiv: 1912 . 10499. URL: http://arxiv.org/abs/1912.10499.

[Wan+17] Zhihui Wang et al. “The Quantum Approximation Optimization Algorithm for MaxCut: A Fermionic View”. In: *Physical Review A* 97.2 (2017), pp. 1–13. ISSN: 24699934. DOI: 10.1103/PhysRevA.97.022304. arXiv: 1706.02998. URL: http://arxiv.org/abs/1706.02998.

[Wau+20] Matteo M Wauters et al. “Reinforcement Learning assisted Quantum Optimization”. In: (2020), pp. 1–5. arXiv: 2004.12323. URL: http://arxiv.org/abs/2004.12323.

[WG94] D P Williamson and Michael Goemans. “Improved Maximum Approximation Algorithms for Using Cut and Satisfiability Programming Problems Semidefinite”. In: *Science* 42.6 (1994), pp. 1115–1145.

[WGK20] David Wierichs, Christian Gogolin and Michael Kastoryano. “Avoiding local minima in variational quantum eigensolvers with the natural gradient optimizer”. In: (2020), pp. 1–16. arXiv: 2004.14666. URL: http://arxiv.org/abs/2004.14666.

[Wil+19] Madita Willsch et al. “Benchmarking the Quantum Approximate Optimization Algorithm”. In: 1 (2019), pp. 1–12. arXiv: 1907.02359.

[WMS20] Matteo M Wauters, Glen Bigan Mbeng and Giuseppe E Santoro. “Polynomial scaling of QAOA for ground-state preparation: taming first-order phase transitions”. In: (2020), pp. 1–10. arXiv: 2003.07419. URL: http://arxiv.org/abs/2003.07419.

[Zho+18] Leo Zhou et al. “Quantum Approximate Optimization Algorithm: Performance, Mechanism, and Implementation on Near-Term Devices”. In: (2018). arXiv: 1812.01041. URL: http://arxiv.org/abs/1812.01041.

Chapter 8

Appendix

8.1 Example Numerical Experiment Code

```
# Python Public Packages
import networkx as nx
import numpy as np
import math as m
import time
import csv
import random as rand

# My Quantum Numerical Experiment Python Code Files
import my_quantum_simulator_objects as qs
import my_quantum_simulator_helper_functions as qsf


# Loop through the number of vertices/qubits
for dimension in range(2,9):
    my_graph = nx.cycle_graph(dimension)
    graph_name = "Cycle"
    my_maxcut_graph = qs.QAOAGraph(weight_list='No_Weights', my_networkX_graph=my_graph, accelerate=True)
    my_initial_state = qs.PureQuantumState.all_plus_state(dimension)
    MaxCut_Hamiltonian = qs.MaxCutHamiltonian(my_maxcut_graph, use_negative=True)
    Transverse_Hamiltonian = qs.MixerHamiltonian.transverse_operator(dimension)
    beta_limits = [0, m.pi]
    gamma_limits = [0, 2*m.pi]
    myQAOA = qs.QAOA(Transverse_Hamiltonian, MaxCut_Hamiltonian, my_initial_state, my_maxcut_graph, beta_limits, gamma_limits)
    my_optimizer = qs.HybridOptimisation(myQAOA)


    # Search for the minimum expectation value
    minimum = 'min'
    depth = 10
    beta_divisions = 17
    gamma_divisions= 33


    # Run the QAOA optimizer/Strategy
    time_start = time.perf_counter()
    optimal_data, search_data = my_optimizer.run_greedy_newton_search_original(depth=depth, beta_divisions=beta_divisions,
gamma_divisions=gamma_divisions, search_for=minimum)
    time_elapsed = (time.perf_counter() - time_start)
    print(f"Time Taken for Greedy Newton Search of Graph {graph_name}_{dimension}:  {time_elapsed}")


    # Show data
    print(f"The object type of optimal_data is {optimal_data.name}")
    optimal_data.show()
    print(f"The object type of search_data is {search_data.name}")
    search_data.show()


    # Save results
    filename = "Newton_" + graph_name + "_" + str(dimension)
    filename_2 = graph_name + "_" + str(dimension)
    optimal_data.save(filename)
    search_data.save(filename_2)
```

Figure 8.1.1: The numerical experiment code to obtain raw data for Cycle graphs, up to 8 vertices, using Greedy Newton hybrid strategy.

8.2 Probability Distribution of Binary Cut Strings

8.2.1 1 Regular

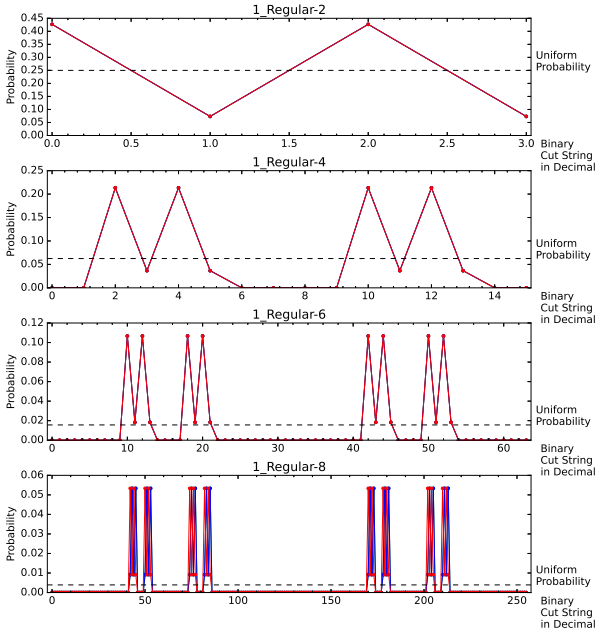

Figure 8.2.1: Probability Distribution of the binary cut strings in decimal for 1 Regular Graphs. Note that the probability the calculated by modulus squaring of the amplitudes. Also, note that the Greedy Standard (in green) and Greedy Subsearch (in blue) distributions are almost completely covered by Greedy Newton (in red). The leading binary zeros in the cut string are removed before converting them into decimal.

8.2.2 Path

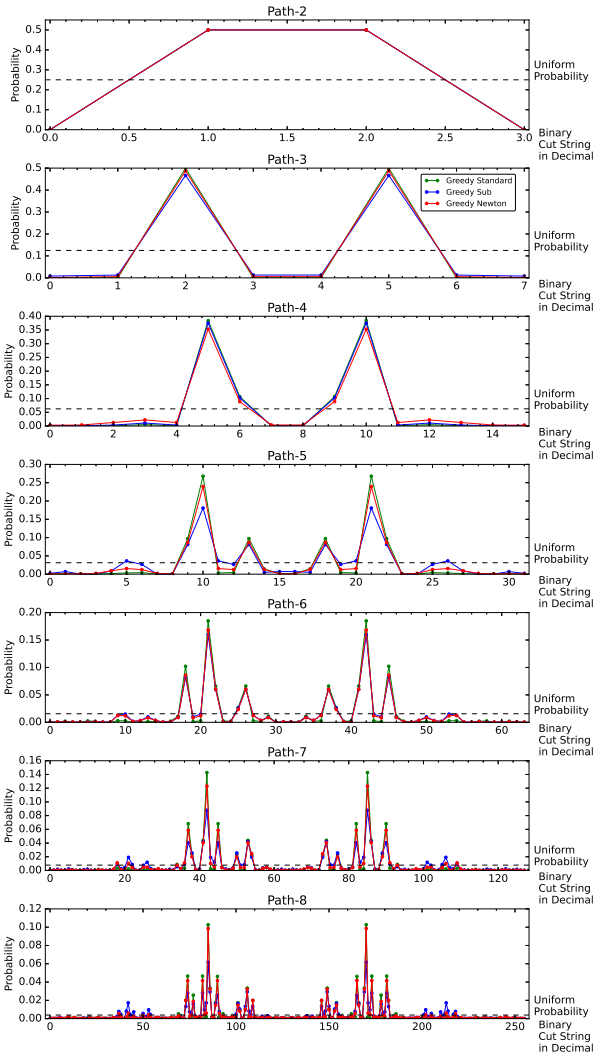

Figure 8.2.2: Probability Distribution of the binary cut strings in decimal for Path Graphs. Note that the probability the calculated by modulus squaring of the amplitudes. Also, note that in some plots, the Greedy Standard (in green) and Greedy Subsearch (in blue) distributions are almost completely covered by Greedy Newton (in red). The leading binary zeros in the cut string are removed before converting them into decimal.

8.2.3 Cycle

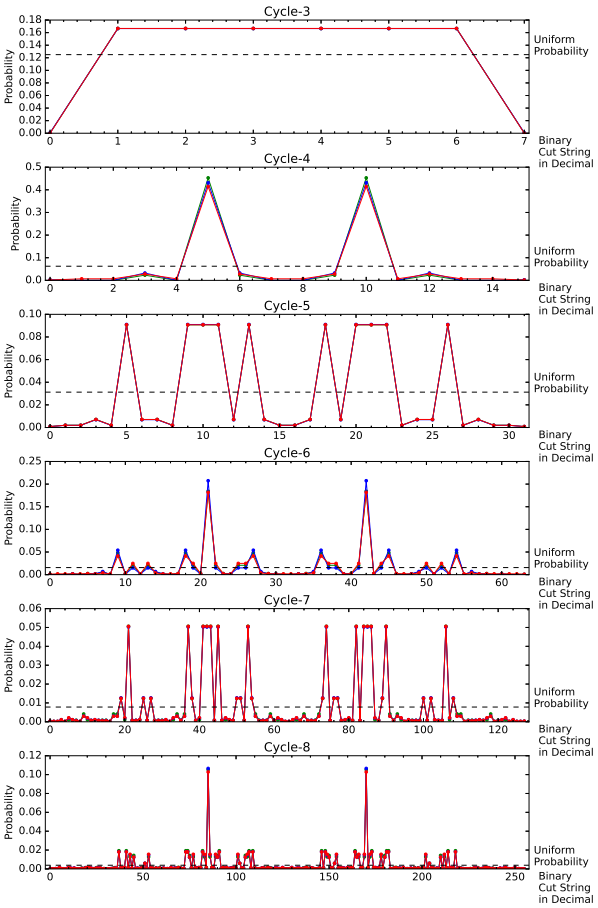

Figure 8.2.3: Probability Distribution of the binary cut strings in decimal for Cycle Graphs. Note that the probability the calculated by modulus squaring of the amplitudes. Also, note that in some plots, the Greedy Standard (in green) and Greedy Subsearch (in blue) distributions are almost completely covered by Greedy Newton (in red). The leading binary zeros in the cut string are removed before converting them into decimal.

8.2.4 Complete

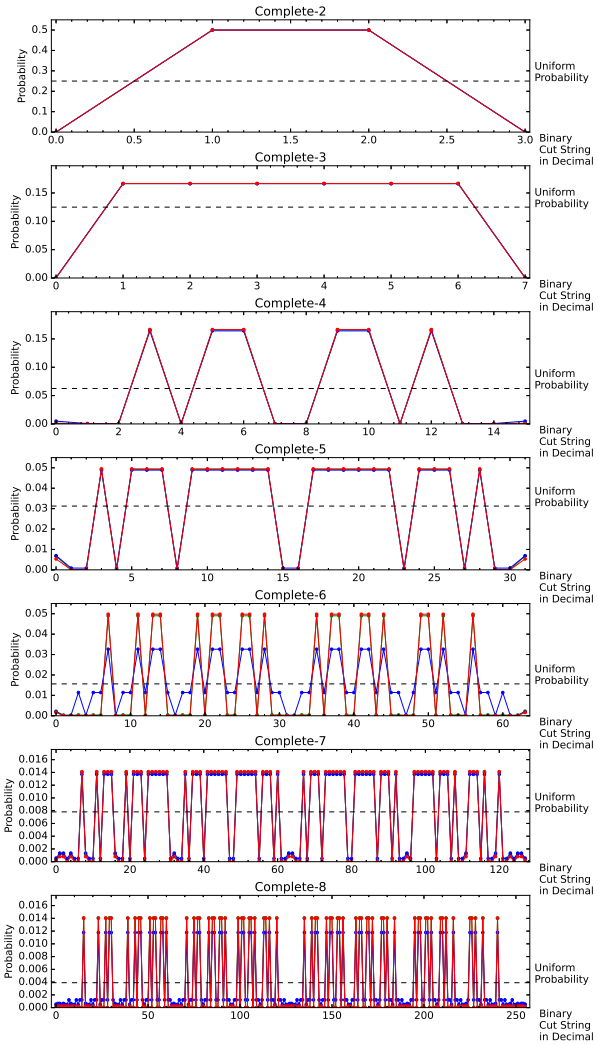

Figure 8.2.4: Probability Distribution of the binary cut strings in decimal for Complete Graphs. Note that the probability the calculated by modulus squaring of the amplitudes. Also, note that in some plots, the Greedy Standard (in green) and Greedy Subsearch (in blue) distributions are almost completely covered by Greedy Newton (in red). The leading binary zeros in the cut string are removed before converting them into decimal.

8.2.5 3 Regular

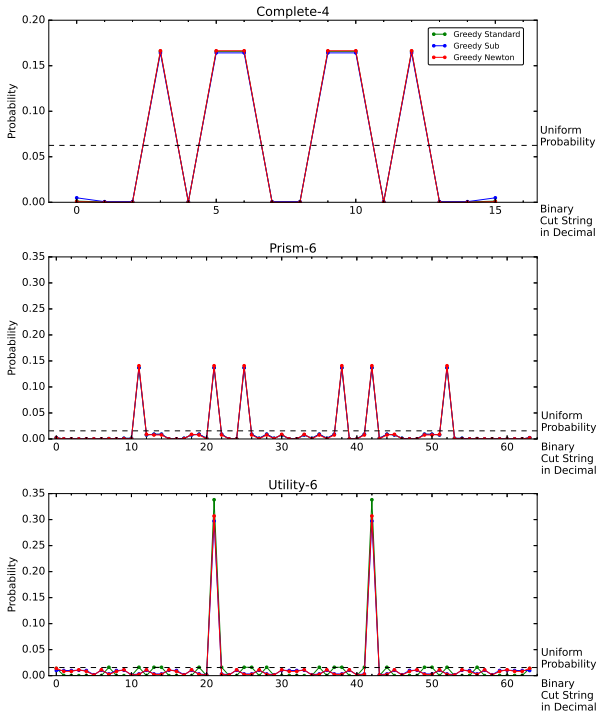

Figure 8.2.5: Plot 1 of 2. See below for the next plot.

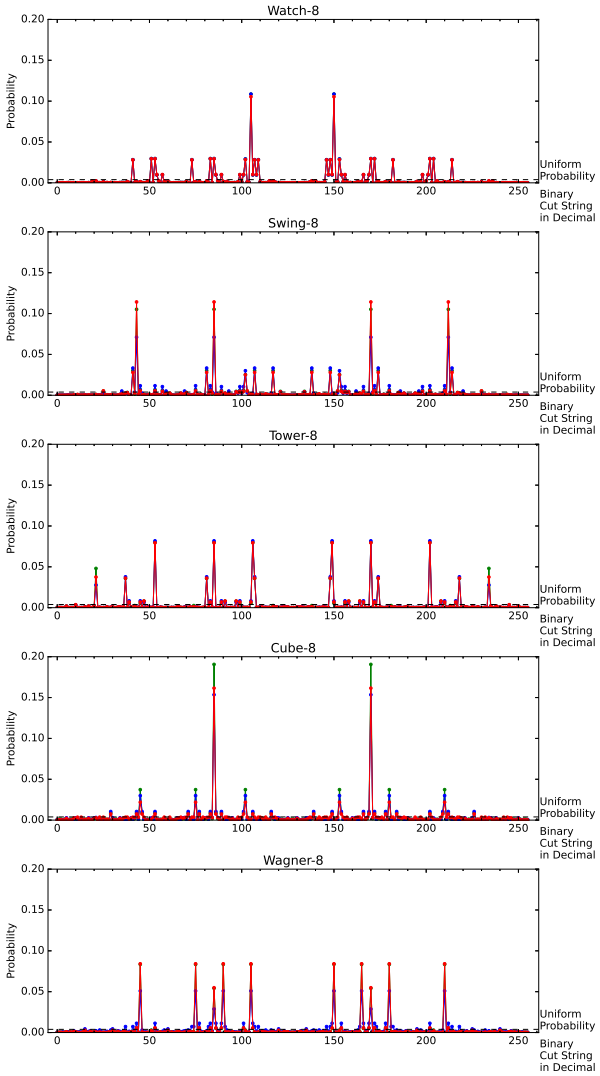

Figure 8.2.6: Plot 2 of 2. Probability distribution of the binary cut strings in decimal for 3 Regular Graphs. Note that the probability the calculated by modulus squaring of the amplitudes. Also, note that in some plots, the Greedy Standard (in green) and Greedy Subsearch (in blue) distributions are almost completely covered by Greedy Newton (in red). The leading binary zeros in the cut string are removed before converting them into decimal.

8.3 Simple Example: Pauli Decomposition of a Triangle

Let us consider a simple example to demonstrate the new way of calculation of the expectation $\langle\phi|\hat{C}|\phi\rangle$ at some QAOA depth p. Suppose the graph of interest is a simple unweighted triangle with three vertices $V = \{0,1,2\}$ and three edges $E = \{(0,1),(1,2),(2,0)\}$. We will calculate the expectation $\langle\phi|\hat{C}|\phi\rangle$ using Pauli Decomposition. Let us organise the calculation step by step, as given in the box on page 37. Starting with the first equation 5.2.60, the summation terms explicitly given in the table 8.3.1.

Edge	Summation Terms of $\langle\phi\|\hat{C}\|\phi\rangle$
$(0,1)$	$\frac{1}{2}\left(\cos^2 2\beta\,\langle\psi'\|\hat{Z}_0\hat{Z}_1\|\psi'\rangle + \frac{1}{2}\sin 4\beta\,\langle\psi'\|\hat{Y}_0\hat{Z}_1+\hat{Z}_0\hat{Y}_1\|\psi'\rangle + \sin^2 2\beta\,\langle\psi'\|\hat{Y}_0\hat{Y}_1\|\psi'\rangle - 1\right)$
$(1,2)$	$\frac{1}{2}\left(\cos^2 2\beta\,\langle\psi'\|\hat{Z}_1\hat{Z}_2\|\psi'\rangle + \frac{1}{2}\sin 4\beta\,\langle\psi'\|\hat{Y}_1\hat{Z}_2+\hat{Z}_1\hat{Y}_2\|\psi'\rangle + \sin^2 2\beta\,\langle\psi'\|\hat{Y}_1\hat{Y}_2\|\psi'\rangle - 1\right)$
$(2,0)$	$\frac{1}{2}\left(\cos^2 2\beta\,\langle\psi'\|\hat{Z}_2\hat{Z}_0\|\psi'\rangle + \frac{1}{2}\sin 4\beta\,\langle\psi'\|\hat{Y}_2\hat{Z}_0+\hat{Z}_2\hat{Y}_0\|\psi'\rangle + \sin^2 2\beta\,\langle\psi'\|\hat{Y}_2\hat{Y}_0\|\psi'\rangle - 1\right)$

Table 8.3.1: Summation terms, indexed by edges, of equation 5.2.60.

From the summation terms, we may expand it in terms of the QAOA output state $|\phi_{p-1}\rangle$ of depth $p-1$, using equations 5.2.61 to 5.2.64. Note that for every edge in the triangle, $\ell_{ij} = \xi_{ij} = 1$. The summation terms of the expanded expressions of the various expectation $\langle\psi'|\_|\psi'\rangle$ in terms of $|\phi_{p-1}\rangle$ and are organised in the table 8.3.2.

Expectations	Summation Terms of the Expanded Expressions
$\langle\psi'\vert\hat{Z}_0\hat{Z}_1\vert\psi'\rangle$	$\langle\phi_{p-1}\vert\hat{Z}_1\hat{Z}_2\vert\phi_{p-1}\rangle$
$\langle\psi'\vert\hat{Y}_0\hat{Z}_1\vert\psi'\rangle$	$\cos\gamma\left(\cos\gamma\langle\phi_{p-1}\vert\hat{Y}_0\hat{Z}_1\vert\phi_{p-1}\rangle+\sin\gamma\langle\phi_{p-1}\vert\hat{X}_0\vert\phi_{p-1}\rangle\right)$
	$-i\sin\gamma\left(\cos\gamma\langle\phi_{p-1}\vert\hat{Y}_0\hat{Z}_1\hat{Z}_0\hat{Z}_2\vert\phi_{p-1}\rangle+\sin\gamma\langle\phi_{p-1}\vert\hat{X}_0\hat{Z}_0\hat{Z}_2\vert\phi_{p-1}\rangle\right)$
$\langle\psi'\vert\hat{Z}_0\hat{Y}_1\vert\psi'\rangle$	$\cos\gamma\left(\cos\gamma\langle\phi_{p-1}\vert\hat{Z}_0\hat{Y}_1\vert\phi_{p-1}\rangle+\sin\gamma\langle\phi_{p-1}\vert\hat{X}_1\vert\phi_{p-1}\rangle\right)$
	$-i\sin\gamma\left(\cos\gamma\langle\phi_{p-1}\vert\hat{Z}_0\hat{Y}_1\hat{Z}_1\hat{Z}_2\vert\phi_{p-1}\rangle+\sin\gamma\langle\phi_{p-1}\vert\hat{X}_1\hat{Z}_1\hat{Z}_2\vert\phi_{p-1}\rangle\right)$
$\langle\psi'\vert\hat{Y}_0\hat{Y}_1\vert\psi'\rangle$	$\cos^2\gamma\langle\phi_{p-1}\vert\hat{Y}_0\hat{Y}_1\vert\phi_{p-1}\rangle$
	$-i\cos\gamma\sin\gamma\langle\phi_{p-1}\vert\hat{Y}_0\hat{Y}_1\hat{Z}_0\hat{Z}_2\vert\phi_{p-1}\rangle$
	$-i\cos\gamma\sin\gamma\langle\phi_{p-1}\vert\hat{Y}_0\hat{Y}_1\hat{Z}_1\hat{Z}_2\vert\phi_{p-1}\rangle$
	$-\sin^2\gamma\langle\phi_{p-1}\vert\hat{Y}_0\hat{Y}_1\hat{Z}_0\hat{Z}_1\vert\phi_{p-1}\rangle$
$\langle\psi'\vert\hat{Z}_1\hat{Z}_2\vert\psi'\rangle$	$\langle\phi_{p-1}\vert\hat{Z}_1\hat{Z}_2\vert\phi_{p-1}\rangle$
$\langle\psi'\vert\hat{Y}_1\hat{Z}_2\vert\psi'\rangle$	$\cos\gamma\left(\cos\gamma\langle\phi_{p-1}\vert\hat{Y}_1\hat{Z}_2\vert\phi_{p-1}\rangle+\sin\gamma\langle\phi_{p-1}\vert\hat{X}_1\vert\phi_{p-1}\rangle\right)$
	$-i\sin\gamma\left(\cos\gamma\langle\phi_{p-1}\vert\hat{Y}_1\hat{Z}_2\hat{Z}_1\hat{Z}_0\vert\phi_{p-1}\rangle+\sin\gamma\langle\phi_{p-1}\vert\hat{X}_1\hat{Z}_1\hat{Z}_0\vert\phi_{p-1}\rangle\right)$
$\langle\psi'\vert\hat{Z}_1\hat{Y}_2\vert\psi'\rangle$	$\cos\gamma\left(\cos\gamma\langle\phi_{p-1}\vert\hat{Z}_1\hat{Y}_2\vert\phi_{p-1}\rangle+\sin\gamma\langle\phi_{p-1}\vert\hat{X}_2\vert\phi_{p-1}\rangle\right)$
	$-i\sin\gamma\left(\cos\gamma\langle\phi_{p-1}\vert\hat{Z}_1\hat{Y}_2\hat{Z}_2\hat{Z}_0\vert\phi_{p-1}\rangle+\sin\gamma\langle\phi_{p-1}\vert\hat{X}_2\hat{Z}_2\hat{Z}_0\vert\phi_{p-1}\rangle\right)$
$\langle\psi'\vert\hat{Y}_1\hat{Y}_2\vert\psi'\rangle$	$\cos^2\gamma\langle\phi_{p-1}\vert\hat{Y}_1\hat{Y}_2\vert\phi_{p-1}\rangle$
	$-i\cos\gamma\sin\gamma\langle\phi_{p-1}\vert\hat{Y}_1\hat{Y}_2\hat{Z}_1\hat{Z}_0\vert\phi_{p-1}\rangle$
	$-i\cos\gamma\sin\gamma\langle\phi_{p-1}\vert\hat{Y}_1\hat{Y}_2\hat{Z}_2\hat{Z}_0\vert\phi_{p-1}\rangle$
	$-\sin^2\gamma\langle\phi_{p-1}\vert\hat{Y}_1\hat{Y}_2\hat{Z}_1\hat{Z}_2\vert\phi_{p-1}\rangle$
$\langle\psi'\vert\hat{Z}_2\hat{Z}_0\vert\psi'\rangle$	$\langle\phi_{p-1}\vert\hat{Z}_2\hat{Z}_0\vert\phi_{p-1}\rangle$
$\langle\psi'\vert\hat{Y}_2\hat{Z}_0\vert\psi'\rangle$	$\cos\gamma\left(\cos\gamma\langle\phi_{p-1}\vert\hat{Y}_2\hat{Z}_0\vert\phi_{p-1}\rangle+\sin\gamma\langle\phi_{p-1}\vert\hat{X}_2\vert\phi_{p-1}\rangle\right)$
	$-i\sin\gamma\left(\cos\gamma\langle\phi_{p-1}\vert\hat{Y}_2\hat{Z}_0\hat{Z}_2\hat{Z}_1\vert\phi_{p-1}\rangle+\sin\gamma\langle\phi_{p-1}\vert\hat{X}_2\hat{Z}_2\hat{Z}_1\vert\phi_{p-1}\rangle\right)$
$\langle\psi'\vert\hat{Z}_2\hat{Y}_0\vert\psi'\rangle$	$\cos\gamma\left(\cos\gamma\langle\phi_{p-1}\vert\hat{Z}_2\hat{Y}_0\vert\phi_{p-1}\rangle+\sin\gamma\langle\phi_{p-1}\vert\hat{X}_0\vert\phi_{p-1}\rangle\right)$
	$-i\sin\gamma\left(\cos\gamma\langle\phi_{p-1}\vert\hat{Z}_2\hat{Y}_0\hat{Z}_0\hat{Z}_1\vert\phi_{p-1}\rangle+\sin\gamma\langle\phi_{p-1}\vert\hat{X}_0\hat{Z}_0\hat{Z}_1\vert\phi_{p-1}\rangle\right)$
$\langle\psi'\vert\hat{Y}_2\hat{Y}_0\vert\psi'\rangle$	$\cos^2\gamma\langle\phi_{p-1}\vert\hat{Y}_2\hat{Y}_0\vert\phi_{p-1}\rangle$
	$-i\cos\gamma\sin\gamma\langle\phi_{p-1}\vert\hat{Y}_2\hat{Y}_0\hat{Z}_2\hat{Z}_1\vert\phi_{p-1}\rangle$
	$-i\cos\gamma\sin\gamma\langle\phi_{p-1}\vert\hat{Y}_2\hat{Y}_0\hat{Z}_0\hat{Z}_1\vert\phi_{p-1}\rangle$
	$-\sin^2\gamma\langle\phi_{p-1}\vert\hat{Y}_2\hat{Y}_0\hat{Z}_2\hat{Z}_0\vert\phi_{p-1}\rangle$

Table 8.3.2: Summation terms of the expanded expression of the various expectations $\langle\psi'\vert\_\vert\psi'\rangle$ in terms of QAOA Output state $\vert\phi_{p-1}\rangle$ of depth $p-1$.

You may count the total number of various expectation of the Pauli Compositions, which sums to 39. By substituting the terms in table 8.3.2 into the main table 8.3.1, we will obtain the full explict expansion of $\langle\phi\vert\hat{C}\vert\phi\rangle$ in terms of the local QAOA parameter β, γ of depth p and QAOA output state $\vert\phi_{p-1}\rangle$ of depth $p-1$. We may differentiate expansion of $\langle\phi\vert\hat{C}\vert\phi\rangle$ with respect to local QAOA parameter β, γ to get the gradient and Hessian respectively.

8.4 All Plus State Simplifications on Unweighted Graph Case

At times, we may be interested in the first QAOA depth $P = 1$. We may want to find out its reduced expression of the expectation $\langle\phi|\hat{C}|\phi\rangle$, when the initial QAOA state $|\psi\rangle$ is given as the all plus state where each qubit is initialised as $|+\rangle = \frac{1}{\sqrt{2}}(|0\rangle + |1\rangle)$. The result of substituting $|\psi\rangle = |+\rangle^{\otimes n}$ into $\langle\phi|\hat{C}|\phi\rangle$ for depth $p = 1$ leads to an amazing all plus simplification of $\langle\phi|\hat{C}|\phi\rangle$ that can be easily calculated. Before doing so, it is worthwhile to review the properties of expectation of Pauli operators,

$$\langle+|\hat{X}_j|+\rangle = 1, \quad \langle+|f_1\left(\sigma_j^{a/1}\right)\hat{X}_i f_2\left(\sigma_j^{a/1}\right)|+\rangle = 0, \quad \langle+|f\left(\sigma_j^{a/1}\right)|+\rangle = 0 \tag{8.4.1}$$

where $f\left(\sigma_j^{a/1}\right)$ refers to any composite Pauli operators, excluding $\sigma_j^1 = \hat{X}_j$. In order words, the expectation of the Pauli composition will be a contributing term if the Pauli composition consist solely of $\hat{X}$, otherwise, it will be a zero term. Then, by the substitution of $|\psi\rangle = |+\rangle^{\otimes n} = |\phi_0\rangle$ into set of expectations of Pauli compositions in figure 5.2.8, we have the calculated results given in figure 8.4.1 below.

$$\langle+|\hat{Z}_i\hat{Z}_j|+\rangle = 0 \tag{8.4.2}$$

$$\sum_{\lambda\in\Lambda_k^{\ell_{ij}}}\langle+|\hat{Y}_i\hat{Z}_j\left(\hat{Z}_i\right)^k\left(I\prod_{a\in\lambda}\hat{Z}_{l_a}\right)|+\rangle = 0 \quad \forall k\geq 0 \tag{8.4.3}$$

$$\sum_{\lambda\in\Lambda_k^{\ell_{ij}}}\langle+|\hat{X}_i\left(\hat{Z}_i\right)^k\left(I\prod_{a\in\lambda}\hat{Z}_{l_a}\right)|+\rangle = \begin{cases}0 & \forall k>0\\ 1 & k=0\end{cases} \tag{8.4.4}$$

$$\sum_{\lambda\in\Lambda_k^{\xi_{ij}}}\langle+|\hat{Z}_i\hat{Y}_j\left(\hat{Z}_j\right)^k\left(I\prod_{b\in\lambda}\hat{Z}_{r_b}\right)|+\rangle = 0 \quad \forall k\geq 0 \tag{8.4.5}$$

$$\sum_{\lambda\in\Lambda_k^{\xi_{ij}}}\langle+|\hat{X}_j\left(\hat{Z}_j\right)^k\left(I\prod_{b\in\lambda}\hat{Z}_{r_b}\right)|+\rangle = \begin{cases}0 & \forall k>0\\ 1 & k=0\end{cases} \tag{8.4.6}$$

Figure 8.4.1: Calculated results of the expectations of Pauli compositions at QAOA depth $p = 1$ using the all plus state $|+\rangle^{\otimes n}$ as the initial state.

Note that we have avoid calculating

$$\sum_{\lambda_1\in\Lambda_m^{\ell_{ij}}}\sum_{\lambda_2\in\Lambda_n^{\xi_{ij}}}\langle+|\hat{Y}_i\hat{Y}_j\left(\hat{Z}_i\right)^m\left(\hat{Z}_j\right)^n\left(I\prod_{a\in\lambda_1}\hat{Z}_{l_a}\right)\left(\prod_{b\in\lambda_2}\hat{Z}_{r_b}\right)|+\rangle \tag{8.4.7}$$

as it is slightly more complicated. Here, note that the contributing Pauli composition is a double $\hat{X}_j\hat{X}_i$. It is necessary that $m = n =$ odd such that the Pauli composition consists a double $\hat{X}_j\hat{X}_i$, so that,

$$-\sum_{\lambda_1\in\Lambda_m^{\ell_{ij}}}\sum_{\lambda_2\in\Lambda_n^{\xi_{ij}}}\langle+|\hat{X}_j\hat{X}_i\left(I\prod_{a\in\lambda_1}\hat{Z}_{l_a}\right)\left(\prod_{b\in\lambda_2}\hat{Z}_{r_b}\right)|+\rangle, \quad m=n=\text{odd} \tag{8.4.8}$$

However, it is insufficient for simplification as the term $\left(I\prod_{a\in\lambda_1}\hat{Z}_{l_a}\right)\left(\prod_{b\in\lambda_2}\hat{Z}_{r_b}\right)$ may or may not be an identity I. $\prod_{a\in\lambda_1}\hat{Z}_{l_a}\prod_{b_2\in\lambda_2}\hat{Z}_{r_b} = I$ whenever the sets $\lambda_1\equiv\lambda_2$ are equivalent. Under this set

equivalent condition, each of both sets has $\begin{pmatrix} T_{ij} \\ m \end{pmatrix}$ number of indexes that corresponds to the label of the common vertex, such that the common vertex forms a triangle with a common edge (i, j). Note that we use T_{ij} to denote the number of triangles with a common edge (i, j). Thus, $\sum_{\lambda_1 \in \Lambda_m^{\ell_{ij}}} \sum_{\lambda_2 \in \Lambda_m^{\xi_{ij}}} \left(I \prod_{a \in \lambda_1} \hat{Z}_{l_a}\right) \left(\prod_{b \in \lambda_2} \hat{Z}_{r_b}\right)$ will contain $\begin{pmatrix} T_{ij} \\ m \end{pmatrix}$ number of such identities. Therefore,

$$\sum_{\lambda_1 \in \Lambda_m^{\ell_{ij}}} \sum_{\lambda_2 \in \Lambda_n^{\xi_{ij}}} \langle + | \hat{Y}_i \hat{Y}_j \left(\hat{Z}_i\right)^m \left(\hat{Z}_j\right)^n \left(I \prod_{a \in \lambda_1} \hat{Z}_{l_a}\right) \left(\prod_{b \in \lambda_2} \hat{Z}_{r_b}\right) | + \rangle = \begin{cases} -\begin{pmatrix} T_{ij} \\ m \end{pmatrix} & m = n = \text{odd} \\ 0 & \text{Otherwise} \end{cases} \tag{8.4.9}$$

We now have all the calculated results of the expectation of the various Pauli composition and we may substitute them into summation terms of $\langle \phi | \hat{C} | \phi \rangle$ using equations 5.2.61 to 5.2.64. To simplify the calculations after substitution, we may split up ℓ_{ij} and ξ_{ij} the number of left and right edges into edges that does and does not form a triangle with edge (i, j). Let L_{ij} and R_{ij} be the number of left and right edges that does not form a triangle with edge (i, j). Then, we rewrite,

$$\ell_{ij} = L_{ij} + T_{ij} \tag{8.4.10}$$

$$\xi_{ij} = R_{ij} + T_{ij} \tag{8.4.11}$$

As a result, we have our all plus simplification of the QAOA depth $P = 1$ expectation value of the unweighted MaxCut Hamiltonian $\langle \phi | \hat{C} | \phi \rangle$ as given in the box below. The explicit derivation of $\langle \psi' | \hat{Y}_i \hat{Y}_j | \psi' \rangle$ in equation 8.4.16 is given in figure 8.4.3 below. The calculation of the gradient and Hessian of $\langle \phi | \hat{C} | \phi \rangle$ are pretty straightforward, therefore, explicit derivation will not be given, the results are given in the following boxes below. The simplified expression of $\langle \phi | \hat{C} | \phi \rangle$ was first found analytically by Wang et al [Wan+17], followed by Sevag et al [GPRA18], Stuart Hadfield [Had18] independently. It was later noted that Wang et al's results was corrected by Mario Szegedy [Sze19]. A graphical representation of a subgraph of edge (i, j) is given in figure 8.4.2. At higher depths, however, analytical calculations of the expectation may quickly become intractable and cumbersome, even for a single edge graph with the all plus simplification, as noted by Wang et al who managed to obtain an analytical expression for QAOA depth $P = 2$ $\left\langle \hat{C} \right\rangle$ for non-weighted cycle graphs [Wan+17].

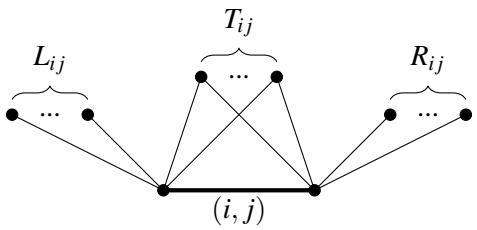

Figure 8.4.2: A subgraph of unweighted edge (i, j) that is connected to L_{ij}, R_{ij} and T_{ij} number of vertices on the left, right and both of the vertices of the edge (i, j) respectively.

All Plus Simplification of the QAOA Expectation Value of Unweighted MaxCut Hamiltonian

$$\langle\phi|\hat{C}|\phi\rangle = \sum_{(i,j)\in\text{edges}} \frac{1}{2}\left(\frac{1}{2}\sin 4\beta\,\langle\psi'|\hat{Y}_i\hat{Z}_j+\hat{Z}_i\hat{Y}_j|\psi'\rangle+\sin^2 2\beta\,\langle\psi'|\hat{Y}_i\hat{Y}_j|\psi'\rangle-1\right) \tag{8.4.12}$$

where,

$$\langle\psi'|\hat{Z}_i\hat{Z}_j|\psi'\rangle = 0 \tag{8.4.13}$$
$$\langle\psi'|\hat{Y}_i\hat{Z}_j|\psi'\rangle = \sin\gamma(\cos\gamma)^{L_{ij}+T_{ij}} \tag{8.4.14}$$
$$\langle\psi'|\hat{Z}_i\hat{Y}_j|\psi'\rangle = \sin\gamma(\cos\gamma)^{R_{ij}+T_{ij}} \tag{8.4.15}$$
$$\langle\psi'|\hat{Y}_i\hat{Y}_j|\psi'\rangle = \frac{1}{2}(\cos\gamma)^{L_{ij}+R_{ij}}\left(1-\cos^{T_{ij}}2\gamma\right) \tag{8.4.16}$$

$$\langle\psi'|\hat{Y}_i\hat{Y}_j|\psi'\rangle \tag{8.4.17}$$
$$= \sum_{n=0}^{\xi_{ij}}\sum_{m=0}^{\ell_{ij}}(\cos\gamma I)^{\ell_{ij}+\xi_{ij}-m-n}(-i\sin\gamma)^{m+n}\langle+|y_iy_jz_i^kz_j^k|+\rangle \tag{8.4.18}$$
$$= -\begin{pmatrix}T_{ij}\\1\end{pmatrix}(\cos\gamma I)^{\ell_{ij}+\xi_{ij}-2}(-i\sin\gamma)^2-\begin{pmatrix}T_{ij}\\3\end{pmatrix}(\cos\gamma I)^{\ell_{ij}+\xi_{ij}-6}(-i\sin\gamma)^6-\ldots \tag{8.4.19}$$
$$= \begin{pmatrix}T_{ij}\\1\end{pmatrix}(\cos\gamma)^{L_{ij}+R_{ij}+2T_{ij}-2}(\sin\gamma)^2+\begin{pmatrix}T_{ij}\\3\end{pmatrix}(\cos\gamma)^{L_{ij}+R_{ij}+2T_{ij}-6}(\sin\gamma)^6+\ldots \tag{8.4.20}$$
$$= (\cos\gamma)^{L_{ij}+R_{ij}}\sum_{k=odd}\begin{pmatrix}T_{ij}\\k\end{pmatrix}\left(\cos^2\gamma\right)^{T_{ij}-k}\left(\sin^2\gamma\right)^k \tag{8.4.21}$$
| Using sum of odd terms of a binomial expansion theorem
$$= (\cos\gamma)^{L_{ij}+R_{ij}}\frac{1}{2}\left[\left(\cos^2\gamma+\sin^2\gamma\right)^{T_{ij}}-\left(\cos^2\gamma-\sin^2\gamma\right)^{T_{ij}}\right] \tag{8.4.22}$$
$$= \frac{1}{2}(\cos\gamma)^{L_{ij}+R_{ij}}\left(1-\cos^{T_{ij}}2\gamma\right) \tag{8.4.23}$$

Figure 8.4.3: The explicit derivation of the result of $\langle+|e^{i\gamma\hat{C}}\hat{Y}_i\hat{Y}_je^{-i\gamma\hat{C}}|+\rangle$.

All Plus Simplification of the Gradient of the Expectation Value (Unweighted)

$$\nabla\langle\phi|\hat{C}|\phi\rangle = \sum_{(i,j)\in\mathrm{E}}\frac{1}{2}\begin{pmatrix}\frac{\partial}{\partial\beta}\\\frac{\partial}{\partial\gamma}\end{pmatrix}\langle\phi|\hat{Z}_i\hat{Z}_j|\phi\rangle \tag{8.4.24}$$

where,

$$\frac{\partial}{\partial\beta}\langle\phi|\hat{Z}_i\hat{Z}_j|\phi\rangle = 2\cos 4\beta\,\langle\psi'|\hat{Y}_i\hat{Z}_j+\hat{Z}_i\hat{Y}_j|\psi'\rangle+2\sin 4\beta\,\langle\psi'|\hat{Y}_i\hat{Y}_j|\psi'\rangle \tag{8.4.25}$$
$$\frac{\partial}{\partial\gamma}\langle\phi|\hat{Z}_i\hat{Z}_j|\phi\rangle = \frac{1}{2}\sin 4\beta\frac{\partial}{\partial\gamma}\langle\psi'|\hat{Y}_i\hat{Z}_j+\hat{Z}_i\hat{Y}_j|\psi'\rangle+\sin^2 2\beta\frac{\partial}{\partial\gamma}\langle\psi'|\hat{Y}_i\hat{Y}_j|\psi'\rangle \tag{8.4.26}$$

and,

$$\frac{\partial}{\partial\gamma}\langle\psi'|\hat{Y}_i\hat{Z}_j|\psi'\rangle = \sin\gamma(\cos\gamma)^{L_{ij}+T_{ij}}\left[\cot\gamma-\left(L_{ij}+T_{ij}\right)\tan\gamma\right] \tag{8.4.27}$$
$$\frac{\partial}{\partial\gamma}\langle\psi'|\hat{Z}_i\hat{Y}_j|\psi'\rangle = \sin\gamma(\cos\gamma)^{R_{ij}+T_{ij}}\left[\cot\gamma-\left(R_{ij}+T_{ij}\right)\tan\gamma\right] \tag{8.4.28}$$
$$\frac{\partial}{\partial\gamma}\langle\psi'|\hat{Y}_i\hat{Y}_j|\psi'\rangle = -\frac{1}{2}\cos^{L_{ij}+R_{ij}}\gamma\left[2T_{ij}\cos^{T_{ij}}2\gamma\tan 2\gamma-\left(L_{ij}+R_{ij}\right)\left(1-\cos^{T_{ij}}2\gamma\right)\tan\gamma\right] \tag{8.4.29}$$

All Plus Simplification of the Hessian of the Expectation Value (Unweighted)

$$\nabla^2 \langle \phi | \hat{C} | \phi \rangle = \sum_{(i,j) \in \mathrm{E}} \frac{1}{2} \begin{pmatrix} \frac{\partial^2}{\partial \beta^2} & \frac{\partial^2}{\partial \gamma \partial \beta} \\ \frac{\partial^2}{\partial \beta \partial \gamma} & \frac{\partial^2}{\partial \gamma^2} \end{pmatrix} \langle \phi | \hat{Z}_i \hat{Z}_j | \phi \rangle \tag{8.4.30}$$

where,

$$\frac{\partial^2}{\partial \beta^2} \langle \phi | \hat{Z}_i \hat{Z}_j | \phi \rangle = -8 \sin 4\beta \langle \psi' | \hat{Y}_i \hat{Z}_j + \hat{Z}_i \hat{Y}_j | \psi' \rangle + 8 \cos 4\beta \langle \psi' | \hat{Y}_i \hat{Y}_j | \psi' \rangle \tag{8.4.31}$$

$$\frac{\partial^2}{\partial \gamma^2} \langle \phi | \hat{Z}_i \hat{Z}_j | \phi \rangle = \frac{1}{2} \sin 4\beta \frac{\partial^2}{\partial \gamma^2} \langle \psi' | \hat{Y}_i \hat{Z}_j + \hat{Z}_i \hat{Y}_j | \psi' \rangle + \sin^2 2\beta \frac{\partial^2}{\partial \gamma^2} \langle \psi' | \hat{Y}_i \hat{Y}_j | \psi' \rangle \tag{8.4.32}$$

$$\frac{\partial^2}{\partial \beta \partial \gamma} \langle \phi | \hat{Z}_i \hat{Z}_j | \phi \rangle = 2 \cos 4\beta \frac{\partial}{\partial \gamma} \langle \psi' | \hat{Y}_i \hat{Z}_j + \hat{Z}_i \hat{Y}_j | \psi' \rangle + 2 \sin 4\beta \frac{\partial}{\partial \gamma} \langle \psi' | \hat{Y}_i \hat{Y}_j | \psi' \rangle \tag{8.4.33}$$

$$= \frac{\partial^2}{\partial \gamma \partial \beta} \langle \phi | \hat{Z}_i \hat{Z}_j | \phi \rangle \tag{8.4.34}$$

and,

$$\frac{\partial^2}{\partial \gamma^2} \langle \psi' | \hat{Y}_i \hat{Z}_j | \psi' \rangle =$$
$$\sin \gamma (\cos \gamma)^{L_{ij}+T_{ij}} \left\{ \left[\cot \gamma - \left(L_{ij} + T_{ij} \right) \tan \gamma \right]^2 + \left[-\csc^2 \gamma - \left(L_{ij} + T_{ij} \right) \sec^2 \gamma \right] \right\} \tag{8.4.35}$$

$$\frac{\partial^2}{\partial \gamma^2} \langle \psi' | \hat{Z}_i \hat{Y}_j | \psi' \rangle =$$
$$\sin \gamma (\cos \gamma)^{R_{ij}+T_{ij}} \left\{ \left[\cot \gamma - \left(R_{ij} + T_{ij} \right) \tan \gamma \right]^2 + \left[-\csc^2 \gamma - \left(R_{ij} + T_{ij} \right) \sec^2 \gamma \right] \right\} \tag{8.4.36}$$

$$\frac{\partial^2}{\partial \gamma^2} \langle \psi' | \left(\hat{Y}_i \hat{Y}_j \right) | \psi' \rangle =$$
$$-\frac{1}{2} \cos^{L_{ij}+R_{ij}} \gamma \left\{ \left(1 - \cos^{T_{ij}} 2\gamma \right) \left[\left(L_{ij} + R_{ij} \right)^2 \tan^2 \gamma - \left(L_{ij} + R_{ij} \right) \sec^2 \gamma \right] \right.$$
$$\left. -4 \cos^{T_{ij}} 2\gamma \left[T_{ij}^2 \tan^2 2\gamma - T_{ij} \sec^2 2\gamma \right] - 4 T_{ij} \left(L_{ij} + R_{ij} \right) \cos^{T_{ij}} 2\gamma \tan 2\gamma \tan \gamma \right\} \tag{8.4.37}$$

8.5 Optimal Parameters for QAOA of Depth $P = 1$

We will obtain some useful new theoretical results by applying the results obtained from the all plus simplification of the QAOA depth $P = 1$ expectation value of the unweighted MaxCut Hamiltonian $\langle \phi | \hat{C} | \phi \rangle$ on several common types of graphs: 0-Regular (Unconnected Graph), 1-Regular, 2-Regular, Cycle, Linear, 3-Regular, k-Regular and Complete ($n-1$-Regular). In addition, we may find the optimal points of the expectation value landscape and find it corresponding optimal parameters.

Recall that a k-regular graph is any graph whose any vertex has k connected neighbours. That is every edge of a k-regular graph has $k-1$ left and $k-1$ right neighbours, which may or may not be common. A cycle graph is a special case of 2-Regular graph whereby every vertex must be connected in a single ring. A linear graph is simply a single chain of connected vertices.

To avoid cumbersome writing, in this section only, we denote the expectation value of any operator $\hat{G}_i$, with respect to an arbitrary QAOA initial state $|\psi\rangle$, as

$$\langle \psi | \hat{G}_i | \psi \rangle = \langle g_i \rangle \tag{8.5.1}$$

8.5.1 0-Regular Graph

For the sake of a sanity check, the expectation value of the unweighted MaxCut Hamiltonian for a 0 Regular graph is unsurprisingly calculated to be zero, since there are no edges to speak of. Thus, the MaxCut value is zero. Quantum mechanically, any 2^nD computational basis state may be admitted as a reasonable MaxCut solution state. Hence, there is no need for any quantum algorithm to solve this trivial case.

8.5.2 1-Regular Graph

A 1-Regular graph with n-vertices is any graph whose any vertex has only other connected neighbour. That is every edge of a 1-regular graph has neither left nor right neighbours. This also means that any 1 regular graph has even number of vertices, otherwise an odd number will result in at least one unconnected vertex. This also means that there are $\frac{n}{2}$ number of edges. The MaxCut solution value is simply just equal the number of edges. A MaxCut Solution state is any complex superposition of any computation basis that corresponds to having only pairs of disagreeing connected qubits. We may substitute $\ell_{ij} = \xi_{ij} = 0$ in equations 8.4.13 to 8.4.16 to obtain a simplified expectation value of the unweighted MaxCut Hamiltonian, its gradient and the hessian

QAOA Depth $P = 1$ Expectation Value of Unweighted MaxCut Hamiltonian (1-Regular)

$$\langle\phi|\hat{C}|\phi\rangle = \sum_{(i,j)\in \mathrm{E}} \frac{1}{2}\left(\cos^2 2\beta\,\langle z_i z_j\rangle + \frac{1}{2}\sin 4\beta\left(\cos\gamma\langle y_i z_j + z_i y_j\rangle + \sin\gamma\langle x_i + x_j\rangle\right) + \sin^2 2\beta\,\langle y_i y_j\rangle - 1\right) \tag{8.5.2}$$

QAOA Depth $P = 1$ Gradient of the Expectation Value (1-Regular)

$$\nabla\langle\phi|\hat{C}|\phi\rangle = \sum_{(i,j)\in \mathrm{E}} \frac{1}{2}\begin{pmatrix} \frac{\partial}{\partial\beta} \\ \frac{\partial}{\partial\gamma} \end{pmatrix}\langle\phi|\hat{Z}_i\hat{Z}_j|\phi\rangle \tag{8.5.3}$$

where,

$$\frac{\partial}{\partial\beta}\langle\phi|\hat{Z}_i\hat{Z}_j|\phi\rangle = 2\cos 4\beta\left(\cos\gamma\langle y_i z_j + z_i y_j\rangle + \sin\gamma\langle x_i + x_j\rangle\right) + 2\sin 4\beta\,\langle y_i y_j - z_i z_j\rangle \tag{8.5.4}$$

$$\frac{\partial}{\partial\gamma}\langle\phi|\hat{Z}_i\hat{Z}_j|\phi\rangle = \frac{1}{2}\sin 4\beta\left(\cos\gamma\langle x_i + x_j\rangle - \sin\gamma\langle y_i z_j + z_i y_j\rangle\right) \tag{8.5.5}$$

QAOA Depth $P = 1$ Hessian of the Expectation Value (1-Regular)

$$\nabla^2 \langle \phi | \hat{C} | \phi \rangle = \sum_{(i,j) \in \mathrm{E}} \frac{1}{2} \begin{pmatrix} \frac{\partial^2}{\partial \beta^2} & \frac{\partial^2}{\partial \gamma \partial \beta} \\ \frac{\partial^2}{\partial \beta \partial \gamma} & \frac{\partial^2}{\partial \gamma^2} \end{pmatrix} \langle \phi | \hat{Z}_i \hat{Z}_j | \phi \rangle \tag{8.5.6}$$

where,

$$\frac{\partial^2}{\partial \beta^2} \langle \phi | \hat{Z}_i \hat{Z}_j | \phi \rangle = -8 \sin 4\beta \left(\cos \gamma \langle y_i z_j + z_i y_j \rangle + \sin \gamma \langle x_i + x_j \rangle \right) + 8 \cos 4\beta \langle y_i y_j - z_i z_j \rangle \tag{8.5.7}$$

$$\frac{\partial^2}{\partial \gamma^2} \langle \phi | \hat{Z}_i \hat{Z}_j | \phi \rangle = \frac{1}{2} \sin 4\beta \left(-\sin \gamma \langle x_i + x_j \rangle - \cos \gamma \langle y_i z_j + z_i y_j \rangle \right) \tag{8.5.8}$$

$$\frac{\partial^2}{\partial \beta \partial \gamma} \langle \phi | \hat{Z}_i \hat{Z}_j | \phi \rangle = 2 \cos 4\beta \left(\cos \gamma \langle x_i + x_j \rangle - \sin \gamma \langle y_i z_j + z_i y_j \rangle \right) \tag{8.5.9}$$

$$= \frac{\partial^2}{\partial \gamma \partial \beta} \langle \phi | \hat{Z}_i \hat{Z}_j | \phi \rangle \tag{8.5.10}$$

Optimal Parameters of QAOA Depth $P = 1$ (1-Regular)

β^*	γ^*	Hessian	Critical Type
$\frac{\pi k}{4}$	$\arctan\left[-\frac{\Sigma_{(i,j)\in \mathrm{E}} \langle x_i + x_j \rangle}{\Sigma_{(i,j)\in \mathrm{E}} \langle y_i z_j + z_i y_j \rangle} \right]$	$\begin{pmatrix} 0 & b \\ b & d \end{pmatrix}$, for some real b, d	Saddle
$\frac{1}{4} \arctan\left[\pm \frac{\sqrt{\left(\Sigma_{(i,j)\in \mathrm{E}} \langle y_i z_j + z_i y_j \rangle \right)^2 + \left(\Sigma_{(i,j)\in \mathrm{E}} \langle x_i + x_j \rangle \right)^2}}{\Sigma_{(i,j)\in \mathrm{E}} \langle y_i y_j - z_i z_j \rangle} \right]$	$\arctan\left[\frac{\Sigma_{(i,j)\in \mathrm{E}} \langle x_i + x_j \rangle}{\Sigma_{(i,j)\in \mathrm{E}} \langle y_i z_j + z_i y_j \rangle} \right]$	(No concise expression available)	Inconclusive

All Plus Simplification of QAOA Depth $P = 1$ (1-Regular)

$$\langle \phi | \hat{C} | \phi \rangle = \frac{n}{4} \left(\frac{1}{2} \sin 4\beta \sin \gamma - 1 \right) \tag{8.5.11}$$

$$\nabla \langle \phi | \hat{C} | \phi \rangle = \frac{n}{16} \begin{pmatrix} 4 \cos 4\beta \sin \gamma \\ \sin 4\beta \cos \gamma \end{pmatrix} \tag{8.5.12}$$

$$\nabla^2 \langle \phi | \hat{C} | \phi \rangle = \frac{n}{16} \begin{pmatrix} -16 \sin 4\beta \sin \gamma & 4 \cos 4\beta \cos \gamma \\ 4 \cos 4\beta \cos \gamma & -\sin 4\beta \sin \gamma \end{pmatrix} \tag{8.5.13}$$

All Plus Simplification of Optimal Parameters of QAOA Depth $P = 1$ (1-Regular)

β^*	γ^*	Hessian	Critical Type
$\frac{\pi k}{4}$	πk	$\frac{n}{16}\begin{pmatrix} 0 & \pm 4 \\ \pm 4 & 0 \end{pmatrix}$	Saddle
$\frac{\pi}{8}(2k+1)$	$\frac{\pi}{2}(2k+1)$	$\frac{n}{16}\begin{pmatrix} +16 & 0 \\ 0 & +1 \end{pmatrix}$, Both k even or odd	Local Minimum
		$\frac{n}{16}\begin{pmatrix} -16 & 0 \\ 0 & -1 \end{pmatrix}$, Otherwise	Local Maximum

8.5.3 2-Regular

A 2-Regular graph with n-vertices is any graph whose any vertex has two other connected neighbour. That is every edge of a 2-regular graph has one pair of left and right neighbours, which may or may not be a common neighbour. The MaxCut solution is not trivial as it is graph structure is not unique, but it is consider easy solve as 2-Regular graph may consist of one or multiple cycles as sub-graphs. A single cycle is a special case of 2-Regular graph which will be covered in the next section. We may substitute $\ell_{ij} = \xi_{ij} = 1$ in equation 8.4.13 to 8.4.16 to obtain a simplified expectation value of the unweighted MaxCut Hamiltonian,

QAOA Depth $P = 1$ Expectation Value of Unweighted MaxCut Hamiltonian (2-Regular)

$$\langle \phi | \hat{C} | \phi \rangle = \sum_{(i,j)\in \mathrm{E}} \frac{1}{2}\left(\cos^2 2\beta \langle z_i z_j \rangle + \frac{1}{2}\sin 4\beta \langle \psi' | \hat{Y}_i \hat{Z}_j + \hat{Z}_i \hat{Y}_j | \psi' \rangle + \sin^2 2\beta \langle \psi' | \hat{Y}_i \hat{Y}_j | \psi' \rangle - 1\right) \tag{8.5.14}$$

where,

$$\langle \psi' | \hat{Y}_i \hat{Z}_j | \psi' \rangle = \cos^2\gamma \langle y_i z_j \rangle + \frac{1}{2}\sin 2\gamma \left\langle x_i + x_i z_j \left(\sum_{\lambda \in \Lambda_1^1} \prod_{a\in\lambda} z_{l_a}\right)\right\rangle - \sin^2\gamma \left\langle y_i \left(\sum_{\lambda\in\Lambda_1^1}\prod_{b\in\lambda} z_{l_a}\right)\right\rangle \tag{8.5.15}$$

$$\langle \psi' | \hat{Z}_i \hat{Y}_j | \psi' \rangle = \cos^2\gamma \langle z_i y_j \rangle + \frac{1}{2}\sin 2\gamma \left\langle x_j + z_i x_j \left(\sum_{\lambda \in \Lambda_1^1} \prod_{b\in\lambda} z_{r_b}\right)\right\rangle - \sin^2\gamma \left\langle y_j \left(\sum_{\lambda\in\Lambda_1^1}\prod_{b\in\lambda} z_{r_b}\right)\right\rangle \tag{8.5.16}$$

$$\langle \psi' | \hat{Y}_i \hat{Y}_j | \psi' \rangle = \cos^2\gamma \langle y_i y_j \rangle + \frac{1}{2}\sin 2\gamma \left\langle y_i x_j \left(\sum_{\lambda_2 \in \Lambda_1^1} \prod_{b\in\lambda_2} z_{r_b}\right) + x_i y_j \left(\sum_{\lambda_1 \in \Lambda_1^1} \prod_{a\in\lambda_1} z_{l_a}\right)\right\rangle + \sin^2\gamma \left\langle x_i x_j \left(\sum_{\lambda_1\in\Lambda_1^1}\prod_{a\in\lambda_1} z_{l_a}\right)\left(\sum_{\lambda_2\in\Lambda_1^1}\prod_{b\in\lambda_2} z_{r_b}\right)\right\rangle \tag{8.5.17}$$

QAOA Depth $P = 1$ Gradient of the Expectation Value (2-Regular)

$$\nabla \langle \phi | \hat{C} | \phi \rangle = \sum_{(i,j) \in \mathrm{E}} \frac{1}{2} \begin{pmatrix} \frac{\partial}{\partial \beta} \\ \frac{\partial}{\partial \gamma} \end{pmatrix} \langle \phi | \hat{Z}_i \hat{Z}_j | \phi \rangle \tag{8.5.18}$$

where,

$$\frac{\partial}{\partial \beta} \langle \phi | \hat{Z}_i \hat{Z}_j | \phi \rangle = 2 \cos 4\beta \langle \psi' | \hat{Y}_i \hat{Z}_j + \hat{Z}_i \hat{Y}_j | \psi' \rangle + 2 \sin 4\beta \left(\langle \psi' | \hat{Y}_i \hat{Y}_j | \psi' \rangle - \langle z_i z_j \rangle \right) \tag{8.5.19}$$

$$\frac{\partial}{\partial \gamma} \langle \phi | \hat{Z}_i \hat{Z}_j | \phi \rangle = \frac{1}{2} \sin 4\beta \frac{\partial}{\partial \gamma} \langle \psi' | \hat{Y}_i \hat{Z}_j + \hat{Z}_i \hat{Y}_j | \psi' \rangle + \sin^2 2\beta \frac{\partial}{\partial \gamma} \langle \psi' | \hat{Y}_i \hat{Y}_j | \psi' \rangle \tag{8.5.20}$$

and,

$$\frac{\partial}{\partial \gamma} \langle \psi' | \hat{Y}_i \hat{Z}_j | \psi' \rangle =$$

$$\cos 2\gamma \left\langle x_i + x_i z_j \left(\sum_{\lambda \in \Lambda_1^1} \prod_{a \in \lambda} z_{l_a} \right) \right\rangle - \sin 2\gamma \left\langle y_i z_j + y_i \left(\sum_{\lambda \in \Lambda_1^1} \prod_{b \in \lambda} z_{l_a} \right) \right\rangle \tag{8.5.21}$$

$$\frac{\partial}{\partial \gamma} \langle \psi' | \hat{Z}_i \hat{Y}_j | \psi' \rangle =$$

$$\cos 2\gamma \left\langle x_j + z_i x_j \left(\sum_{\lambda \in \Lambda_1^1} \prod_{b \in \lambda} z_{r_b} \right) \right\rangle - \sin 2\gamma \left\langle z_i y_j + y_j \left(\sum_{\lambda \in \Lambda_1^1} \prod_{b \in \lambda} z_{r_b} \right) \right\rangle \tag{8.5.22}$$

$$\frac{\partial}{\partial \gamma} \langle \psi' | \hat{Y}_i \hat{Y}_j | \psi' \rangle =$$

$$\cos 2\gamma \left\langle y_i x_j \left(\sum_{\lambda_2 \in \Lambda_1^1} \prod_{b \in \lambda_2} z_{r_b} \right) + x_i y_j \left(\sum_{\lambda_1 \in \Lambda_1^1} \prod_{a \in \lambda_1} z_{l_a} \right) \right\rangle - \sin 2\gamma \left\langle y_i y_j - x_i x_j \left(\sum_{\lambda_1 \in \Lambda_1^1} \prod_{a \in \lambda_1} z_{l_a} \right) \left(\sum_{\lambda_2 \in \Lambda_1^1} \prod_{b \in \lambda_2} z_{r_b} \right) \right\rangle \tag{8.5.23}$$

QAOA Depth $P = 1$ Hessian of the Expectation Value (2-Regular)

$$\nabla^2 \langle \phi | \hat{C} | \phi \rangle = \sum_{(i,j) \in \mathrm{E}} \frac{1}{2} \begin{pmatrix} \frac{\partial^2}{\partial \beta^2} & \frac{\partial^2}{\partial \gamma \partial \beta} \\ \frac{\partial^2}{\partial \beta \partial \gamma} & \frac{\partial^2}{\partial \gamma^2} \end{pmatrix} \langle \phi | \hat{Z}_i \hat{Z}_j | \phi \rangle \tag{8.5.24}$$

where,

$$\frac{\partial^2}{\partial \beta^2} \langle \phi | \hat{Z}_i \hat{Z}_j | \phi \rangle = -8 \sin 4\beta \langle \psi' | \hat{Y}_i \hat{Z}_j + \hat{Z}_i \hat{Y}_j | \psi' \rangle + 8 \cos 4\beta \left(\langle \psi' | \hat{Y}_i \hat{Y}_j | \psi' \rangle - \langle z_i z_j \rangle \right) \tag{8.5.25}$$

$$\frac{\partial^2}{\partial \gamma^2} \langle \phi | \hat{Z}_i \hat{Z}_j | \phi \rangle = \frac{1}{2} \sin 4\beta \frac{\partial^2}{\partial \gamma^2} \langle \psi' | \hat{Y}_i \hat{Z}_j + \hat{Z}_i \hat{Y}_j | \psi' \rangle + \sin^2 2\beta \frac{\partial^2}{\partial \gamma^2} \langle \psi' | \hat{Y}_i \hat{Y}_j | \psi' \rangle \tag{8.5.26}$$

$$\frac{\partial^2}{\partial \beta \partial \gamma} \langle \phi | \hat{Z}_i \hat{Z}_j | \phi \rangle = 2 \cos 4\beta \frac{\partial}{\partial \gamma} \langle \psi' | \hat{Y}_i \hat{Z}_j + \hat{Z}_i \hat{Y}_j | \psi' \rangle + 2 \sin 4\beta \frac{\partial}{\partial \gamma} \langle \psi' | \hat{Y}_i \hat{Y}_j | \psi' \rangle \tag{8.5.27}$$

$$= \frac{\partial^2}{\partial \gamma \partial \beta} \langle \phi | \hat{Z}_i \hat{Z}_j | \phi \rangle \tag{8.5.28}$$

and,

$$\frac{\partial^2}{\partial \gamma^2} \langle \psi' | \hat{Y}_i \hat{Z}_j | \psi' \rangle =$$

$$-2 \sin 2\gamma \left\langle x_i + x_i z_j \left(\sum_{\lambda \in \Lambda_1^1} \prod_{a \in \lambda} z_{l_a} \right) \right\rangle - 2 \cos 2\gamma \left\langle y_i z_j + y_i \left(\sum_{\lambda \in \Lambda_1^1} \prod_{b \in \lambda} z_{l_a} \right) \right\rangle \tag{8.5.29}$$

$$\frac{\partial^2}{\partial \gamma^2} \langle \psi' | \hat{Z}_i \hat{Y}_j | \psi' \rangle =$$

$$-2 \sin 2\gamma \left\langle x_j + z_i x_j \left(\sum_{\lambda \in \Lambda_1^1} \prod_{b \in \lambda} z_{r_b} \right) \right\rangle - 2 \cos 2\gamma \left\langle z_i y_j + y_j \left(\sum_{\lambda \in \Lambda_1^1} \prod_{b \in \lambda} z_{r_b} \right) \right\rangle \tag{8.5.30}$$

$$\frac{\partial^2}{\partial \gamma^2} \langle \psi' | \left(\hat{Y}_i \hat{Y}_j \right) | \psi' \rangle =$$

$$-2 \sin 2\gamma \left\langle y_i x_j \left(\sum_{\lambda_2 \in \Lambda_1^1} \prod_{b \in \lambda_2} z_{r_b} \right) + x_i y_j \left(\sum_{\lambda_1 \in \Lambda_1^1} \prod_{a \in \lambda_1} z_{l_a} \right) \right\rangle - 2 \cos 2\gamma \left\langle y_i y_j - x_i x_j \left(\sum_{\lambda_1 \in \Lambda_1^1} \prod_{a \in \lambda_1} z_{l_a} \right) \left(\sum_{\lambda_2 \in \Lambda_1^1} \prod_{b \in \lambda_2} z_{r_b} \right) \right\rangle \tag{8.5.31}$$

Optimal Parameters of QAOA Depth $P = 1$ (2-Regular)

β^*	γ^*	Hessian	Critical Type
(Not calculated due to unknown expectation values)			

All Plus Simplification of QAOA Depth $P=1$ (2-Regular)

$$\text{Let } \left\langle x_i x_j \left(z_{l_a}\right)\left(z_{r_b}\right)\right\rangle = \left\langle x_i x_j \left(\sum_{\lambda_1 \in \Lambda_1^1} \prod_{a \in \lambda_1} z_{l_a}\right)\left(\sum_{\lambda_2 \in \Lambda_1^1} \prod_{b \in \lambda_2} z_{r_b}\right)\right\rangle$$

$$\langle \phi | \hat{C} | \phi \rangle = \sum_{(i,j)\in \mathrm{E}} \frac{1}{2}\left[\frac{1}{2}\sin 4\beta \sin 2\gamma + \sin^2 2\beta \sin^2 \gamma \left\langle x_i x_j \left(z_{l_a}\right)\left(z_{r_b}\right)\right\rangle - 1\right] \tag{8.5.32}$$

$$\nabla \langle \phi | \hat{C} | \phi \rangle = \sum_{(i,j)\in \mathrm{E}} \frac{1}{2}\begin{pmatrix} 2\cos 4\beta \sin 2\gamma + 2\sin 4\beta \sin^2 \gamma \left\langle x_i x_j \left(z_{l_a}\right)\left(z_{r_b}\right)\right\rangle \\ \sin 4\beta \cos 2\gamma + \sin^2 2\beta \sin 2\gamma \left\langle x_i x_j \left(z_{l_a}\right)\left(z_{r_b}\right)\right\rangle \end{pmatrix} \tag{8.5.33}$$

$$\nabla^2 \langle \phi | \hat{C} | \phi \rangle = \sum_{(i,j)\in \mathrm{E}} \frac{1}{2}\begin{pmatrix} \frac{\partial^2}{\partial \beta^2} & \frac{\partial^2}{\partial \gamma \partial \beta} \\ \frac{\partial^2}{\partial \beta \partial \gamma} & \frac{\partial^2}{\partial \gamma^2} \end{pmatrix} \langle \phi | \hat{Z}_i \hat{Z}_j | \phi \rangle \tag{8.5.34}$$

$$\frac{\partial^2}{\partial \beta^2} \langle \phi | \hat{Z}_i \hat{Z}_j | \phi \rangle = -8\sin 4\beta \sin 2\gamma + 8\cos 4\beta \sin^2 \gamma \left\langle x_i x_j \left(z_{l_a}\right)\left(z_{r_b}\right)\right\rangle \tag{8.5.35}$$

$$\frac{\partial^2}{\partial \gamma^2} \langle \phi | \hat{Z}_i \hat{Z}_j | \phi \rangle = -2\sin 4\beta \sin 2\gamma + 2\sin^2 2\beta \cos 2\gamma \left\langle x_i x_j \left(z_{l_a}\right)\left(z_{r_b}\right)\right\rangle \tag{8.5.36}$$

$$\frac{\partial^2}{\partial \beta \partial \gamma} \langle \phi | \hat{Z}_i \hat{Z}_j | \phi \rangle = 4\cos 4\beta \cos 2\gamma + 2\sin 4\beta \sin 2\gamma \left\langle x_i x_j \left(z_{l_a}\right)\left(z_{r_b}\right)\right\rangle \tag{8.5.37}$$

$$= \frac{\partial^2}{\partial \gamma \partial \beta} \langle \phi | \hat{Z}_i \hat{Z}_j | \phi \rangle \tag{8.5.38}$$

Note: Even under the all plus simplification, the term $\left\langle x_i x_j \left(z_{l_a}\right)\left(z_{r_b}\right)\right\rangle$ cannot be further simplified as it is dependent on the actual graph structure. However, for any 2-Regular graph structure, this term can only take values 1 or 0.

All Plus Simplification of Optimal Parameters of QAOA Depth $P=1$ (2-Regular)

β^*	γ^*	Hessian	Critical Type
$\frac{\pi k}{2}$	πk	$\begin{pmatrix} 0 & 2\lvert E\rvert \\ 2\lvert E\rvert & 0 \end{pmatrix}$	Saddle

Ignoring the trivial set of of optimised parameters, one may obtain other non-trivial solutions by solving the two equations,

$$\tan 4\beta^* \tan \gamma^* = g = -\frac{2|E|}{\sum_{(i,j)\in \mathrm{E}} \left\langle x_i x_j \left(z_{l_a}\right)\left(z_{r_b}\right)\right\rangle} \tag{8.5.39}$$

$$\tan 2\beta^* \tan 2\gamma^* = g \tag{8.5.40}$$

where $g \leq -2$, since $0 \leq \sum_{(i,j)\in \mathrm{E}} \left\langle x_i x_j \left(z_{l_a}\right)\left(z_{r_b}\right)\right\rangle \leq |E|$. As the actual graph structure are unknown, the extremal angles β^*, γ^* are not calculated.

8.5.4 Cycles

A cycle graph with $n \geq 3$ vertices has n edges, where all vertices are connected in a single ring. For even number of edges, its MaxCut solution value is n and its MaxCut solution state is trivial for even n whereby all the edges are cut. Quantum mechanically, this means that the cut state $|\text{Sol}\rangle$ is simply any complex superposition of two computation basis, which there are no consecutively equal qubits, that is,

$$|\text{Sol}\rangle = \left(\alpha_1 \left| \underbrace{01010\ldots}_{n \text{ qubits}} \right\rangle + \alpha_2 \left| \underbrace{10101\ldots}_{n \text{ qubits}} \right\rangle \right) \quad \alpha_1, \alpha_2 \in \mathbb{C} \tag{8.5.41}$$

This solution cut state for even cycle is commonly known as the ring of disagrees. For odd number of edges, the MaxCut value is $n-1$ and its MaxCut solution state is a uniform superposition of all computational basis states where there is only one pair of consecutively equal qubits. Suppose we label each vertex using index i, then a single cycle is a special case of 2-Regular graph, where every vertex i is connected to the next vertex $i+1$ and last vertex $i=n$ must be connected to the first vertex $i=1$. Following the results obtained in the 2-Regular example, we make several substitutions:

1. The edge of the cycle may be relabelled as $(i,j) \to (i,i+1)$.
2. The summation iterates over the vertex labels instead of edges $\sum_{(i,j)\in \text{E}} \to \sum_{i=1}^{n}$
3. The left neighbour of edge $(i,i+1)$ is labelled as $i-1$, therefore $\left(\sum_{\lambda\in\Lambda_1^1} \prod_{a\in\lambda} z_{l_a}\right) = z_{i-1}$.
4. The right neighbour of edge $(i,i+1)$ is labelled as $i+2$, therefore $\left(\sum_{\lambda\in\Lambda_1^1} \prod_{b\in\lambda} z_{r_b}\right) = z_{i+2}$

Then, we may obtain a simplified expectation value of the unweighted MaxCut Hamiltonian,

QAOA Depth $P=1$ Expectation Value of Unweighted MaxCut Hamiltonian (Cycle)

$$\langle\phi|\hat{C}|\phi\rangle = \sum_{i=1}^{n} \frac{1}{2}\left[\cos^2 2\beta \langle z_i z_{i+1}\rangle + \frac{1}{2}\sin 4\beta \langle\psi'|\hat{Y}_i\hat{Z}_{i+1} + \hat{Z}_i\hat{Y}_{i+2}|\psi'\rangle + \sin^2 2\beta \langle\psi'|\hat{Y}_i\hat{Y}_{i+1}|\psi'\rangle - 1\right] \tag{8.5.42}$$

where,

$$\langle\psi'|\hat{Y}_i\hat{Z}_j|\psi'\rangle = \cos^2\gamma\langle y_i z_{i+1}\rangle + \frac{1}{2}\sin 2\gamma\langle x_i + z_{i-1}x_i z_{i+1}\rangle - \sin^2\gamma\langle z_{i-1}y_i\rangle \tag{8.5.43}$$

$$\langle\psi'|\hat{Z}_i\hat{Y}_j|\psi'\rangle = \cos^2\gamma\langle z_i y_{i+1}\rangle + \frac{1}{2}\sin 2\gamma\langle x_{i+1} + z_i x_{i+1} z_{i+2}\rangle - \sin^2\gamma\langle y_{i+1}z_{i+2}\rangle \tag{8.5.44}$$

$$\langle\psi'|\hat{Y}_i\hat{Y}_j|\psi'\rangle = \cos^2\gamma\langle y_i y_{i+1}\rangle + \frac{1}{2}\sin 2\gamma\langle y_i x_{i+1} z_{i+2} + z_{i-1}x_i y_{i+1}\rangle + \sin^2\gamma\langle z_{i-1}x_i x_{i+1}z_{i+2}\rangle \tag{8.5.45}$$

QAOA Depth $P = 1$ Gradient of the Expectation Value (Cycle)

$$\nabla \langle \phi | \hat{C} | \phi \rangle = \sum_{i=1}^{n} \frac{1}{2} \begin{pmatrix} \frac{\partial}{\partial \beta} \\ \frac{\partial}{\partial \gamma} \end{pmatrix} \langle \phi | \hat{Z}_i \hat{Z}_j | \phi \rangle \tag{8.5.46}$$

where,

$$\frac{\partial}{\partial \beta} \langle \phi | \hat{Z}_i \hat{Z}_j | \phi \rangle = 2\cos 4\beta \left\langle \psi' \right| \hat{Y}_i \hat{Z}_{i+1} + \hat{Z}_i \hat{Y}_{i+1} \left| \psi' \right\rangle + 2\sin 4\beta \left(\left\langle \psi' \right| \hat{Y}_i \hat{Y}_{i+1} \left| \psi' \right\rangle - \langle z_i z_{i+1} \rangle \right) \tag{8.5.47}$$

$$\frac{\partial}{\partial \gamma} \langle \phi | \hat{Z}_i \hat{Z}_j | \phi \rangle = \frac{1}{2} \sin 4\beta \frac{\partial}{\partial \gamma} \left\langle \psi' \right| \hat{Y}_i \hat{Z}_{i+1} + \hat{Z}_i \hat{Y}_{i+1} \left| \psi' \right\rangle + \sin^2 2\beta \frac{\partial}{\partial \gamma} \left\langle \psi' \right| \hat{Y}_i \hat{Y}_{i+1} \left| \psi' \right\rangle \tag{8.5.48}$$

and,

$$\frac{\partial}{\partial \gamma} \left\langle \psi' \right| \hat{Y}_i \hat{Z}_j \left| \psi' \right\rangle = \cos 2\gamma \langle x_i + z_{i-1} x_i z_{i+1} \rangle - \sin 2\gamma \langle y_i z_{i+1} + z_{i-1} y_i \rangle \tag{8.5.49}$$

$$\frac{\partial}{\partial \gamma} \left\langle \psi' \right| \hat{Z}_i \hat{Y}_j \left| \psi' \right\rangle = \cos 2\gamma \langle x_{i+1} + z_i x_{i+1} z_{i+2} \rangle - \sin 2\gamma \langle z_i y_{i+1} + y_{i+1} z_{i+2} \rangle \tag{8.5.50}$$

$$\frac{\partial}{\partial \gamma} \left\langle \psi' \right| \hat{Y}_i \hat{Y}_j \left| \psi' \right\rangle = \cos 2\gamma \langle z_{i-1} x_i y_{i+1} + y_i x_{i+1} z_{i+2} \rangle - \sin 2\gamma \langle y_i y_{i+1} - z_{i-1} x_i x_{i+1} z_{i+2} \rangle \tag{8.5.51}$$

QAOA Depth $P = 1$ Hessian of the Expectation Value (Cycle)

$$\nabla^2 \langle \phi | \hat{C} | \phi \rangle = \sum_{i=1}^{n} \frac{1}{2} \begin{pmatrix} \frac{\partial^2}{\partial \beta^2} & \frac{\partial^2}{\partial \gamma \partial \beta} \\ \frac{\partial^2}{\partial \beta \partial \gamma} & \frac{\partial^2}{\partial \gamma^2} \end{pmatrix} \langle \phi | \hat{Z}_i \hat{Z}_j | \phi \rangle \tag{8.5.52}$$

where,

$$\frac{\partial^2}{\partial \beta^2} \langle \phi | \hat{Z}_i \hat{Z}_j | \phi \rangle = -8\sin 4\beta \left\langle \psi' \right| \hat{Y}_i \hat{Z}_{i+1} + \hat{Z}_i \hat{Y}_{i+1} \left| \psi' \right\rangle + 8\cos 4\beta \left(\left\langle \psi' \right| \hat{Y}_i \hat{Y}_{i+1} \left| \psi' \right\rangle - \langle z_i z_{i+1} \rangle \right) \tag{8.5.53}$$

$$\frac{\partial^2}{\partial \gamma^2} \langle \phi | \hat{Z}_i \hat{Z}_j | \phi \rangle = \frac{1}{2} \sin 4\beta \frac{\partial^2}{\partial \gamma^2} \left\langle \psi' \right| \hat{Y}_i \hat{Z}_{i+1} + \hat{Z}_i \hat{Y}_{i+1} \left| \psi' \right\rangle + \sin^2 2\beta \frac{\partial^2}{\partial \gamma^2} \left\langle \psi' \right| \hat{Y}_i \hat{Y}_{i+1} \left| \psi' \right\rangle \tag{8.5.54}$$

$$\frac{\partial^2}{\partial \beta \partial \gamma} \langle \phi | \hat{Z}_i \hat{Z}_j | \phi \rangle = 2\cos 4\beta \frac{\partial}{\partial \gamma} \left\langle \psi' \right| \hat{Y}_i \hat{Z}_{i+1} + \hat{Z}_i \hat{Y}_{i+1} \left| \psi' \right\rangle + 2\sin 4\beta \frac{\partial}{\partial \gamma} \left\langle \psi' \right| \hat{Y}_i \hat{Y}_{i+1} \left| \psi' \right\rangle \tag{8.5.55}$$

$$= \frac{\partial^2}{\partial \gamma \partial \beta} \langle \phi | \hat{Z}_i \hat{Z}_j | \phi \rangle \tag{8.5.56}$$

and,

$$\frac{\partial^2}{\partial \gamma^2} \left\langle \psi' \right| \hat{Y}_i \hat{Z}_j \left| \psi' \right\rangle = -2\sin 2\gamma \langle x_i + z_{i-1} x_i z_{i+1} \rangle - 2\cos 2\gamma \langle y_i z_{i+1} + z_{i-1} y_i \rangle \tag{8.5.57}$$

$$\frac{\partial^2}{\partial \gamma^2} \left\langle \psi' \right| \hat{Z}_i \hat{Y}_j \left| \psi' \right\rangle = -2\sin 2\gamma \langle x_{i+1} + z_i x_{i+1} z_{i+2} \rangle - 2\cos 2\gamma \langle z_i y_{i+1} + y_{i+1} z_{i+2} \rangle \tag{8.5.58}$$

$$\frac{\partial^2}{\partial \gamma^2} \left\langle \psi' \right| \hat{Y}_i \hat{Y}_j \left| \psi' \right\rangle = -2\sin 2\gamma \langle z_{i-1} x_i y_{i+1} + y_i x_{i+1} z_{i+2} \rangle - 2\cos 2\gamma \langle y_i y_{i+1} - z_{i-1} x_i x_{i+1} z_{i+2} \rangle \tag{8.5.59}$$

Optimal Parameters of QAOA Depth $P = 1$ (Cycle)

β^*	γ^*	Hessian	Critical Type
(Not calculated, see below)			

Solving $\nabla \langle \phi | \hat{C} | \phi \rangle = \vec{0}$ yields the following set of equations,

$$\begin{aligned}
\frac{\partial}{\partial \beta} \langle \phi | \hat{C} | \phi \rangle &= 0 \\
\Rightarrow \tan 4\beta^* &= -\frac{\sum_{i=1}^{n} \left(\cos^2 \gamma^* \langle y_i z_{i+1} + z_i y_{i+1} \rangle + \frac{1}{2} \sin 2\gamma^* \langle x_i + z_{i-1} x_i z_{i+1} + x_{i+1} + z_i x_{i+1} z_{i+2} \rangle - \sin^2 \gamma^* \langle z_{i-1} y_i + y_{i+1} z_{i+2} \rangle \right)}{\sum_{i=1}^{n} \left(\cos^2 \gamma^* \langle y_i y_{i+1} \rangle + \frac{1}{2} \sin 2\gamma^* \langle y_i x_{i+1} z_{i+2} + z_{i-1} x_i y_{i+1} \rangle + \sin^2 \gamma^* \langle z_{i-1} x_i x_{i+1} z_{i+2} \rangle - \langle z_i z_{i+1} \rangle \right)} \qquad (8.5.60) \\
\frac{\partial}{\partial \gamma} \langle \phi | \hat{C} | \phi \rangle &= 0 \\
\Rightarrow \tan 2\beta^* &= -\frac{\sum_{i=1}^{n} \left(\cos 2\gamma^* \langle x_i + z_{i-1} x_i z_{i+1} + x_{i+1} + z_i x_{i+1} z_{i+2} \rangle - \sin 2\gamma^* \langle y_i z_{i+1} + z_{i-1} y_i + z_i y_{i+1} + y_{i+1} z_{i+2} \rangle \right)}{\sum_{i=1}^{n} \left(\cos 2\gamma^* \langle z_{i-1} x_i y_{i+1} + y_i x_{i+1} z_{i+2} \rangle - \sin 2\gamma^* \langle y_i y_{i+1} + z_{i-1} x_i x_{i+1} z_{i+2} \rangle \right)} \qquad (8.5.61)
\end{aligned}$$

which are to be solved to obtain the optimised angles β^*, γ^*. Solving for the optimised angles β^*, γ^* here, by equating the two equations above using the the double angle tangent formulae, is equivalent to solving for the roots of a trigonometric polynomial of degree 6 , that consist complicated real coefficients which are polynomials of various expectations values. As β^*, γ^* remains unsolved, the second partial derivative test will not be carried out.

All Plus Simplification of QAOA Depth $P = 1$ (Cycle)

For $n = 3$, a triangle, note that for any index $i = 1,2,3$, the boundary relation $i+2 = i-1$ holds, as a result, this particular expectation value $\langle z_{i-1}x_ix_{i+1}z_{i+2}\rangle = 1$. This is not the case for $n \geq 4$, where the boundary relation is $i+n-1 = i-1$ and $\langle z_{i-1}x_ix_{i+1}z_{i+2}\rangle = 0$. Consider the case of triangle, a cycle with 3 vertices, also known as a triangle graph, then the above results simplifies to,

$$\langle\phi|\hat{C}|\phi\rangle = \frac{3}{4}\sin 4\beta\sin 2\gamma + \frac{3}{2}\sin^2 2\beta\sin^2\gamma - \frac{3}{2} \tag{8.5.62}$$

$$\nabla\langle\phi|\hat{C}|\phi\rangle = \begin{pmatrix} 3\cos 4\beta\sin 2\gamma + 3\sin 4\beta\sin^2\gamma \\ \frac{3}{2}\sin 4\beta\cos 2\gamma + \frac{3}{2}\sin^2 2\beta\sin 2\gamma \end{pmatrix} \tag{8.5.63}$$

$$\nabla^2\langle\phi|\hat{C}|\phi\rangle = \begin{pmatrix} \frac{\partial^2}{\partial\beta^2} & \frac{\partial^2}{\partial\gamma\partial\beta} \\ \frac{\partial^2}{\partial\beta\partial\gamma} & \frac{\partial^2}{\partial\gamma^2} \end{pmatrix}\langle\phi|\hat{C}|\phi\rangle \tag{8.5.64}$$

$$\frac{\partial^2}{\partial\beta^2}\langle\phi|\hat{C}|\phi\rangle = -12\sin 4\beta\sin 2\gamma + 12\cos 4\beta\sin^2\gamma \tag{8.5.65}$$

$$\frac{\partial^2}{\partial\gamma^2}\langle\phi|\hat{C}|\phi\rangle = -3\sin 4\beta\sin 2\gamma + 3\sin^2 2\beta\cos 2\gamma \tag{8.5.66}$$

$$\frac{\partial^2}{\partial\beta\partial\gamma}\langle\phi|\hat{C}|\phi\rangle = 12\cos 4\beta\cos 2\gamma + 3\sin 4\beta\sin 2\gamma \tag{8.5.67}$$

$$= \frac{\partial^2}{\partial\gamma\partial\beta}\langle\phi|\hat{Z}_i\hat{Z}_j|\phi\rangle \tag{8.5.68}$$

Next, consider the case of a cycle with $n \geq 4$ vertices, then the above results simplifies to,

$$\langle\phi|\hat{C}|\phi\rangle = \frac{n}{4}\sin 4\beta\sin 2\gamma - \frac{n}{2} \tag{8.5.69}$$

$$\nabla\langle\phi|\hat{C}|\phi\rangle = \begin{pmatrix} n\cos 4\beta\sin 2\gamma \\ \frac{n}{2}\sin 4\beta\cos 2\gamma \end{pmatrix} \tag{8.5.70}$$

$$\nabla^2\langle\phi|\hat{C}|\phi\rangle = \begin{pmatrix} \frac{\partial^2}{\partial\beta^2} & \frac{\partial^2}{\partial\gamma\partial\beta} \\ \frac{\partial^2}{\partial\beta\partial\gamma} & \frac{\partial^2}{\partial\gamma^2} \end{pmatrix}\langle\phi|\hat{C}|\phi\rangle \tag{8.5.71}$$

$$\frac{\partial^2}{\partial\beta^2}\langle\phi|\hat{C}|\phi\rangle = -4n\sin 4\beta\sin 2\gamma \tag{8.5.72}$$

$$\frac{\partial^2}{\partial\gamma^2}\langle\phi|\hat{C}|\phi\rangle = -n\sin 4\beta\sin 2\gamma \tag{8.5.73}$$

$$\frac{\partial^2}{\partial\beta\partial\gamma}\langle\phi|\hat{C}|\phi\rangle = 2n\cos 4\beta\cos 2\gamma \tag{8.5.74}$$

$$= \frac{\partial^2}{\partial\gamma\partial\beta}\langle\phi|\hat{Z}_i\hat{Z}_j|\phi\rangle \tag{8.5.75}$$

All Plus Simplification of Optimal Parameters of QAOA Depth $P = 1$ (Cycle)

Triangle ($n = 3$)

β^*	γ^*	Hessian	Critical Type
$\frac{\pi}{4}(2k+1)$	$\frac{\pi}{2}(2k+1)$	$\begin{pmatrix} 0 & 12 \\ 12 & 0 \end{pmatrix}$	Saddle
$\frac{\pi}{2}(2k+1)$	$\frac{\pi}{2}(2k+1)$	$\begin{pmatrix} 0 & -12 \\ -12 & 0 \end{pmatrix}$	Inconclusive
$\frac{\pi}{4}(2k+1)$	$\pi(2k+1)$	$\begin{pmatrix} 0 & -12 \\ -12 & 0 \end{pmatrix}$	Inconclusive
$\frac{\pi}{2}(2k+1)$	$\pi(2k+1)$	$\begin{pmatrix} 0 & 12 \\ 12 & 0 \end{pmatrix}$	Saddle
$\frac{\pi k}{2} + \frac{1}{2}\arctan\left(\frac{1}{\sqrt{2}}\right)$	$\pi k + \arctan\left(-\frac{1}{\sqrt{2}}\right)$	$\begin{pmatrix} 12 & -\frac{4}{3} \\ -\frac{4}{3} & 3 \end{pmatrix}$	Local Minimum
$\frac{\pi k}{2} + \frac{1}{2}\arctan\left(-\frac{1}{\sqrt{2}}\right)$	$\pi k + \arctan\left(\frac{1}{\sqrt{2}}\right)$	$\begin{pmatrix} 12 & -\frac{4}{3} \\ -\frac{4}{3} & 3 \end{pmatrix}$	Local Minimum

Cycle ($n \geq 4$)

β^*	γ^*	Hessian	Critical Type
$\frac{\pi}{8}(2k+1)$	$\frac{\pi}{4}(2k+1)$	$\begin{pmatrix} 4n & 0 \\ 0 & n \end{pmatrix}$, Both k even or odd	Local Minimum
		$\begin{pmatrix} -4n & 0 \\ 0 & -n \end{pmatrix}$, Otherwise	Local Maximum
$\frac{\pi k}{4}$	$\frac{\pi k}{2}$	$\begin{pmatrix} 0 & 1 \\ 1 & 0 \end{pmatrix}$	Saddle

8.5.5 Path

A path graph with n vertices has $n-1$ edges, where all vertices are connected in a single chain, where we label each vertex using index i, starting from the left vertex as $i = 1$. The MaxCut value is simply $n-1$ and the the MaxCut solution state is trivial whereby all the edges are cut. Quantum mechanically, this means that the cut state $|\text{Sol}\rangle$ is simply any complex superposition of two computation basis, which there are no consecutively equal qubits. That is,

$$|\text{Sol}\rangle = \left(\alpha_1 \left|\underbrace{01010\ldots}_{n \text{ qubits}}\right\rangle + \alpha_2 \left|\underbrace{10101\ldots}_{n \text{ qubits}}\right\rangle\right)$$

Although, the MaxCut value and the solution state of a path graph is the same as that of a cycle graph with even number of vertices, the expectation value of the unweighted MaxCut Hamiltonian of the path graph is different and more complicated that of the cycle due to presence fixed boundary conditions. The fixed boundary conditions are that any index $i > n$ or $i < 1$ does not exist and its term must be eliminated from the summation in the expectation value. As a result, the overall expression is more awkward and tedious to handle, but one may note the mathematical semblance to that of the cycle. The expectation of the unweighted MaxCut Hamiltonian is calculated to be

QAOA Depth $P = 1$ Expectation Value of Unweighted MaxCut Hamiltonian (Path)

$$\begin{aligned}
&\langle\phi|\hat{C}|\phi\rangle = \\
&\frac{1-n}{2} + \frac{1}{2}\cos^2 2\beta \sum_{i=1}^{n-1} \langle z_i z_{i+1}\rangle + \\
&+\frac{1}{4}\sin 4\beta \left[\left\langle\psi'\right|\hat{Y}_1\hat{Z}_2 + \hat{Z}_{n-1}\hat{Y}_n\left|\psi'\right\rangle + \left(\sum_{i=2}^{n-1}\left\langle\psi'\right|\hat{Y}_i\hat{Z}_{i+1}\left|\psi'\right\rangle\right) + \left(\sum_{i=1}^{n-2}\left\langle\psi'\right|\hat{Z}_i\hat{Y}_{i+1}\left|\psi'\right\rangle\right)\right] \\
&+\frac{1}{2}\sin^2 2\beta \left[\left\langle\psi'\right|\hat{Y}_1\hat{Y}_2 + \hat{Y}_{n-1}\hat{Y}_n\left|\psi'\right\rangle + \left(\sum_{i=2}^{n-2}\left\langle\psi'\right|\hat{Y}_i\hat{Y}_{i+1}\left|\psi'\right\rangle\right)\right] \qquad (8.5.76)
\end{aligned}$$

where,

$$\left\langle\psi'\right|\hat{Y}_1\hat{Z}_2 + \hat{Z}_{n-1}\hat{Y}_n\left|\psi'\right\rangle = \cos\gamma\langle y_1 y_2 + z_{n-1}y_n\rangle + \sin\gamma\langle x_1 + x_n\rangle \qquad (8.5.77)$$

$$\left\langle\psi'\right|\hat{Y}_1\hat{Y}_2 + \hat{Y}_{n-1}\hat{Y}_n\left|\psi'\right\rangle = \cos\gamma\langle y_1 y_2 + y_{n-1}y_n\rangle + \sin\gamma\langle y_1 x_2 z_3 + z_{n-2}x_{n-2}y_n\rangle \qquad (8.5.78)$$

$$\left\langle\psi'\right|\hat{Y}_i\hat{Z}_{i+1}\left|\psi'\right\rangle = \cos^2\gamma\langle y_i z_{i+1}\rangle + \frac{1}{2}\sin 2\gamma\langle x_i + z_{i-1}x_i z_{i+1}\rangle - \sin^2\gamma\langle z_{i-1}y_i\rangle \qquad (8.5.79)$$

$$\left\langle\psi'\right|\hat{Z}_i\hat{Y}_{i+1}\left|\psi'\right\rangle = \cos^2\gamma\langle z_i y_{i+1}\rangle + \frac{1}{2}\sin 2\gamma\langle x_{i+1} + z_i x_{i+1} z_{i+2}\rangle - \sin^2\gamma\langle y_{i+1}z_{i+2}\rangle \qquad (8.5.80)$$

$$\left\langle\psi'\right|\hat{Y}_i\hat{Y}_{i+1}\left|\psi'\right\rangle = \cos^2\gamma\langle y_i y_{i+1}\rangle + \frac{1}{2}\sin 2\gamma\langle z_{i-1}x_i y_{i+1} + y_i x_{i+1} z_{i+2}\rangle - \sin^2\gamma\langle z_{i-1}x_i x_{i+1}z_{i+2}\rangle \qquad (8.5.81)$$

QAOA Depth $P = 1$ Gradient of the Expectation Value (Path)

$$\nabla \langle \phi | \hat{C} | \phi \rangle = \sum_{i=1}^{n} \frac{1}{2} \begin{pmatrix} \frac{\partial}{\partial \beta} \\ \frac{\partial}{\partial \gamma} \end{pmatrix} \langle \phi | \hat{Z}_i \hat{Z}_j | \phi \rangle \tag{8.5.82}$$

where,

$$\begin{aligned} &\frac{\partial}{\partial \beta} \langle \phi | \hat{C} | \phi \rangle = \\ &\sin 4\beta \left[\langle \psi' | \hat{Y}_1 \hat{Y}_2 + \hat{Y}_{n-1} \hat{Y}_n | \psi' \rangle + \left(\sum_{i=2}^{n-2} \langle \psi' | \hat{Y}_i \hat{Y}_{i+1} | \psi' \rangle \right) - \left(\sum_{i=1}^{n-1} \langle z_i z_{i+1} \rangle \right) \right] \\ &+ \cos 4\beta \left[\langle \psi' | \hat{Y}_1 \hat{Z}_2 + \hat{Z}_{n-1} \hat{Y}_n | \psi' \rangle + \left(\sum_{i=2}^{n-1} \langle \psi' | \hat{Y}_i \hat{Z}_{i+1} | \psi' \rangle \right) + \left(\sum_{i=1}^{n-2} \langle \psi' | \hat{Z}_i \hat{Y}_{i+1} | \psi' \rangle \right) \right] \end{aligned} \tag{8.5.83}$$

$$\begin{aligned} &\frac{\partial}{\partial \gamma} \langle \phi | \hat{C} | \phi \rangle = \\ &\frac{1}{2} \sin^2 2\beta \left[\frac{\partial}{\partial \gamma} \langle \psi' | \hat{Y}_1 \hat{Y}_2 + \hat{Y}_{n-1} \hat{Y}_n | \psi' \rangle + \left(\sum_{i=2}^{n-2} \frac{\partial}{\partial \gamma} \langle \psi' | \hat{Y}_i \hat{Y}_{i+1} | \psi' \rangle \right) \right] \\ &+ \frac{1}{4} \sin 4\beta \left[\frac{\partial}{\partial \gamma} \langle \psi' | \hat{Y}_1 \hat{Z}_2 + \hat{Z}_{n-1} \hat{Y}_n | \psi' \rangle + \left(\sum_{i=2}^{n-1} \frac{\partial}{\partial \gamma} \langle \psi' | \hat{Y}_i \hat{Z}_{i+1} | \psi' \rangle \right) + \left(\sum_{i=1}^{n-2} \frac{\partial}{\partial \gamma} \langle \psi' | \hat{Z}_i \hat{Y}_{i+1} | \psi' \rangle \right) \right] \end{aligned} \tag{8.5.84}$$

and,

$$\frac{\partial}{\partial \gamma} \langle \psi' | \hat{Y}_1 \hat{Z}_2 + \hat{Z}_{n-1} \hat{Y}_n | \psi' \rangle = \cos \gamma \langle x_1 + x_n \rangle - \sin \gamma \langle y_1 y_2 + z_{n-1} y_n \rangle \tag{8.5.85}$$

$$\frac{\partial}{\partial \gamma} \langle \psi' | \hat{Y}_1 \hat{Y}_2 + \hat{Y}_{n-1} \hat{Y}_n | \psi' \rangle = \cos \gamma \langle y_1 x_2 z_3 + z_{n-2} x_{n-2} y_n \rangle - \sin \gamma \langle y_1 y_2 + y_{n-1} y_n \rangle \tag{8.5.86}$$

$$\frac{\partial}{\partial \gamma} \langle \psi' | \hat{Y}_i \hat{Z}_{i+1} | \psi' \rangle = \cos 2\gamma \langle x_i + z_{i-1} x_i z_{i+1} \rangle - \sin 2\gamma \langle y_i z_{i+1} + z_{i-1} y_i \rangle \tag{8.5.87}$$

$$\frac{\partial}{\partial \gamma} \langle \psi' | \hat{Z}_i \hat{Y}_{i+1} | \psi' \rangle = \cos 2\gamma \langle x_{i+1} + z_i x_{i+1} z_{i+2} \rangle - \sin 2\gamma \langle z_i y_{i+1} + y_{i+1} z_{i+2} \rangle \tag{8.5.88}$$

$$\frac{\partial}{\partial \gamma} \langle \psi' | \hat{Y}_i \hat{Y}_{i+1} | \psi' \rangle = \cos 2\gamma \langle z_{i-1} x_i y_{i+1} + y_i x_{i+1} z_{i+2} \rangle - \sin 2\gamma \langle y_i y_{i+1} + z_{i-1} x_i x_{i+1} z_{i+2} \rangle \tag{8.5.89}$$

QAOA Depth $P = 1$ Hessian of the Expectation Value (Path)

$$\nabla^2 \langle \phi | \hat{C} | \phi \rangle = \sum_{i=1}^{n} \frac{1}{2} \begin{pmatrix} \frac{\partial^2}{\partial \beta^2} & \frac{\partial^2}{\partial \gamma \partial \beta} \\ \frac{\partial^2}{\partial \beta \partial \gamma} & \frac{\partial^2}{\partial \gamma^2} \end{pmatrix} \langle \phi | \hat{Z}_i \hat{Z}_j | \phi \rangle \tag{8.5.90}$$

where,

$$\begin{aligned} &\frac{\partial^2}{\partial \beta^2} \langle \phi | \hat{C} | \phi \rangle = \\ &4 \cos 4\beta \left[\langle \psi' | \hat{Y}_1 \hat{Y}_2 + \hat{Y}_{n-1} \hat{Y}_n | \psi' \rangle + \left(\sum_{i=2}^{n-2} \langle \psi' | \hat{Y}_i \hat{Y}_{i+1} | \psi' \rangle \right) - \left(\sum_{i=1}^{n-1} \langle \psi | \hat{Z}_i \hat{Z}_{i+1} | \psi \rangle \right) \right] \\ &-4 \sin 4\beta \left[\langle \psi' | \hat{Y}_1 \hat{Z}_2 + \hat{Z}_{n-1} \hat{Y}_n | \psi' \rangle + \left(\sum_{i=2}^{n-1} \langle \psi' | \hat{Y}_i \hat{Z}_{i+1} | \psi' \rangle \right) + \left(\sum_{i=1}^{n-2} \langle \psi' | \hat{Z}_i \hat{Y}_{i+1} | \psi' \rangle \right) \right] \end{aligned} \tag{8.5.91}$$

$$\begin{aligned} &\frac{\partial^2}{\partial \gamma^2} \langle \phi | \hat{C} | \phi \rangle = \\ &\frac{1}{2} \sin^2 2\beta \left[\frac{\partial^2}{\partial \gamma^2} \langle \psi' | \hat{Y}_1 \hat{Y}_2 + \hat{Y}_{n-1} \hat{Y}_n | \psi' \rangle + \left(\sum_{i=2}^{n-2} \frac{\partial^2}{\partial \gamma^2} \langle \psi' | \hat{Y}_i \hat{Y}_{i+1} | \psi' \rangle \right) \right] \\ &+ \frac{1}{4} \sin 4\beta \left[\frac{\partial^2}{\partial \gamma^2} \langle \psi' | \hat{Y}_1 \hat{Z}_2 + \hat{Z}_{n-1} \hat{Y}_n | \psi' \rangle + \left(\sum_{i=2}^{n-1} \frac{\partial^2}{\partial \gamma^2} \langle \psi' | \hat{Y}_i \hat{Z}_{i+1} | \psi' \rangle \right) + \left(\sum_{i=1}^{n-2} \frac{\partial^2}{\partial \gamma^2} \langle \psi' | \hat{Z}_i \hat{Y}_{i+1} | \psi' \rangle \right) \right] \end{aligned} \tag{8.5.92}$$

$$\begin{aligned} &\frac{\partial^2}{\partial \beta \partial \gamma} \langle \phi | \hat{C} | \phi \rangle = \frac{\partial^2}{\partial \gamma \partial \beta} \langle \phi | \hat{Z}_i \hat{Z}_j | \phi \rangle = \\ &\sin 4\beta \left[\frac{\partial}{\partial \gamma} \langle \psi' | \hat{Y}_1 \hat{Y}_2 + \hat{Y}_{n-1} \hat{Y}_n | \psi' \rangle + \left(\sum_{i=2}^{n-2} \frac{\partial}{\partial \gamma} \langle \psi' | \hat{Y}_i \hat{Y}_{i+1} | \psi' \rangle \right) \right] \\ &+ \cos 4\beta \left[\frac{\partial}{\partial \gamma} \langle \psi' | \hat{Y}_1 \hat{Z}_2 + \hat{Z}_{n-1} \hat{Y}_n | \psi' \rangle + \left(\sum_{i=2}^{n-1} \frac{\partial}{\partial \gamma} \langle \psi' | \hat{Y}_i \hat{Z}_{i+1} | \psi' \rangle \right) + \left(\sum_{i=1}^{n-2} \frac{\partial}{\partial \gamma} \langle \psi' | \hat{Z}_i \hat{Y}_{i+1} | \psi' \rangle \right) \right] \end{aligned} \tag{8.5.93}$$

and,

$$\frac{\partial^2}{\partial \gamma^2} \langle \psi' | \hat{Y}_1 \hat{Z}_2 + \hat{Z}_{n-1} \hat{Y}_n | \psi' \rangle = -\sin \gamma \langle x_1 + x_n \rangle - \cos \gamma \langle y_1 y_2 + z_{n-1} y_n \rangle \tag{8.5.94}$$

$$\frac{\partial^2}{\partial \gamma^2} \langle \psi' | \hat{Y}_1 \hat{Y}_2 + \hat{Y}_{n-1} \hat{Y}_n | \psi' \rangle = -\sin \gamma \langle y_1 x_2 z_3 + z_{n-2} x_{n-2} y_n \rangle - \cos \gamma \langle y_1 y_2 + y_{n-1} y_n \rangle \tag{8.5.95}$$

$$\frac{\partial^2}{\partial \gamma^2} \langle \psi' | \hat{Y}_i \hat{Z}_{i+1} | \psi' \rangle = -2 \sin 2\gamma \langle x_i + z_{i-1} x_i z_{i+1} \rangle - 2 \cos 2\gamma \langle y_i z_{i+1} + z_{i-1} y_i \rangle \tag{8.5.96}$$

$$\frac{\partial^2}{\partial \gamma^2} \langle \psi' | \hat{Z}_i \hat{Y}_{i+1} | \psi' \rangle = -2 \sin 2\gamma \langle x_{i+1} + z_i x_{i+1} z_{i+2} \rangle - 2 \cos 2\gamma \langle z_i y_{i+1} + y_{i+1} z_{i+2} \rangle \tag{8.5.97}$$

$$\frac{\partial^2}{\partial \gamma^2} \langle \psi' | \hat{Y}_i \hat{Y}_{i+1} | \psi' \rangle = -2 \sin 2\gamma \langle z_{i-1} x_i y_{i+1} + y_i x_{i+1} z_{i+2} \rangle - 2 \cos 2\gamma \langle y_i y_{i+1} + z_{i-1} x_i x_{i+1} z_{i+2} \rangle \tag{8.5.98}$$

Optimal Parameters of QAOA Depth $P = 1$ (Path)

β^*	γ^*	Hessian	Critical Type
(Not calculated, see below)			

Solving $\nabla \langle \phi | \hat{C} | \phi \rangle = \vec{0}$ yields the following set of equations,

$$\begin{aligned}
\frac{\partial}{\partial \beta} \langle \phi | \hat{C} | \phi \rangle &= 0 \\
\Rightarrow \tan 4\beta^* &= -\frac{\langle \psi' | \hat{Y}_1 \hat{Z}_2 + \hat{Z}_{n-1} \hat{Y}_n | \psi' \rangle + \left(\sum_{i=2}^{n-1} \langle \psi' | \hat{Y}_i \hat{Z}_{i+1} | \psi' \rangle \right) + \left(\sum_{i=1}^{n-2} \langle \psi' | \hat{Z}_i \hat{Y}_{i+1} | \psi' \rangle \right)}{\langle \psi' | \hat{Y}_1 \hat{Y}_2 + \hat{Y}_{n-1} \hat{Y}_n | \psi' \rangle + \left(\sum_{i=2}^{n-2} \langle \psi' | \hat{Y}_i \hat{Y}_{i+1} | \psi' \rangle \right) - \left(\sum_{i=1}^{n-1} \langle \psi | \hat{Z}_i \hat{Z}_{i+1} | \psi \rangle \right)} \qquad (8.5.99) \\
\frac{\partial}{\partial \gamma} \langle \phi | \hat{C} | \phi \rangle &= 0 \\
\Rightarrow \tan 2\beta^* &= -\frac{\frac{\partial}{\partial \gamma} \langle \psi' | \hat{Y}_1 \hat{Z}_2 + \hat{Z}_{n-1} \hat{Y}_n | \psi' \rangle + \left(\sum_{i=2}^{n-1} \frac{\partial}{\partial \gamma} \langle \psi' | \hat{Y}_i \hat{Z}_{i+1} | \psi' \rangle \right) + \left(\sum_{i=1}^{n-2} \frac{\partial}{\partial \gamma} \langle \psi' | \hat{Z}_i \hat{Y}_{i+1} | \psi' \rangle \right)}{\frac{\partial}{\partial \gamma} \langle \psi' | \hat{Y}_1 \hat{Y}_2 + \hat{Y}_{n-1} \hat{Y}_n | \psi' \rangle + \left(\sum_{i=2}^{n-2} \frac{\partial}{\partial \gamma} \langle \psi' | \hat{Y}_i \hat{Y}_{i+1} | \psi' \rangle \right)} \qquad (8.5.100)
\end{aligned}$$

which are to be solved to obtain the optimised angles β^*, γ^*. Solving for the optimised angles β^*, γ^* here, by equating the two equations above using the the double angle tangent formulae, is equivalent to solving for the roots of a trigonometric polynomial of degree 6 , that consist complicated real coefficients which are polynomials of various expectations values. As β^*, γ^* remains unsolved, the second partial derivative test will not be carried out.

All Plus Simplification of QAOA Depth $P = 1$ (Path)

$$\langle \phi | \hat{C} | \phi \rangle = \frac{1-n}{2} + \frac{1}{4} \sin 4\beta \left(2 \sin \gamma + (n-2) \sin 2\gamma \right) \qquad (8.5.101)$$

$$\nabla \langle \phi | \hat{C} | \phi \rangle = \begin{pmatrix} \cos 4\beta \left[2 \sin \gamma + (n-2) \sin 2\gamma \right] \\ \frac{1}{2} \sin 4\beta \left[\cos \gamma + (n-2) \cos 2\gamma \right] \end{pmatrix} \qquad (8.5.102)$$

$$\nabla^2 \langle \phi | \hat{C} | \phi \rangle = \begin{pmatrix} \frac{\partial^2}{\partial \beta^2} & \frac{\partial^2}{\partial \gamma \partial \beta} \\ \frac{\partial^2}{\partial \beta \partial \gamma} & \frac{\partial^2}{\partial \gamma^2} \end{pmatrix} \langle \phi | \hat{C} | \phi \rangle \qquad (8.5.103)$$

$$\begin{aligned}
\frac{\partial^2}{\partial \beta^2} \langle \phi | \hat{C} | \phi \rangle &= -4 \sin 4\beta \left(2 \sin \gamma + (n-2) \sin 2\gamma \right) && (8.5.104) \\
\frac{\partial^2}{\partial \gamma^2} \langle \phi | \hat{C} | \phi \rangle &= -\frac{1}{2} \sin 4\beta \left[\sin \gamma + 2 (n-2) \sin 2\gamma \right] && (8.5.105) \\
\frac{\partial^2}{\partial \beta \partial \gamma} \langle \phi | \hat{C} | \phi \rangle &= 2 \cos 4\beta \left[\cos \gamma + (n-2) \cos 2\gamma \right] && (8.5.106) \\
&= \frac{\partial^2}{\partial \gamma \partial \beta} \langle \phi | \hat{Z}_i \hat{Z}_j | \phi \rangle && (8.5.107)
\end{aligned}$$

All Plus Simplification of Optimal Parameters of QAOA Depth $P=1$

	β^*	γ^*	Hessian	Critical Type
(Path)	$\frac{\pi}{8}(2k+1)$	$2k\pi \pm \arccos\left(\frac{-1+\sqrt{8n^2-32n+33}}{4n-8}\right)$, where $\frac{\pi}{4} < \lvert\gamma_1^*\rvert \leq \frac{\pi}{2}, \forall n \geq 4, k=0$	$\begin{pmatrix} \pm\alpha_1 & 0 \\ 0 & \pm\alpha_2 \end{pmatrix}$, where $\alpha_1, \alpha_2 \in \mathbb{R}$	Local Max/Min, depending on the integer value of both indexes k in β_1^*, γ_1^* and the sign of $\pm$ in γ_1^*
	$\frac{\pi k}{4}$	$2k\pi \pm \arccos\left(\frac{1}{2-n}\right)$	$\begin{pmatrix} 0 & \pm 2\left[\frac{1}{n-2}-(n-2)\right] \\ \pm 2\left[\frac{1}{n-2}-(n-2)\right] & 0 \end{pmatrix}$	Saddle
	$\frac{\pi k}{4}$	$k\pi$	$\begin{pmatrix} 0 & \pm 2[\pm 1+(n-2)] \\ \pm 2[\pm 1+(n-2)] & 0 \end{pmatrix}$	Saddle

8.5.6 3 Regular graphs

A 3-Regular graph with n-vertices is any graph whose any vertex has three other connected neighbours. That is every edge of a 3 regular graph has two left and two right neighbours, which some neighbours may or may not be a common neighbour. The MaxCut value and solution is not trivial and it is consider to be a computationally and significantly harder problem than that of other simpler graphs with vertices having at most two other connected neighbours. One may obtain the expectation value of the unweighted MaxCut Hamiltonian by simply substituting $\ell_{ij} = L_{ij} + T_{ij} = \xi_{ij} = R_{ij} + T_{ij} = 2$. However, the full expression is will still be cumbersome write down, it shall be left to the reader to derive the full expression, the relevant derivatives and the extremal parameters as an exercise. In this section we will consider the use of all plus state simplifications. Suppose the all plus state is used as the QAOA initial state $|+\rangle$, and let L_{ij}, R_{ij} be the number of non-common left and right neighbours of edge (i,j) and T_{ij} is the number of common neighbours of edge (i,j), then the expressions simplifies to,

All Plus Simplification of QAOA Depth $P=1$ (3 Regular)

$$\langle\phi|\hat{C}|\phi\rangle = \sum_{(i,j)\in \text{edges}} -\frac{1}{2} + \frac{1}{2}\left(\frac{1}{2}\sin 4\beta \langle\psi'|\hat{Y}_i\hat{Z}_j + \hat{Z}_i\hat{Y}_j|\psi'\rangle + \sin^2 2\beta \langle\psi'|\hat{Y}_i\hat{Y}_j|\psi'\rangle\right) \tag{8.5.108}$$

where,

$$\langle\psi'|\hat{Y}_i\hat{Z}_j|\psi'\rangle = \sin\gamma\cos^2\gamma \tag{8.5.109}$$

$$\langle\psi'|\hat{Z}_i\hat{Y}_j|\psi'\rangle = \sin\gamma\cos^2\gamma \tag{8.5.110}$$

$$\langle\psi'|\hat{Y}_i\hat{Y}_j|\psi'\rangle = \frac{1}{2}(\cos\gamma)^{L_{ij}+R_{ij}}\left(1-\cos^{T_{ij}}2\gamma\right) \tag{8.5.111}$$

All Plus Simplification of the Gradient (3 Regular)

$$\nabla \langle \phi | \hat{C} | \phi \rangle = \sum_{(i,j) \in \mathrm{E}} \frac{1}{2} \begin{pmatrix} \frac{\partial}{\partial \beta} \\ \frac{\partial}{\partial \gamma} \end{pmatrix} \langle \phi | \hat{Z}_i \hat{Z}_j | \phi \rangle \tag{8.5.112}$$

where,

$$\frac{\partial}{\partial \beta} \langle \phi | \hat{Z}_i \hat{Z}_j | \phi \rangle = 2\cos 4\beta \langle \psi' | \hat{Y}_i \hat{Z}_j + \hat{Z}_i \hat{Y}_j | \psi' \rangle + 2\sin 4\beta \langle \psi' | \hat{Y}_i \hat{Y}_j | \psi' \rangle \tag{8.5.113}$$

$$\frac{\partial}{\partial \gamma} \langle \phi | \hat{Z}_i \hat{Z}_j | \phi \rangle = \frac{1}{2} \sin 4\beta \frac{\partial}{\partial \gamma} \langle \psi' | \hat{Y}_i \hat{Z}_j + \hat{Z}_i \hat{Y}_j | \psi' \rangle + \sin^2 2\beta \frac{\partial}{\partial \gamma} \langle \psi' | \hat{Y}_i \hat{Y}_j | \psi' \rangle \tag{8.5.114}$$

and,

$$\frac{\partial}{\partial \gamma} \langle \psi' | \hat{Y}_i \hat{Z}_j | \psi' \rangle = \sin \gamma \cos^2 \gamma (\cot \gamma - 2\tan \gamma) \tag{8.5.115}$$

$$\frac{\partial}{\partial \gamma} \langle \psi' | \hat{Z}_i \hat{Y}_j | \psi' \rangle = \sin \gamma \cos^2 \gamma (\cot \gamma - 2\tan \gamma) \tag{8.5.116}$$

$$\frac{\partial}{\partial \gamma} \langle \psi' | \hat{Y}_i \hat{Y}_j | \psi' \rangle = -\frac{1}{2} \cos^{L_{ij}+R_{ij}} \gamma \left[2T_{ij} \cos^{T_{ij}} 2\gamma \tan 2\gamma - \left(L_{ij} + R_{ij} \right) \left(1 - \cos^{T_{ij}} 2\gamma \right) \tan \gamma \right] \tag{8.5.117}$$

All Plus Simplification of the Hessian (3 Regular)

$$\nabla^2 \langle \phi | \hat{C} | \phi \rangle = \sum_{(i,j) \in \mathrm{E}} \frac{1}{2} \begin{pmatrix} \frac{\partial^2}{\partial \beta^2} & \frac{\partial^2}{\partial \gamma \partial \beta} \\ \frac{\partial^2}{\partial \beta \partial \gamma} & \frac{\partial^2}{\partial \gamma^2} \end{pmatrix} \langle \phi | \hat{Z}_i \hat{Z}_j | \phi \rangle \tag{8.5.118}$$

where,

$$\frac{\partial^2}{\partial \beta^2} \langle \phi | \hat{Z}_i \hat{Z}_j | \phi \rangle = -8\sin 4\beta \langle \psi' | \hat{Y}_i \hat{Z}_j + \hat{Z}_i \hat{Y}_j | \psi' \rangle + 8\cos 4\beta \langle \psi' | \hat{Y}_i \hat{Y}_j | \psi' \rangle \tag{8.5.119}$$

$$\frac{\partial^2}{\partial \gamma^2} \langle \phi | \hat{Z}_i \hat{Z}_j | \phi \rangle = \frac{1}{2} \sin 4\beta \frac{\partial^2}{\partial \gamma^2} \langle \psi' | \hat{Y}_i \hat{Z}_j + \hat{Z}_i \hat{Y}_j | \psi' \rangle + \sin^2 2\beta \frac{\partial^2}{\partial \gamma^2} \langle \psi' | \hat{Y}_i \hat{Y}_j | \psi' \rangle \tag{8.5.120}$$

$$\frac{\partial^2}{\partial \beta \partial \gamma} \langle \phi | \hat{Z}_i \hat{Z}_j | \phi \rangle = 2\cos 4\beta \frac{\partial}{\partial \gamma} \langle \psi' | \hat{Y}_i \hat{Z}_j + \hat{Z}_i \hat{Y}_j | \psi' \rangle + 2\sin 4\beta \frac{\partial}{\partial \gamma} \langle \psi' | \hat{Y}_i \hat{Y}_j | \psi' \rangle \tag{8.5.121}$$

$$= \frac{\partial^2}{\partial \gamma \partial \beta} \langle \phi | \hat{Z}_i \hat{Z}_j | \phi \rangle \tag{8.5.122}$$

and,

$$\frac{\partial^2}{\partial \gamma^2} \langle \psi' | \hat{Y}_i \hat{Z}_j | \psi' \rangle = \sin \gamma \cos^2 \gamma \left[(\cot \gamma - 2\tan \gamma)^2 - \left(\csc^2 \gamma + 2\sec^2 \gamma \right) \right] \tag{8.5.123}$$

$$\frac{\partial^2}{\partial \gamma^2} \langle \psi' | \hat{Z}_i \hat{Y}_j | \psi' \rangle = \sin \gamma \cos^2 \gamma \left[(\cot \gamma - 2\tan \gamma)^2 - \left(\csc^2 \gamma + 2\sec^2 \gamma \right) \right] \tag{8.5.124}$$

$$\frac{\partial^2}{\partial \gamma^2} \langle \psi' | \hat{Y}_i \hat{Y}_j | \psi' \rangle = -\frac{1}{2} \cos^{L_{ij}+R_{ij}} \gamma \left\{ \left(1 - \cos^{T_{ij}} 2\gamma \right) \left[\left(L_{ij} + R_{ij} \right)^2 \tan^2 \gamma - \left(L_{ij} + R_{ij} \right) \sec^2 \gamma \right] \right. \tag{8.5.125}$$

$$-4\cos^{T_{ij}} 2\gamma \left[T_{ij}^2 \tan^2 2\gamma - T_{ij} \sec^2 2\gamma \right] \tag{8.5.126}$$

$$\left. -4T_{ij} \left(L_{ij} + R_{ij} \right) \cos^{T_{ij}} 2\gamma \tan 2\gamma \tan \gamma \right\} \tag{8.5.127}$$

All Plus Simplification of Optimal Parameters of QAOA Depth $P=1$ (3 Regular)

β^*	γ^*	Hessian	Critical Type
$\frac{\pi k}{2}$	πk	$\Sigma_{(i,j)\in \mathrm{E}} \frac{1}{2} \begin{pmatrix} 8\langle\psi'\vert\hat{Y}_i\hat{Y}_j\vert\psi'\rangle & \pm 4 \\ \pm 4 & 0 \end{pmatrix}$, where $+$: even k, $-$: odd k for k in γ_1^*	Saddle
$\forall \beta_2^* \in \mathbb{R}$	$\frac{\pi}{2}(2k+1)$	$\Sigma_{(i,j)\in \mathrm{E}} \frac{1}{2} \begin{pmatrix} 0 & 0 \\ 0 & \frac{\partial^2}{\partial \gamma^2}\langle\gamma,\beta\vert\hat{Z}_i\hat{Z}_j\vert\gamma,\beta\rangle\Big\vert_{\gamma_2^*} \end{pmatrix}$	Inconclusive

To obtain the non-trivial optimised parameters γ^*, β^*, by $\nabla \langle\phi\vert\hat{C}\vert\phi\rangle = 0$, we have to solve the following set of equations,

$$\frac{\partial}{\partial\beta}\langle\phi\vert\hat{C}\vert\phi\rangle = 0 \tag{8.5.128}$$

$$\Rightarrow \tan 4\beta^* = -\frac{4\vert E\vert \sin\gamma\cos^2\gamma}{\Sigma_{(i,j)\in \mathrm{E}} (\cos\gamma)^{L_{ij}+R_{ij}}\left(1-\cos^{T_{ij}}2\gamma\right)}\Bigg|_{\gamma^*} \tag{8.5.129}$$

$$\frac{\partial}{\partial\gamma}\langle\phi\vert\hat{C}\vert\phi\rangle = 0 \tag{8.5.130}$$

$$\Rightarrow \tan 2\beta^* = -\frac{2\vert E\vert \sin\gamma\cos^2\gamma(\cot\gamma - 2\tan\gamma)}{-\sum_{(i,j)\in \mathrm{E}} \frac{1}{2}\cos^{L_{ij}+R_{ij}}\gamma\left[2T_{ij}\cos^{T_{ij}}2\gamma\tan 2\gamma - (L_{ij}+R_{ij})\left(1-\cos^{T_{ij}}2\gamma\right)\tan\gamma\right]}\Bigg|_{\gamma^*} \tag{8.5.131}$$

As non-trivial β^*, γ^* remains unsolved, the second partial derivative test will not be carried out.

8.5.7 g Regular graphs

We may generalise the above example to a g-Regular graph with n-vertices where $4 \leq g < n-2$. It is any graph whose any vertex has g other connected neighbours. That is every edge of a g regular graph has $g-1$ left and two right neighbours, which some neighbours may or may not be a common neighbour. The MaxCut value and solution is definitely not trivial and it is considered an even harder problem than all of the encountered previous examples. One may obtain the expectation value of the unweighted MaxCut Hamiltonian by simply substituting $\ell_{ij} = L_{ij} + T_{ij} = \xi_{ij} = R_{ij} + T_{ij} = g-1$ which may not lead to any significant theoretical results. Similar to the previous sections we shall consider the use of all plus state simplifications. Suppose the all plus state is used as the QAOA initial state $\vert+\rangle$, and let L_{ij}, R_{ij} be the number of non-common left and right neighbours of edge (i,j) and T_{ij} is the number of common neighbours of edge (i,j), then the expressions simplifies to,

All Plus Simplification of QAOA Depth $P=1$ (g Regular)

$$\langle\phi\vert\hat{C}\vert\phi\rangle = \sum_{(i,j)\in \text{edges}} -\frac{1}{2} + \frac{1}{2}\left(\frac{1}{2}\sin 4\beta\,\langle\psi'\vert\hat{Y}_i\hat{Z}_j + \hat{Z}_i\hat{Y}_j\vert\psi'\rangle + \sin^2 2\beta\,\langle\psi'\vert\hat{Y}_i\hat{Y}_j\vert\psi'\rangle\right) \tag{8.5.132}$$

where,

$$\langle\psi'\vert\hat{Y}_i\hat{Z}_j\vert\psi'\rangle = \sin\gamma\cos^{g-1}\gamma \tag{8.5.133}$$

$$\langle\psi'\vert\hat{Z}_i\hat{Y}_j\vert\psi'\rangle = \sin\gamma\cos^{g-1}\gamma \tag{8.5.134}$$

$$\langle\psi'\vert\hat{Y}_i\hat{Y}_j\vert\psi'\rangle = \frac{1}{2}(\cos\gamma)^{L_{ij}+R_{ij}}\left(1-\cos^{T_{ij}}2\gamma\right) \tag{8.5.135}$$

All Plus Simplification of the Gradient (g Regular)

$$\nabla \langle \phi | \hat{C} | \phi \rangle = \sum_{(i,j) \in \mathrm{E}} \frac{1}{2} \begin{pmatrix} \frac{\partial}{\partial \beta} \\ \frac{\partial}{\partial \gamma} \end{pmatrix} \langle \phi | \hat{Z}_i \hat{Z}_j | \phi \rangle \tag{8.5.136}$$

where,

$$\frac{\partial}{\partial \beta} \langle \phi | \hat{Z}_i \hat{Z}_j | \phi \rangle = 2\cos 4\beta \langle \psi' | \hat{Y}_i \hat{Z}_j + \hat{Z}_i \hat{Y}_j | \psi' \rangle + 2\sin 4\beta \langle \psi' | \hat{Y}_i \hat{Y}_j | \psi' \rangle \tag{8.5.137}$$

$$\frac{\partial}{\partial \gamma} \langle \phi | \hat{Z}_i \hat{Z}_j | \phi \rangle = \frac{1}{2} \sin 4\beta \frac{\partial}{\partial \gamma} \langle \psi' | \hat{Y}_i \hat{Z}_j + \hat{Z}_i \hat{Y}_j | \psi' \rangle + \sin^2 2\beta \frac{\partial}{\partial \gamma} \langle \psi' | \hat{Y}_i \hat{Y}_j | \psi' \rangle \tag{8.5.138}$$

and,

$$\frac{\partial}{\partial \gamma} \langle \psi' | \hat{Y}_i \hat{Z}_j | \psi' \rangle = \sin \gamma \cos^{g-1} \gamma (\cot \gamma - (g-1) \tan \gamma) \tag{8.5.139}$$

$$\frac{\partial}{\partial \gamma} \langle \psi' | \hat{Z}_i \hat{Y}_j | \psi' \rangle = \sin \gamma \cos^{g-1} \gamma (\cot \gamma - (g-1) \tan \gamma) \tag{8.5.140}$$

$$\frac{\partial}{\partial \gamma} \langle \psi' | \hat{Y}_i \hat{Y}_j | \psi' \rangle = -\frac{1}{2} \cos^{L_{ij}+R_{ij}} \gamma \left[2T_{ij} \cos^{T_{ij}} 2\gamma \tan 2\gamma - \left(L_{ij} + R_{ij} \right) \left(1 - \cos^{T_{ij}} 2\gamma \right) \tan \gamma \right] \tag{8.5.141}$$

All Plus Simplification of the Hessian (g Regular)

$$\nabla^2 \langle \phi | \hat{C} | \phi \rangle = \sum_{(i,j) \in \mathrm{E}} \frac{1}{2} \begin{pmatrix} \frac{\partial^2}{\partial \beta^2} & \frac{\partial^2}{\partial \gamma \partial \beta} \\ \frac{\partial^2}{\partial \beta \partial \gamma} & \frac{\partial^2}{\partial \gamma^2} \end{pmatrix} \langle \phi | \hat{Z}_i \hat{Z}_j | \phi \rangle \tag{8.5.142}$$

where,

$$\frac{\partial^2}{\partial \beta^2} \langle \phi | \hat{Z}_i \hat{Z}_j | \phi \rangle = -8\sin 4\beta \langle \psi' | \hat{Y}_i \hat{Z}_j + \hat{Z}_i \hat{Y}_j | \psi' \rangle + 8\cos 4\beta \langle \psi' | \hat{Y}_i \hat{Y}_j | \psi' \rangle \tag{8.5.143}$$

$$\frac{\partial^2}{\partial \gamma^2} \langle \phi | \hat{Z}_i \hat{Z}_j | \phi \rangle = \frac{1}{2} \sin 4\beta \frac{\partial^2}{\partial \gamma^2} \langle \psi' | \hat{Y}_i \hat{Z}_j + \hat{Z}_i \hat{Y}_j | \psi' \rangle + \sin^2 2\beta \frac{\partial^2}{\partial \gamma^2} \langle \psi' | \hat{Y}_i \hat{Y}_j | \psi' \rangle \tag{8.5.144}$$

$$\frac{\partial^2}{\partial \beta \partial \gamma} \langle \phi | \hat{Z}_i \hat{Z}_j | \phi \rangle = 2\cos 4\beta \frac{\partial}{\partial \gamma} \langle \psi' | \hat{Y}_i \hat{Z}_j + \hat{Z}_i \hat{Y}_j | \psi' \rangle + 2\sin 4\beta \frac{\partial}{\partial \gamma} \langle \psi' | \hat{Y}_i \hat{Y}_j | \psi' \rangle \tag{8.5.145}$$

$$= \frac{\partial^2}{\partial \gamma \partial \beta} \langle \phi | \hat{Z}_i \hat{Z}_j | \phi \rangle \tag{8.5.146}$$

and,

$$\frac{\partial^2}{\partial \gamma^2} \langle \psi' | \hat{Y}_i \hat{Z}_j | \psi' \rangle = \sin \gamma \cos^{g-1} \gamma \left[(\cot \gamma - (g-1) \tan \gamma)^2 - \left(\csc^2 \gamma + (g-1) \sec^2 \gamma \right) \right] \tag{8.5.147}$$

$$\frac{\partial^2}{\partial \gamma^2} \langle \psi' | \hat{Z}_i \hat{Y}_j | \psi' \rangle = \sin \gamma \cos^{g-1} \gamma \left[(\cot \gamma - (g-1) \tan \gamma)^2 - \left(\csc^2 \gamma + (g-1) \sec^2 \gamma \right) \right] \tag{8.5.148}$$

$$\frac{\partial^2}{\partial \gamma^2} \langle \psi' | \hat{Y}_i \hat{Y}_j | \psi' \rangle = -\frac{1}{2} \cos^{L_{ij}+R_{ij}} \gamma \left\{ \left(1 - \cos^{T_{ij}} 2\gamma \right) \left[\left(L_{ij} + R_{ij} \right)^2 \tan^2 \gamma - \left(L_{ij} + R_{ij} \right) \sec^2 \gamma \right] \right. \tag{8.5.149}$$

$$-4\cos^{T_{ij}} 2\gamma \left[T_{ij}^2 \tan^2 2\gamma - T_{ij} \sec^2 2\gamma \right] \tag{8.5.150}$$

$$\left. -4T_{ij} \left(L_{ij} + R_{ij} \right) \cos^{T_{ij}} 2\gamma \tan 2\gamma \tan \gamma \right\} \tag{8.5.151}$$

All Plus Simplification of Optimal Parameters of QAOA Depth $P = 1$ (g Regular)

β^*	γ^*	Hessian	Critical Type
$\frac{\pi k}{2}$	πk	$\Sigma_{(i,j)\in \mathrm{E}} \frac{1}{2} \begin{pmatrix} 8\langle\psi'\lvert\hat{Y}_i\hat{Y}_j\rvert\psi'\rangle & \pm 4 \\ \pm 4 & 0 \end{pmatrix}$, where $+$: even g & any k or odd g & even k, $-$: odd g & odd k for k in γ_1^*	Saddle
$\frac{\pi k}{2}$	$\frac{\pi}{2}(2k+1)$	$\Sigma_{(i,j)\in \mathrm{E}} \frac{1}{2} \begin{pmatrix} 8\langle\psi'\lvert\hat{Y}_i\hat{Y}_j\rvert\psi'\rangle\rvert_{\gamma_2^*} & 0 \\ 0 & 0 \end{pmatrix}$	Inconclusive

To obtain the non-trivial optimised parameters γ^*, β^*, by $\nabla \langle\phi\lvert\hat{C}\rvert\phi\rangle = 0$, we have to solve the following set of equations,

$$\frac{\partial}{\partial\beta}\langle\phi\lvert\hat{C}\rvert\phi\rangle = 0 \tag{8.5.152}$$

$$\Rightarrow \tan 4\beta^* = -\frac{4|E|\sin\gamma(\cos\gamma)^{g-1}}{\Sigma_{(i,j)\in \mathrm{E}}(\cos\gamma)^{L_{ij}+R_{ij}}\left(1-\cos^{T_{ij}}2\gamma\right)}\Bigg|_{\gamma^*} \tag{8.5.153}$$

$$\frac{\partial}{\partial\gamma}\langle\phi\lvert\hat{C}\rvert\phi\rangle = 0 \tag{8.5.154}$$

$$\Rightarrow \tan 2\beta^* = -\frac{2|E|\sin\gamma(\cos\gamma)^{g-1}\left[\cot\gamma-(g-1)\tan\gamma\right]}{-\sum_{(i,j)\in \mathrm{E}}\frac{1}{2}\cos^{L_{ij}+R_{ij}}\gamma\left[2T_{ij}\cos^{T_{ij}}2\gamma\tan 2\gamma-\left(L_{ij}+R_{ij}\right)\left(1-\cos^{T_{ij}}2\gamma\right)\tan\gamma\right]}\Bigg|_{\gamma^*} \tag{8.5.155}$$

As non-trivial β^*, γ^* remains unsolved, the second partial derivative test will not be carried out.

8.5.8 Complete graphs ($n-1$ Regular)

A complete graph with n vertices is a graph where all vertices are connected to every other vertices. It has $|E| = \frac{n(n-1)}{2}$ number of edges. The MaxCut value and solution are not trivial and it may seem to be difficult to solve for at first glance, however, it can be solved by hand, though its proof is may not be easy. The solution to be done by hand is to arrange the vertices of the complete graph in a circular ring. The MaxCut line would be along the diameter of the circular ring, where the diameter must separate the vertices evenly. If there is an odd number of vertices, then the number difference between the both separations must be at most one. As a result, the MaxCut value is $\frac{1}{8}\left(2n^2-1+(-1)^n\right)$ and the solution state is simply having vertices on different separation sides to disagree with each other and agree if they are on the same side. One may obtain the expectation value of the unweighted MaxCut Hamiltonian by simply substituting $\ell_{ij} = \xi_{ij} = T_{ij} = n-2$, however, it may not yield any significant insights. Similar to the previous sections we shall consider the use of all plus state simplifications. Suppose the all plus state is used as the QAOA initial state $|+\rangle$, and let $L_{ij} = R_{ij} = 0$ as there are no non-common left and right neighbours of at any edge, then the expressions simplifies to,

All Plus Simplification of QAOA Depth $P = 1$ (Complete)

$$\langle \phi | \hat{C} | \phi \rangle =$$
$$\sum_{(i,j) \in \text{edges}} -\frac{1}{2} + \frac{1}{2} \left(\frac{1}{2} \sin 4\beta \left\langle \psi' \right| \hat{Y}_i \hat{Z}_j + \hat{Z}_i \hat{Y}_j \left| \psi' \right\rangle + \sin^2 2\beta \left\langle \psi' \right| \hat{Y}_i \hat{Y}_j \left| \psi' \right\rangle \right) \tag{8.5.156}$$

where,

$$\left\langle \psi' \right| \hat{Y}_i \hat{Z}_j \left| \psi' \right\rangle = \sin \gamma \cos^{n-2} \gamma \tag{8.5.157}$$
$$\left\langle \psi' \right| \hat{Z}_i \hat{Y}_j \left| \psi' \right\rangle = \sin \gamma \cos^{n-2} \gamma \tag{8.5.158}$$
$$\left\langle \psi' \right| \hat{Y}_i \hat{Y}_j \left| \psi' \right\rangle = \frac{1}{2} \left(1 - \cos^{n-2} 2\gamma \right) \tag{8.5.159}$$

All Plus Simplification of the Gradient (Complete)

$$\nabla \langle \phi | \hat{C} | \phi \rangle = \sum_{(i,j) \in \mathrm{E}} \frac{1}{2} \begin{pmatrix} \frac{\partial}{\partial \beta} \\ \frac{\partial}{\partial \gamma} \end{pmatrix} \langle \phi | \hat{Z}_i \hat{Z}_j | \phi \rangle \tag{8.5.160}$$

where,

$$\frac{\partial}{\partial \beta} \langle \phi | \hat{Z}_i \hat{Z}_j | \phi \rangle = 2 \cos 4\beta \left\langle \psi' \right| \hat{Y}_i \hat{Z}_j + \hat{Z}_i \hat{Y}_j \left| \psi' \right\rangle + 2 \sin 4\beta \left\langle \psi' \right| \hat{Y}_i \hat{Y}_j \left| \psi' \right\rangle \tag{8.5.161}$$
$$\frac{\partial}{\partial \gamma} \langle \phi | \hat{Z}_i \hat{Z}_j | \phi \rangle = \frac{1}{2} \sin 4\beta \frac{\partial}{\partial \gamma} \left\langle \psi' \right| \hat{Y}_i \hat{Z}_j + \hat{Z}_i \hat{Y}_j \left| \psi' \right\rangle + \sin^2 2\beta \frac{\partial}{\partial \gamma} \left\langle \psi' \right| \hat{Y}_i \hat{Y}_j \left| \psi' \right\rangle \tag{8.5.162}$$

and,

$$\frac{\partial}{\partial \gamma} \left\langle \psi' \right| \hat{Y}_i \hat{Z}_j \left| \psi' \right\rangle = \sin \gamma \cos^{n-2} \gamma (\cot \gamma - (n-2) \tan \gamma) \tag{8.5.163}$$
$$\frac{\partial}{\partial \gamma} \left\langle \psi' \right| \hat{Z}_i \hat{Y}_j \left| \psi' \right\rangle = \sin \gamma \cos^{n-2} \gamma (\cot \gamma - (n-2) \tan \gamma) \tag{8.5.164}$$
$$\frac{\partial}{\partial \gamma} \left\langle \psi' \right| \hat{Y}_i \hat{Y}_j \left| \psi' \right\rangle = -(n-2) \cos^{n-2} 2\gamma \tan 2\gamma \tag{8.5.165}$$

All Plus Simplification of the Hessian (Complete)

$$\nabla^2 \langle \phi | \hat{C} | \phi \rangle = \sum_{(i,j) \in \mathrm{E}} \frac{1}{2} \begin{pmatrix} \frac{\partial^2}{\partial \beta^2} & \frac{\partial^2}{\partial \gamma \partial \beta} \\ \frac{\partial^2}{\partial \beta \partial \gamma} & \frac{\partial^2}{\partial \gamma^2} \end{pmatrix} \langle \phi | \hat{Z}_i \hat{Z}_j | \phi \rangle \tag{8.5.166}$$

where,

$$\frac{\partial^2}{\partial \beta^2} \langle \phi | \hat{Z}_i \hat{Z}_j | \phi \rangle = -8 \sin 4\beta \left\langle \psi' \middle| \hat{Y}_i \hat{Z}_j + \hat{Z}_i \hat{Y}_j \middle| \psi' \right\rangle + 8 \cos 4\beta \left\langle \psi' \middle| \hat{Y}_i \hat{Y}_j \middle| \psi' \right\rangle \tag{8.5.167}$$

$$\frac{\partial^2}{\partial \gamma^2} \langle \phi | \hat{Z}_i \hat{Z}_j | \phi \rangle = \frac{1}{2} \sin 4\beta \frac{\partial^2}{\partial \gamma^2} \left\langle \psi' \middle| \hat{Y}_i \hat{Z}_j + \hat{Z}_i \hat{Y}_j \middle| \psi' \right\rangle + \sin^2 2\beta \frac{\partial^2}{\partial \gamma^2} \left\langle \psi' \middle| \hat{Y}_i \hat{Y}_j \middle| \psi' \right\rangle \tag{8.5.168}$$

$$\frac{\partial^2}{\partial \beta \partial \gamma} \langle \phi | \hat{Z}_i \hat{Z}_j | \phi \rangle = 2 \cos 4\beta \frac{\partial}{\partial \gamma} \left\langle \psi' \middle| \hat{Y}_i \hat{Z}_j + \hat{Z}_i \hat{Y}_j \middle| \psi' \right\rangle + 2 \sin 4\beta \frac{\partial}{\partial \gamma} \left\langle \psi' \middle| \hat{Y}_i \hat{Y}_j \middle| \psi' \right\rangle \tag{8.5.169}$$

$$= \frac{\partial^2}{\partial \gamma \partial \beta} \langle \phi | \hat{Z}_i \hat{Z}_j | \phi \rangle \tag{8.5.170}$$

and,

$$\frac{\partial^2}{\partial \gamma^2} \left\langle \psi' \middle| \hat{Y}_i \hat{Z}_j \middle| \psi' \right\rangle = \sin \gamma \cos^{n-2} \gamma \left[(\cot \gamma - (n-2) \tan \gamma)^2 - \left(\csc^2 \gamma + (n-2) \sec^2 \gamma \right) \right] \tag{8.5.171}$$

$$\frac{\partial^2}{\partial \gamma^2} \left\langle \psi' \middle| \hat{Z}_i \hat{Y}_j \middle| \psi' \right\rangle = \sin \gamma \cos^{n-2} \gamma \left[(\cot \gamma - (n-2) \tan \gamma)^2 - \left(\csc^2 \gamma + (n-2) \sec^2 \gamma \right) \right] \tag{8.5.172}$$

$$\frac{\partial^2}{\partial \gamma^2} \left\langle \psi' \middle| \hat{Y}_i \hat{Y}_j \middle| \psi' \right\rangle = 2 \cos^{n-2} 2\gamma \left[(n-2)^2 \tan^2 2\gamma - (n-2) \sec^2 2\gamma \right] \tag{8.5.173}$$

All Plus Simplification of Optimal Parameters of QAOA Depth $P = 1$ (Complete)

β^*	γ^*	Hessian	Critical Type
$\frac{\pi k_{even}}{4}$	$\frac{\pi k_{even}}{2}$	$\lvert E\rvert \begin{pmatrix} 0 & \pm 4 \\ \pm 4 & 0 \end{pmatrix}$, where $+$: n even & any k or n odd & $\frac{k}{2}$ even, $-$: n odd & $\frac{k}{2}$ odd	Saddle
$\frac{\pi k_{even}}{4}$	$\frac{\pi k_{odd}}{2}$	$\lvert E\rvert \begin{pmatrix} \frac{8\pm 8}{2} & 0 \\ 0 & 0 \end{pmatrix}$, where $+$: n odd, $-$: n even	Inconclusive
$\frac{\pi k_{odd}}{4}$	$\frac{\pi k_{even}}{2}$	$\lvert E\rvert \begin{pmatrix} 0 & \pm 4 \\ \pm 4 & (4-2n) \end{pmatrix}$, where $+$: n even & any k or n odd & $\frac{k}{2}$ even, $-$: n odd & $\frac{k}{2}$ odd	Saddle
$\frac{\pi k_{odd}}{4}$	$\frac{\pi k_{odd}}{2}$	$\lvert E\rvert \begin{pmatrix} \frac{8\pm 8}{2} & 0 \\ 0 & \pm(4-2n) \end{pmatrix}$, where $+$: n odd, $-$: n even	Local Minimum when n is odd, Inconclusive when n is even

To obtain the non-trivial optimised parameters γ^*, β^*, by $\nabla \langle \phi | \hat{C} | \phi \rangle = 0$, we have to solve the following set of equations,

$$\frac{\partial}{\partial \beta} \langle \phi | \hat{C} | \phi \rangle = 0 \tag{8.5.174}$$

$$\Rightarrow \tan 4\beta^* = \frac{-4 \sin \gamma^* \cos^{n-2} \gamma^*}{(1 - \cos^{n-2} 2\gamma^*)} \tag{8.5.175}$$

$$\frac{\partial}{\partial \gamma} \langle \phi | \hat{C} | \phi \rangle = 0 \tag{8.5.176}$$

$$\Rightarrow \tan 2\beta^* = \frac{\sin \gamma \cos^{n-2} \gamma^* (\cot \gamma^* - (n-2) \tan \gamma^*)}{(n-2) \cos^{n-2} 2\gamma^* \tan 2\gamma^*} \tag{8.5.177}$$

As non-trivial β^*, γ^* remains unsolved, the second partial derivative test will not be carried out.

8.6 Pauli Decomposition of Expectation of Weighted MaxCut Hamiltonian

Readers at this section are assumed to have read the Pauli Decomposition of the expectation value of the Unweighted MaxCut Hamiltonian in section 5.2. The derivation of the weighted case is largely similar to the unweighted case, we use the same denotation as in the unweighted case, shall skip any frivolous steps or derivation. Let us start by restating the problem:

> For a given set of QAOA parameters up to depth p, $\vec{\beta} = (\beta_1, \ldots, \beta_p)$ and $\vec{\gamma} = (\gamma_1, \ldots, \gamma_p)$ and the initial state $|\psi\rangle$, what is the expectation value of the Weighted MaxCut Hamiltonian, its gradient and Hessian at QAOA depth p, with respect to the local parameters β_p and γ_p, in terms of Pauli operators? Suppose given a MaxCut problem graph $G = \{V, E\}$ of set of labelled vertices V and labelled weighted edges $E = \{(i, j, w) \mid i, j \in V,\ w \in \mathbb{R}\}$.

Let us denote, $\hat{C}_{ij} = w_{ij}\left(-\frac{1}{2}\mathbb{I} + \frac{1}{2}\hat{Z}_i\hat{Z}_j\right)$ as the Weighted MaxCut Hamiltonian of an edge (i,j). Then, we express the expectation of unweighted MaxCut Hamiltonian $\langle\phi|\hat{C}|\phi\rangle$ as a summation, indexed by edges,

$$\langle\phi|\hat{C}|\phi\rangle = \sum_{(i,j)\in \mathrm{E}} \langle\phi|\hat{C}_{ij}|\phi\rangle \tag{8.6.1}$$

where the expectation value of Weighted MaxCut Hamiltonian of an unweighted edge (i,j), $\langle\phi|\hat{C}_{ij}|\phi\rangle$ is given as,

$$\langle\phi|\hat{C}_{ij}|\phi\rangle = \frac{w_{ij}}{2}\left(-1 + \langle\phi|\hat{Z}_i\hat{Z}_j|\phi\rangle\right) \tag{8.6.2}$$

We observe that $\frac{w_{ij}}{2}$ is our expectation scaling prefactor, and -1 is our expectation offset of the observable $\hat{Z}_i\hat{Z}_j$.

Using the algebraic properties of Pauli Operators, $\langle\phi|\hat{Z}_i\hat{Z}_j|\phi\rangle$ is expressed in terms of local parameter β and the QAOA intermediary state $|\psi'\rangle$ as,

$$\begin{gathered}\langle\phi|\hat{Z}_i\hat{Z}_j|\phi\rangle = \\ \cos^2 2\beta\left\langle\psi'\middle|\hat{Z}_i\hat{Z}_j\middle|\psi'\right\rangle + \frac{1}{2}\sin 4\beta\left\langle\psi'\middle|\hat{Y}_i\hat{Z}_j + \hat{Z}_i\hat{Y}_j\middle|\psi'\right\rangle + \sin^2 2\beta\left\langle\psi'\middle|\hat{Y}_i\hat{Y}_j\middle|\psi'\right\rangle\end{gathered} \tag{8.6.3}$$

which is exactly the same as the unweighted version. To express $\langle\phi|\hat{Z}_i\hat{Z}_j|\phi\rangle$ in terms of local parameter γ, it required of us to re-express three terms $\langle\psi'|\hat{Z}_i\hat{Z}_j|\psi'\rangle$, $\langle\psi'|\hat{Y}_i\hat{Z}_j + \hat{Z}_i\hat{Y}_j|\psi'\rangle$ and $\langle\psi'|\hat{Y}_i\hat{Y}_j|\psi'\rangle$ separately, in terms of QAOA output state $|\phi_{p-1}\rangle$. The first term $\langle\psi'|\hat{Z}_i\hat{Z}_j|\psi'\rangle$ is found to be independent of local parameter γ, that is,

$$\left\langle\psi'\middle|\hat{Z}_i\hat{Z}_j\middle|\psi'\right\rangle = \langle\phi_{p-1}|\hat{Z}_i\hat{Z}_j|\phi_{p-1}\rangle \tag{8.6.4}$$

which is also exactly the same as the unweighted version. By using the same derivation from the unweighted case, the expressions for $\langle\psi'|\hat{Y}_i\hat{Z}_j|\psi'\rangle$, $\langle\psi'|\hat{Z}_i\hat{Y}_j|\psi'\rangle$ and $\langle\psi'|\hat{Y}_i\hat{Y}_j|\psi'\rangle$ are as follows,

$$\langle\psi'|\hat{Y}_i\hat{Z}_j|\psi'\rangle = \langle\phi_{p-1}|\left(\cos w_{ij}\gamma\hat{Y}_i\hat{Z}_j + \sin w_{ij}\gamma\hat{X}_i\right)\left[\prod_{(i,v)\in E_{\{i\}}/ij}\left(\cos w_{iv}\gamma I - i\sin w_{iv}\gamma\hat{Z}_i\hat{Z}_v\right)\right]|\phi_{p-1}\rangle \tag{8.6.5}$$

$$\langle\psi'|\hat{Z}_i\hat{Y}_j|\psi'\rangle = \langle\phi_{p-1}|\left(\cos w_{ij}\gamma\hat{Z}_i\hat{Y}_j + \sin w_{ij}\gamma\hat{X}_j\right)\left[\prod_{(j,v)\in E_{\{j\}}/ij}\left(\cos w_{jv}\gamma I - i\sin w_{jv}\gamma\hat{Z}_j\hat{Z}_v\right)\right]|\phi_{p-1}\rangle \tag{8.6.6}$$

$$\langle\psi'|\hat{Y}_i\hat{Y}_j|\psi'\rangle = \langle\phi_{p-1}|\hat{Y}_i\hat{Y}_j\left[\prod_{(u,v)\in E_{\{i,j\}}/ij}\left(\cos w_{uv}\gamma I - i\sin w_{uv}\gamma\hat{Z}_u\hat{Z}_v\right)\right]|\phi_{p-1}\rangle \tag{8.6.7}$$

where $E_{\{i\}}$ refers to the set of all edges that the includes vertex i, $E_{\{i\}}/ij$ refers to the set $E_{\{i\}}$ excluding edge (i,j) and $E_{\{i,j\}}/ij$ refers to the set of all edges that includes the vertex i or j, excluding edge (i,j).

By a simple substitution of newly found expressions of three terms $\langle\psi'|\hat{Z}_i\hat{Z}_j|\psi'\rangle$, $\langle\psi'|\hat{Y}_i\hat{Z}_j + \hat{Z}_i\hat{Y}_j|\psi'\rangle$ and $\langle\psi'|\hat{Y}_i\hat{Y}_j|\psi'\rangle$, we have successfully re-expressed the expectation of Weighted MaxCut Hamiltonian $\langle\phi_p|\hat{C}|\phi_p\rangle$ in terms of Pauli operators and the QAOA parameters β ,γ of depth p. However, by the same argument from the unweighted case, it is required of us to expand the following product sequences as summation, so that the differentiation will not complicate the expressions.

$$\prod_{(i,v)\in E_{\{i\}}/ij} \left(\cos w_{iv}\gamma I - i\sin w_{iv}\gamma \hat{Z}_i\hat{Z}_v\right) \tag{8.6.8}$$

$$\prod_{(j,v)\in E_{\{j\}}/ij} \left(\cos w_{jv}\gamma I - i\sin w_{jv}\gamma \hat{Z}_j\hat{Z}_v\right) \tag{8.6.9}$$

$$\prod_{(u,v)\in E_{\{i,j\}}/ij} \left(\cos w_{uv}\gamma I - i\sin w_{uv}\gamma \hat{Z}_u\hat{Z}_v\right) \tag{8.6.10}$$

Of course, expanding any of these terms is significantly more difficult as it requires a great deal of mathematical visualisation and intuition. Fortunately, such an product expansion, which we are about to attempt, is closely related to the generalised binomial expansion. Interested readers may wish to consult a standard mathematical textbook in elementary algebra for a refresher on binomial expansion. To reduce the difficultly further, notice that the expression forms of these three terms are the same, expanding one will resolve the other two.

Let us consider the first product sequence. If we refer all the edges (i,v), which consist of vertex i, as the left edges, then there are ℓ_{ij} number of such left edges, excluding edge (i,j). Next, we denote the other vertex $v \to l_a$, where index a ranges from 1 to ℓ_{ij} , then the first product sequence can be written as an summation, iterating through index k, as,

$$\prod_{(i,v)\in E_{\{i\}}/ij} \left(\cos w_{iv}\gamma I - i\sin w_{iv}\gamma \hat{Z}_i\hat{Z}_v\right) = \sum_{m=0}^{\ell_{ij}} \left[\left(-i\hat{Z}_i\right)^m \mathbf{D}_i\left(\ell_{ij},m\right)\right] \tag{8.6.11}$$

$$\text{where } \mathbf{D}_i\left(\ell_{ij},m\right) = \sum_{\lambda\in\Lambda_m^{\ell_{ij}}} \left(I \prod_{a_1\in\Theta_{\ell_{ij}}/\lambda} \cos w_{il_{a_1}}\gamma \prod_{a_2\in\lambda} \sin w_{il_{a_2}}\gamma \prod_{a_2\in\lambda} \hat{Z}_{l_{a_2}} \right) \tag{8.6.12}$$

where we have $\mathbf{D}_i\left(\ell_{ij},m\right)$ to denote a complicated term that has a connection to binomial theorem. Here, $\Lambda_m^{\ell_{ij}}$ is a set of all possible m-combinations of elements λ of the index set $\Theta_{\ell_{ij}} = \left\{a \mid 1 \le a \le \ell_{ij},\ a \in \mathbb{Z}\right\}$. Note the index usage of m as an integer for the element combination and index usage of a as an integer for labelling the other vertex $v \to l_a$ on the left edges. An example of calculation $\mathbf{D}_i\left(\ell_{ij}=3,m\right)$ is given in the figure 8.6.1 below.

Example: If $\ell_{ij}=3$, then $\Theta_3=\{1,2,3\}$ and $\mathbf{D}_i(3,m)$ generates the following terms for $0\le m\le 3$, $m\in\mathbb{Z}$,

$$\begin{aligned} & m=0, && \Lambda_0^3=\emptyset \\ \mathbf{D}_i(3,0) &= && I\prod_{k=1}^{3}\left(\cos w_{il_k}\gamma\right) \end{aligned} \tag{8.6.13}$$

$$\begin{aligned} & m=1, && \Lambda_1^3=\{\{1\},\{2\},\{3\}\} \\ \mathbf{D}_i(3,1) &= && \cos w_{il_2}\gamma\cos w_{il_3}\gamma\sin w_{il_1}\gamma\hat{Z}_{l_1} \\ & && +\cos w_{il_1}\gamma\cos w_{il_3}\sin w_{il_2}\gamma\hat{Z}_{l_2} \\ & && +\cos w_{il_1}\gamma\cos w_{il_2}\sin w_{il_3}\gamma\hat{Z}_{l_3} \end{aligned} \tag{8.6.14}$$

$$\begin{aligned} & m=2, && \Lambda_2^3=\{\{2,3\},\{1,3\},\{1,2\}\} \\ \mathbf{D}_i(3,2) &= && \cos w_{il_1}\gamma\sin w_{il_2}\gamma\sin w_{il_3}\gamma\hat{Z}_{l_2}\hat{Z}_{l_3} \\ & && +\cos w_{il_2}\gamma\sin w_{il_1}\gamma\sin w_{il_3}\gamma\hat{Z}_{l_1}\hat{Z}_{l_3} \\ & && +\cos w_{il_3}\gamma\sin w_{il_1}\gamma\sin w_{il_2}\gamma\hat{Z}_{l_1}\hat{Z}_{l_2} \end{aligned} \tag{8.6.15}$$

$$\begin{aligned} & m=3, && \Lambda_3^3=\{\{1,2,3\}\} \\ \mathbf{D}_i(3,3) &= && \prod_{k=1}^{3}\left(\sin w_{il_k}\gamma\hat{Z}_{l_k}\right) \end{aligned} \tag{8.6.16}$$

Figure 8.6.1: An example of calculating $\mathbf{D}_i(\ell_{ij}=3,m)$.

Similarly, if we refer to the edges (j,v) , which consist of vertex j, as the right edges, then there are ξ_{ij} number of right edges, excluding edge (i,j). Afterwards, we denote the other vertex $v\to r_b$, where index b ranges from 1 to ξ_{ij}. Using the symmetry argument and without explicit derivation, the second product sequence can be written as an summation, iterating through index n, as,

$$\prod_{(j,v)\in E_{\{j\}}/ij}\left(\cos w_{jv}\gamma I-i\sin w_{jv}\gamma\hat{Z}_j\hat{Z}_v\right)=\sum_{n=0}^{\xi_{ij}}\left[\left(-i\hat{Z}_j\right)^n\mathbf{D}_j(\xi_{ij},n)\right] \tag{8.6.17}$$

$$\text{where } \mathbf{D}_j(\xi_{ij},n)=\sum_{\lambda\in\Lambda_n^{\xi_{ij}}}\left(I\prod_{b_1\in\Theta_{\xi_{ij}}/\lambda}\cos w_{jr_{b_1}}\gamma\prod_{b_2\in\lambda}\sin w_{jr_{b_2}}\gamma\prod_{b_2\in\lambda}\hat{Z}_{r_{b_2}}\right) \tag{8.6.18}$$

where $\Lambda_n^{\xi_{ij}}$ is a set of all possible n-combinations of elements λ of the index set $\Theta_{\xi_{ij}}=\left\{b\mid 1\le b\le\xi_{ij},\ b\in\mathbb{Z}\right\}$. Consider the third product sequence, we may split the edge set $E_{\{i,j\}/ij}$ into two mutually exclusive edge sets, $E_{\{i\}/ij}$ and $E_{\{j\}/ij}$. $E_{\{i\}/ij}$ is the set of all left edges that contain vertex i, but not edge (i,j). $E_{\{j\}/ij}$ is the set of all right edges that contain vertex j, but not edge (i,j). That is, $E_{\{i,j\}/ij}=E_{\{i\}/ij}\cup E_{\{j\}/ij}$ and $\emptyset=E_{\{i\}/ij}\cap E_{\{j\}/ij}$. By denoting the vertex l_m and r_n as other vertex of the left and right edges respectively and using the same derivation from the unweighted case, the product expansion of the third product sequence can be expressed as,

$$\begin{aligned} &\prod_{(u,v)\in E_{\{i,j\}/ij}}\left(\cos w_{uv}\gamma I-i\sin w_{uv}\gamma\hat{Z}_u\hat{Z}_v\right)= \\ &\sum_{n=0}^{\xi_{ij}}\sum_{m=0}^{\ell_{ij}}\left[(-i)^{m+n}\left(\hat{Z}_i\right)^m\left(\hat{Z}_j\right)^n\mathbf{D}_i(\ell_{ij},m)\mathbf{D}_j(\xi_{ij},n)\right] \end{aligned} \tag{8.6.19}$$

To avoid cumbersome writing, we shall reuse the same denotation of expressions of expectation

values of the Pauli compositions given in figure 5.2.8 from the unweighted version and new extra ones to represent the corresponding weighted expressions as given in figure 8.6.2. Finally, substituting the results back into the expectation value of weighted MaxCut Hamiltonian, $\langle\phi|\hat{C}|\phi\rangle$, we have our desired expressions. From this point onwards, it is straightforward to calculate all the required higher order derivatives as the QAOA parameters β ,γ of depth p are decoupled from the Pauli operators. Thus, the explicit derivation of the higher order derivatives will not be given. The final Pauli decomposition of the expressions of the expectation value of the Weighted MaxCut Hamiltonian $\left\langle\hat{C}\right\rangle_p$, the gradient $\nabla\left\langle\hat{C}\right\rangle_p$ and the Hessian $\nabla^2\left\langle\hat{C}\right\rangle_p$ are given the following three boxes.

$$\pi_{\lambda ci} = \prod_{a_1\in\Theta_{\ell_{ij}}/\lambda}\cos w_{il_{a_1}}\gamma \tag{8.6.20}$$

$$\pi_{\lambda si} = \prod_{a_2\in\lambda}\sin w_{il_{a_2}}\gamma \tag{8.6.21}$$

$$\pi_{\lambda cj} = \prod_{b_1\in\Theta_{\xi_{ij}}/\lambda}\cos w_{jr_{b_1}}\gamma \tag{8.6.22}$$

$$\pi_{\lambda sj} = \prod_{b_2\in\lambda}\sin w_{jr_{b_2}}\gamma \tag{8.6.23}$$

such that,

$$\mathbf{D}_i(\ell_{ij},m) = \sum_{\lambda\in\Lambda_m^{\ell_{ij}}}\left[I(\pi_{\lambda ci})(\pi_{\lambda si})\prod_{a_2\in\lambda}\hat{Z}_{l_{a_2}}\right] \tag{8.6.24}$$

$$\mathbf{D}_j(\xi_{ij},n) = \sum_{\lambda\in\Lambda_n^{\xi_{ij}}}\left[I(\pi_{\lambda cj})(\pi_{\lambda sj})\prod_{b_2\in\lambda}\hat{Z}_{r_{b_2}}\right] \tag{8.6.25}$$

Figure 8.6.2: Extra denotations to simplify cumbersome writing for the weighted version.

Pauli Decomposition of the QAOA Expectation Value of Weighted MaxCut Hamiltonian

$$\langle\phi|\hat{C}|\phi\rangle =$$

$$\sum_{(i,j)\in \mathrm{E}} \frac{w_{ij}}{2}\left(\cos^2 2\beta \left\langle\psi'\right|\hat{Z}_i\hat{Z}_j\left|\psi'\right\rangle + \frac{1}{2}\sin 4\beta \left\langle\psi'\right|\hat{Y}_i\hat{Z}_j + \hat{Z}_i\hat{Y}_j\left|\psi'\right\rangle + \sin^2 2\beta \left\langle\psi'\right|\hat{Y}_i\hat{Y}_j\left|\psi'\right\rangle - 1\right) \tag{8.6.26}$$

where,

$$\left\langle\psi'\right|\hat{Z}_i\hat{Z}_j\left|\psi'\right\rangle \quad = \quad \left\langle\phi_{p-1}\right|\hat{Z}_i\hat{Z}_j\left|\phi_{p-1}\right\rangle \tag{8.6.27}$$

$$\left\langle\psi'\right|\hat{Y}_i\hat{Z}_j\left|\psi'\right\rangle =$$

$$\sum_{m=0}^{\ell_{ij}} \sum_{\lambda\in\Lambda_m^{\ell_{ij}}} \left[(-i)^m \left(\pi_{\lambda ci}\right)\left(\pi_{\lambda si}\right)\left(\cos w_{ij}\gamma\left\langle y_i z_j z_i^m\right\rangle_\lambda + \sin w_{ij}\gamma\langle x_i z_i^m\rangle_\lambda\right)\right] \tag{8.6.28}$$

$$\left\langle\psi'\right|\hat{Z}_i\hat{Y}_j\left|\psi'\right\rangle =$$

$$\sum_{n=0}^{\xi_{ij}} \sum_{\lambda\in\Lambda_n^{\xi_{ij}}} \left[(-i)^n \left(\pi_{\lambda cj}\right)\left(\pi_{\lambda sj}\right)\left(\cos w_{ij}\gamma\left\langle z_i y_j z_j^n\right\rangle_\lambda + \sin w_{ij}\gamma\left\langle x_j z_j^n\right\rangle_\lambda\right)\right] \tag{8.6.29}$$

$$\left\langle\psi'\right|\hat{Y}_i\hat{Y}_j\left|\psi'\right\rangle =$$

$$\sum_{n=0}^{\xi_{ij}}\sum_{m=0}^{\ell_{ij}} \sum_{\lambda_1\in\Lambda_m^{\ell_{ij}}} \sum_{\lambda_2\in\Lambda_n^{\xi_{ij}}} \left[(-i)^{m+n}\left(\pi_{\lambda_1 ci}\right)\left(\pi_{\lambda_1 si}\right)\left(\pi_{\lambda_2 cj}\right)\left(\pi_{\lambda_2 sj}\right)\left\langle y_i y_j z_i^m z_j^n\right\rangle_{\lambda_1,\lambda_2}\right] \tag{8.6.30}$$

Pauli Decomposition of the Gradient of the Expectation Value (Weighted)

$$\nabla \langle \phi | \hat{C} | \phi \rangle = \sum_{(i,j) \in \mathrm{E}} \frac{w_{ij}}{2} \begin{pmatrix} \frac{\partial}{\partial \beta} \\ \frac{\partial}{\partial \gamma} \end{pmatrix} \langle \phi | \hat{Z}_i \hat{Z}_j | \phi \rangle \tag{8.6.31}$$

where,

$$\frac{\partial}{\partial \beta} \langle \phi | \hat{Z}_i \hat{Z}_j | \phi \rangle = 2\cos 4\beta \langle \psi' | \hat{Y}_i \hat{Z}_j + \hat{Z}_i \hat{Y}_j | \psi' \rangle + 2\sin 4\beta \langle \psi' | \hat{Y}_i \hat{Y}_j - \hat{Z}_i \hat{Z}_j | \psi' \rangle \tag{8.6.32}$$

$$\frac{\partial}{\partial \gamma} \langle \phi | \hat{Z}_i \hat{Z}_j | \phi \rangle = \frac{1}{2} \sin 4\beta \frac{\partial}{\partial \gamma} \langle \psi' | \hat{Y}_i \hat{Z}_j + \hat{Z}_i \hat{Y}_j | \psi' \rangle + \sin^2 2\beta \frac{\partial}{\partial \gamma} \langle \psi' | \hat{Y}_i \hat{Y}_j | \psi' \rangle \tag{8.6.33}$$

and,

$$\frac{\partial}{\partial \gamma} \langle \psi' | \hat{Y}_i \hat{Z}_j | \psi' \rangle =$$

$$\sum_{m=0}^{\ell_{ij}} \sum_{\lambda \in \Lambda_m^{\ell_{ij}}} (-i)^m (\pi_{\lambda ci}) (\pi_{\lambda si})$$

$$\times \left\{ \left[\theta_\lambda^i - w_{ij} \tan w_{ij} \gamma \right] \cos w_{ij} \gamma \left\langle y_i z_j z_i^k \right\rangle_\lambda + \left[\theta_\lambda^i + w_{ij} \cot w_{ij} \gamma \right] \sin w_{ij} \gamma \left\langle x_i z_i^k \right\rangle_\lambda \right\} \tag{8.6.34}$$

$$\frac{\partial}{\partial \gamma} \langle \psi' | \hat{Z}_i \hat{Y}_j | \psi' \rangle =$$

$$\sum_{n=0}^{\xi_{ij}} \sum_{\lambda \in \Lambda_n^{\xi_{ij}}} (-i)^n (\pi_{\lambda cj}) (\pi_{\lambda sj})$$

$$\times \left\{ \left[\theta_\lambda^j - w_{ij} \tan w_{ij} \gamma \right] \cos w_{ij} \gamma \left\langle z_i y_j z_j^n \right\rangle_\lambda + \left[\theta_\lambda^j + w_{ij} \cot w_{ij} \gamma \right] \sin w_{ij} \gamma \left\langle x_j z_j^n \right\rangle_\lambda \right\} \tag{8.6.35}$$

$$\frac{\partial}{\partial \gamma} \langle \psi' | \hat{Y}_i \hat{Y}_j | \psi' \rangle =$$

$$\sum_{n=0}^{\xi_{ij}} \sum_{m=0}^{\ell_{ij}} \sum_{\lambda_1 \in \Lambda_m^{\ell_{ij}}} \sum_{\lambda_2 \in \Lambda_n^{\xi_{ij}}} \left[(-i)^{m+n} (\pi_{\lambda_1 ci}) (\pi_{\lambda_1 si}) (\pi_{\lambda_2 cj}) (\pi_{\lambda_2 sj}) \left(\theta_{\lambda_1}^i + \theta_{\lambda_2}^j \right) \left\langle y_i y_j z_i^m z_j^n \right\rangle_{\lambda_1, \lambda_2} \right] \tag{8.6.36}$$

Note,

$$\theta_\lambda^i = \left(\sum_{a_1 \in \Theta_{\ell_{ij}} / \lambda} -w_{il_{a_1}} \tan w_{il_{a_1}} \gamma \right) + \left(\sum_{a_2 \in \lambda} w_{il_{a_2}} \cot w_{il_{a_2}} \gamma \right) \tag{8.6.37}$$

$$\theta_\lambda^j = \left(\sum_{b_1 \in \Theta_{\xi_{ij}} / \lambda} -w_{jr_{b_1}} \tan w_{jr_{b_1}} \gamma \right) + \left(\sum_{b_2 \in \lambda} w_{jr_{b_2}} \cot w_{jr_{b_2}} \gamma \right) \tag{8.6.38}$$

such that,

$$\frac{\partial}{\partial \gamma} \left[(\pi_{\lambda ci}) (\pi_{\lambda si}) \right] = (\pi_{\lambda ci}) (\pi_{\lambda si}) \left(\theta_\lambda^i \right) \tag{8.6.39}$$

$$\frac{\partial}{\partial \gamma} \left[(\pi_{\lambda cj}) (\pi_{\lambda sj}) \right] = (\pi_{\lambda cj}) (\pi_{\lambda sj}) \left(\theta_\lambda^j \right) \tag{8.6.40}$$

Pauli Decomposition of the Hessian of the Expectation Value (Weighted)

$$\nabla^2 \langle \phi | \hat{C} | \phi \rangle = \sum_{(i,j)\in \mathrm{E}} \frac{w_{ij}}{2} \begin{pmatrix} \frac{\partial^2}{\partial \beta^2} & \frac{\partial^2}{\partial \gamma \partial \beta} \\ \frac{\partial^2}{\partial \beta \partial \gamma} & \frac{\partial^2}{\partial \gamma^2} \end{pmatrix} \langle \phi | \hat{Z}_i \hat{Z}_j | \phi \rangle \tag{8.6.41}$$

where,

$$\frac{\partial^2}{\partial \beta^2} \langle \phi | \hat{Z}_i \hat{Z}_j | \phi \rangle = -8 \sin 4\beta \left\langle \psi' \middle| \hat{Y}_i \hat{Z}_j + \hat{Z}_i \hat{Y}_j \middle| \psi' \right\rangle + 8 \cos 4\beta \left\langle \psi' \middle| \hat{Y}_i \hat{Y}_j - \hat{Z}_i \hat{Z}_j \middle| \psi' \right\rangle \tag{8.6.42}$$

$$\frac{\partial^2}{\partial \gamma^2} \langle \phi | \hat{Z}_i \hat{Z}_j | \phi \rangle = \frac{1}{2} \sin 4\beta \frac{\partial^2}{\partial \gamma^2} \left\langle \psi' \middle| \hat{Y}_i \hat{Z}_j + \hat{Z}_i \hat{Y}_j \middle| \psi' \right\rangle + \sin^2 2\beta \frac{\partial^2}{\partial \gamma^2} \left\langle \psi' \middle| \hat{Y}_i \hat{Y}_j \middle| \psi' \right\rangle \tag{8.6.43}$$

$$\frac{\partial^2}{\partial \beta \partial \gamma} \langle \phi | \hat{Z}_i \hat{Z}_j | \phi \rangle = 2 \cos 4\beta \frac{\partial}{\partial \gamma} \left\langle \psi' \middle| \hat{Y}_i \hat{Z}_j + \hat{Z}_i \hat{Y}_j \middle| \psi' \right\rangle + 2 \sin 4\beta \frac{\partial}{\partial \gamma} \left\langle \psi' \middle| \hat{Y}_i \hat{Y}_j \middle| \psi' \right\rangle \tag{8.6.44}$$

$$= \frac{\partial^2}{\partial \gamma \partial \beta} \langle \phi | \hat{Z}_i \hat{Z}_j | \phi \rangle \tag{8.6.45}$$

and,

$$\frac{\partial^2}{\partial \gamma^2} \left\langle \psi' \middle| \hat{Y}_i \hat{Z}_j \middle| \psi' \right\rangle =$$

$$\sum_{m=0}^{\ell_{ij}} \sum_{\lambda \in \Lambda_m^{\ell_{ij}}} (-i)^m \left(\pi_{\lambda ci}\right) \left(\pi_{\lambda si}\right)$$

$$\times \left\{ \left[\left(\theta_\lambda^i - w_{ij} \tan w_{ij}\gamma \right)^2 + \left(\left(\theta_\lambda^i\right)' - w_{ij}^2 \sec^2 w_{ij}\gamma \right) \right] \cos w_{ij}\gamma \left\langle y_i z_j z_i^m \right\rangle_\lambda \right.$$

$$\left. + \left[\left(\theta_\lambda^i + w_{ij} \cot w_{ij}\gamma \right)^2 + \left(\left(\theta_\lambda^i\right)' - w_{ij}^2 \csc^2 w_{ij}\gamma \right) \right] \sin w_{ij}\gamma \left\langle x_i z_i^m \right\rangle_\lambda \right\} \tag{8.6.46}$$

$$\frac{\partial^2}{\partial \gamma^2} \left\langle \psi' \middle| \hat{Z}_i \hat{Y}_j \middle| \psi' \right\rangle =$$

$$\sum_{n=0}^{\xi_{ij}} \sum_{\lambda \in \Lambda_n^{\xi_{ij}}} (-i)^n \left(\pi_{\lambda cj}\right) \left(\pi_{\lambda sj}\right)$$

$$\times \left\{ \left[\left(\theta_\lambda^j - w_{ij} \tan w_{ij}\gamma \right)^2 + \left(\left(\theta_\lambda^j\right)' - w_{ij}^2 \sec^2 w_{ij}\gamma \right) \right] \cos w_{ij}\gamma \left\langle z_i y_j z_j^n \right\rangle_\lambda \right.$$

$$\left. + \left[\left(\theta_\lambda^j + w_{ij} \cot w_{ij}\gamma \right)^2 + \left(\left(\theta_\lambda^j\right)' - w_{ij}^2 \csc^2 w_{ij}\gamma \right) \right] \sin w_{ij}\gamma \left\langle x_j z_j^n \right\rangle_\lambda \right\} \tag{8.6.47}$$

$$\frac{\partial^2}{\partial \gamma^2} \left\langle \psi' \middle| \left(\hat{Y}_i \hat{Y}_j\right) \middle| \psi' \right\rangle =$$

$$\sum_{n=0}^{\xi_{ij}} \sum_{m=0}^{\ell_{ij}} \sum_{\lambda_1 \in \Lambda_m^{\ell_{ij}}} \sum_{\lambda_2 \in \Lambda_n^{\xi_{ij}}} \left\{ (-i)^{m+n} \left(\pi_{\lambda_1 ci}\right) \left(\pi_{\lambda_1 si}\right) \left(\pi_{\lambda_2 cj}\right) \left(\pi_{\lambda_2 sj}\right) \right.$$

$$\left. \times \left[\left(\theta_{\lambda_1}^i + \theta_{\lambda_2}^j \right)^2 + \left(\theta_{\lambda_1}^i\right)' + \left(\theta_{\lambda_2}^j\right)' \right] \left(\left\langle y_i y_j z_i^m z_j^n \right\rangle_{\lambda_1, \lambda_2} \right) \right\} \tag{8.6.48}$$

note,

$$\left(\theta_\lambda^i\right)' = \left(\sum_{a_1 \in \Theta_{\ell_{ij}}/\lambda} -w_{il_{a_1}}^2 \sec^2 w_{il_{a_1}}\gamma \right) + \left(\sum_{a_2 \in \lambda} -w_{il_{a_2}}^2 \csc^2 w_{il_{a_2}}\gamma \right) \tag{8.6.49}$$

$$\left(\theta_\lambda^j\right)' = \left(\sum_{b_1 \in \Theta_{\xi_{ij}}/\lambda} -w_{jr_{b_1}}^2 \sec^2 w_{jr_{b_1}}\gamma \right) + \left(\sum_{b_2 \in \lambda} -w_{jr_{b_2}}^2 \csc^2 w_{jr_{b_2}}\gamma \right) \tag{8.6.50}$$

8.6.1 All Plus State Simplifications

Readers in this section are assumed to have read the all plus state simplification unweighted case in appendix 8.4. We may apply all plus state simplification on the Pauli decomposition of the expectation value of the Weighted MaxCut Hamiltonian, that is let QAOA total depth $P = 1$ and suppose the initial QAOA state $|\psi\rangle$ is given as the all plus state where each qubit is initialised as $|+\rangle = \frac{1}{\sqrt{2}}(|0\rangle + |1\rangle)$. The same simplification arguments from the unweighted case can be used here. Then, by the substitution of $|\psi\rangle = |+\rangle^{\otimes n} = |\phi_0\rangle$ into summation terms, indexed by m,n of Pauli decomposition of the expectation value of the Weighted MaxCut Hamiltonian, we have,

$$\langle +|\hat{Z}_i\hat{Z}_j|+\rangle = 0 \tag{8.6.51}$$

$$\sum_{\lambda\in\Lambda_m^{\ell_{ij}}}\left[(\pi_{\lambda ci})(\pi_{\lambda si})\langle +|\hat{Y}_i\hat{Z}_j(\hat{Z}_i)^{md}\left(I\prod_{a\in\lambda}\hat{Z}_{l_a}\right)|+\rangle\right] = 0 \quad \forall m\geq 0 \tag{8.6.52}$$

$$\sum_{\lambda\in\Lambda_m^{\ell_{ij}}}\left[(\pi_{\lambda ci})(\pi_{\lambda si})\langle +|\hat{X}_i(\hat{Z}_i)^{m}\left(I\prod_{a\in\lambda}\hat{Z}_{l_a}\right)|+\rangle\right] = \begin{cases}0 & \forall m>0\\ \prod_{k=1}^{\ell_{ij}}(\cos w_{il_k}\gamma) & m=0\end{cases} \tag{8.6.53}$$

$$\sum_{\lambda\in\Lambda_n^{\xi_{ij}}}\left[(\pi_{\lambda cj})(\pi_{\lambda sj})\langle +|\hat{Z}_i\hat{Y}_j(\hat{Z}_j)^{n}\left(I\prod_{b\in\lambda}\hat{Z}_{r_b}\right)|+\rangle\right] = 0 \quad \forall n\geq 0 \tag{8.6.54}$$

$$\sum_{\lambda\in\Lambda_n^{\xi_{ij}}}\left[(\pi_{\lambda cj})(\pi_{\lambda sj})\langle +|\hat{X}_j(\hat{Z}_j)^{n}\left(I\prod_{b\in\lambda}\hat{Z}_{r_b}\right)|+\rangle\right] = \begin{cases}0 & \forall n>0\\ \prod_{k=1}^{\xi_{ij}}(\cos w_{jr_k}\gamma) & n=0\end{cases} \tag{8.6.55}$$

Figure 8.6.3: Calculated results of the summation terms of expectations of Pauli compositions at QAOA depth $p = 1$ using the all plus state $|+\rangle^{\otimes n}$ as the initial state.

Note that we have avoid calculating

$$S = \sum_{\lambda_1\in\Lambda_m^{\ell_{ij}}}\sum_{\lambda_2\in\Lambda_n^{\xi_{ij}}}\left[(\pi_{\lambda_1 ci})(\pi_{\lambda_1 si})(\pi_{\lambda_2 cj})(\pi_{\lambda_2 sj})\langle +|\hat{Y}_i\hat{Y}_j(\hat{Z}_i)^m(\hat{Z}_j)^n\left(I\prod_{a\in\lambda_1}\hat{Z}_{l_a}\right)\left(\prod_{b\in\lambda_2}\hat{Z}_{r_b}\right)|+\rangle\right] \tag{8.6.56}$$

as it is slightly more complicated. Here, note that the contributing Pauli composition is a double $\hat{X}_j\hat{X}_i$. It is necessary that $m = n =$ odd, such that the Pauli composition consists a double $\hat{X}_j\hat{X}_i$, so that,

$$S = -\sum_{\lambda_1\in\Lambda_m^{\ell_{ij}}}\sum_{\lambda_2\in\Lambda_n^{\xi_{ij}}}\left[(\pi_{\lambda_1 ci})(\pi_{\lambda_1 si})(\pi_{\lambda_2 cj})(\pi_{\lambda_2 sj})\langle +|\hat{X}_j\hat{X}_i\left(I\prod_{a\in\lambda_1}\hat{Z}_{l_a}\right)\left(\prod_{b\in\lambda_2}\hat{Z}_{r_b}\right)|+\rangle\right],\quad m=n=\text{odd} \tag{8.6.57}$$

Following the same argument in the unweighted case, the condition $m = n =$ odd, is insufficient for simplification as the term $\left(I\prod_{a\in\lambda_1}\hat{Z}_{l_a}\right)\left(\prod_{b\in\lambda_2}\hat{Z}_{r_b}\right)$ may or may not be an identity I. $\prod_{a\in\lambda_1}\hat{Z}_{l_a}\prod_{b_2\in\lambda_2}\hat{Z}_{r_b} = I$ whenever the sets $\lambda_1\equiv\lambda_2$ are equivalent. Under this set equivalent condition, each of both sets has $\begin{pmatrix} T_{ij} \\ m \end{pmatrix}$ number of indexes that corresponds to the label of the common vertex, such that the common vertex forms a triangle with a common edge (i,j). Note that we use T_{ij} to denote the number of triangles with a common edge (i,j). Thus, $\sum_{\lambda_1\in\Lambda_m^{\ell_{ij}}}\sum_{\lambda_2\in\Lambda_m^{\xi_{ij}}}\left(I\prod_{a\in\lambda_1}\hat{Z}_{l_a}\right)\left(\prod_{b\in\lambda_2}\hat{Z}_{r_b}\right)$ will contain $\begin{pmatrix} T_{ij} \\ m \end{pmatrix}$ number of such identities. To simplify the calculations, we may split up ℓ_{ij} and ξ_{ij} the number of left and right edges into edges that does and does not form a triangle with edge (i,j). Let L_{ij} and R_{ij} be the number of left and right edges that does not form a triangle with edge (i,j). Then, we rewrite, $\ell_{ij} = L_{ij} + T_{ij}$ and $\xi_{ij} = R_{ij} + T_{ij}$. Also, the weights re-denote as follows: Let w_{ifl_k} and

w_{jfr_k} be re-denoted as left and right triangle-free weights attached to edge (i,j) respectively, w_{itl_d} and w_{jtr_d} be left and right triangle weights attached to edge (i,j) respectively. A graphical representation of a weighted subgraph of edge (i,j) of weight w_{ij} is given in figure 8.4.2. As a result, we may express,

$$S = \begin{cases} \left(\prod_{k=1}^{L_{ij}} \cos w_{ifl_k}\gamma\right)\left(\prod_{k=1}^{R_{ij}} \cos w_{jfr_k}\gamma\right)\mathbf{A}_{i,j}\left(T_{ij},m\right) & m=n=\text{odd} \\ 0 & \text{Otherwise} \end{cases} \tag{8.6.58}$$

$$\text{where } \mathbf{A}_{i,j}\left(T_{ij},m\right) = \sum_{\tau\in\Lambda_m^{T_{ij}}}\left[\begin{pmatrix} T_{ij} \\ m \end{pmatrix}\left(\prod_{d_1\in\Theta_{T_{ij}}/\tau} \cos w_{itl_{d_1}}\gamma\cos w_{jtr_{d_1}}\gamma\right)\left(\prod_{d_2\in\tau} \sin w_{itl_{d_2}}\gamma\sin w_{jtr_{d_2}}\gamma\right)\right] \tag{8.6.59}$$

Finally, by substitution and calculation, we have our all plus simplification of the QAOA depth $P=1$ expectation value of the Weighted MaxCut Hamiltonian $\langle\phi|\hat{C}|\phi\rangle$ as given in the box below. The explicit derivation of $\langle\psi'|\hat{Y}_i\hat{Y}_j|\psi'\rangle$ in equation 8.6.64 is given in figure 8.6.5 below. A reduced version of this for weighted triangle-free MaxCut hamiltonian was first obtained by Stuart Hadfield [Had18] and later to include vertex bias by Willsch et al [Wil+19]. Notice that expectation value of the Weighted MaxCut Hamiltonian $\langle\phi|\hat{C}|\phi\rangle$ in equation 8.6.60 can be reduced to unweighted case by taking all edge weights to be 1. The calculation of the gradient and Hessian of $\langle\phi|\hat{C}|\phi\rangle$ are pretty straightforward, therefore, explicit derivation will not be given, the results are given in the following boxes below.

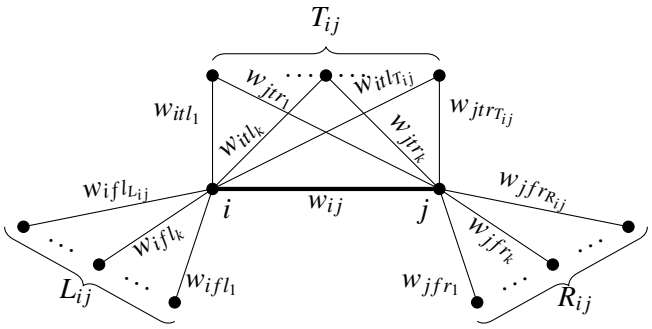

Figure 8.6.4: A weighted subgraph of edge e of weight w_e that is connected to L, R and T number of vertices on the left, right and both of the vertices of the weighted edge e respectively.

All Plus Simplification of the QAOA Expectation Value of Weighted MaxCut Hamiltonian

$$\langle\phi|\hat{C}|\phi\rangle =$$

$$\sum_{(i,j)\in \text{edges}} \frac{w_{ij}}{2}\left(\frac{1}{2}\sin 4\beta \left\langle\psi'\right|\hat{Y}_i\hat{Z}_j+\hat{Z}_i\hat{Y}_j\left|\psi'\right\rangle+\sin^2 2\beta\left\langle\psi'\right|\hat{Y}_i\hat{Y}_j\left|\psi'\right\rangle-1\right) \tag{8.6.60}$$

where,

$$\left\langle\psi'\right|\hat{Z}_i\hat{Z}_j\left|\psi'\right\rangle = 0 \tag{8.6.61}$$

$$\left\langle\psi'\right|\hat{Y}_i\hat{Z}_j\left|\psi'\right\rangle = \sin w_{ij}\gamma\left(\pi_{cifl}\right)\left(\pi_{citl}\right) \tag{8.6.62}$$

$$\left\langle\psi'\right|\hat{Z}_i\hat{Y}_j\left|\psi'\right\rangle = \sin w_{ij}\gamma\left(\pi_{cjfr}\right)\left(\pi_{\lambda cjtr}\right) \tag{8.6.63}$$

$$\left\langle\psi'\right|\hat{Y}_i\hat{Y}_j\left|\psi'\right\rangle = \frac{1}{2}\left(\pi_{cifl}\right)\left(\pi_{cjfr}\right)\left(\pi^{+}_{cijt}-\pi^{-}_{cijt}\right) \tag{8.6.64}$$

note,

$$\pi_{cifl} = \prod_{k=1}^{L_{ij}}\cos w_{ifl_k}\gamma \tag{8.6.65}$$

$$\pi_{citl} = \prod_{k=1}^{T_{ij}}\cos w_{itl_k}\gamma \tag{8.6.66}$$

$$\pi_{cjfr} = \prod_{k=1}^{R_{ij}}\cos w_{jfr_k}\gamma \tag{8.6.67}$$

$$\pi_{\lambda cjtr} = \prod_{k=1}^{T_{ij}}\cos w_{jtr_k}\gamma \tag{8.6.68}$$

$$\pi^{+}_{cijt} = \prod_{k=1}^{T_{ij}}\cos\left(w_{itl_k}\gamma-w_{jtr_k}\gamma\right) \tag{8.6.69}$$

$$\pi^{-}_{cijt} = \prod_{k=1}^{T_{ij}}\cos\left(w_{itl_k}\gamma+w_{jtr_k}\gamma\right) \tag{8.6.70}$$

such that,

$$\left(\pi_{cifl}\right)\left(\pi_{citl}\right) = \prod_{k=1}^{\ell_{ij}}\left(\cos w_{il_k}\gamma\right) \tag{8.6.71}$$

$$\left(\pi_{cjfr}\right)\left(\pi_{\lambda cjtr}\right) = \prod_{k=1}^{\xi_{ij}}\left(\cos w_{jr_k}\gamma\right) \tag{8.6.72}$$

$$\langle \psi' | \hat{Y}_i \hat{Y}_j | \psi' \rangle \tag{8.6.73}$$

$$= \sum_{n=0}^{\xi_{ij}} \sum_{m=0}^{\ell_{ij}} \langle + | (-i)^{m+n} \hat{Y}_i \hat{Y}_j \left(\hat{Z}_i\right)^m \left(\hat{Z}_j\right)^m \mathbf{D}_i \left(\ell_{ij}, m\right) \mathbf{D}_j \left(\xi_{ij}, n\right) | + \rangle \tag{8.6.74}$$

$$| \quad \text{Keeping only } n = m = \text{odd and counting only contributions by triangles.} \tag{8.6.75}$$

$$= \left(\prod_{k=1}^{L_{ij}} \cos w_{ifl_k} \gamma \right) \left(\prod_{k=1}^{R_{ij}} \cos w_{jfr_k} \gamma \right) \sum_{m=n=1,odd}^{m=\xi,\, n=\ell} \mathbf{A}_{ij} \left(T_{ij}, m\right) \underbrace{\langle + | \hat{X}_i \hat{X}_j | + \rangle}_{1} \tag{8.6.76}$$

$$| \quad \text{Using the sum of odd terms of a binomial expansion} \tag{8.6.77}$$

$$= \left(\prod_{k=1}^{L_{ij}} \cos w_{ifl_k} \gamma \right) \left(\prod_{k=1}^{R_{ij}} \cos w_{jfr_k} \gamma \right) \tag{8.6.78}$$

$$\times \frac{1}{2} \left\{ \left[\prod_{k=1}^{T_{ij}} \left(\cos w_{itl_k} \gamma \cos w_{jtr_k} \gamma + \sin w_{itl_k} \gamma \sin w_{jtr_k} \gamma \right) \right] - \left[\prod_{k=1}^{T_{ij}} \cos w_{itl_k} \gamma \cos w_{jtr_k} \gamma - \sin w_{itl_k} \gamma \sin w_{jtr_k} \gamma \right] \right\} \tag{8.6.79}$$

$$= \frac{1}{2} \left(\prod_{k=1}^{L_{ij}} \cos w_{ifl_k} \gamma \right) \left(\prod_{k=1}^{R_{ij}} \cos w_{jfr_k} \gamma \right) \left\{ \left[\prod_{k=1}^{T_{ij}} \cos \left(w_{itl_k} \gamma - w_{jtr_k} \gamma \right) \right] - \left[\prod_{k=1}^{T} \cos \left(w_{itl_k} \gamma + w_{jtr_k} \gamma \right) \right] \right\} \tag{8.6.80}$$

$$= \frac{1}{2} \left(\pi_{cifl} \right) \left(\pi_{cjfr} \right) \left(\pi^{+}_{cijt} - \pi^{-}_{cijt} \right) \tag{8.6.81}$$

Note that we have used,

$$\sum_{m=n=1,odd}^{m=\xi,\, n=\ell} \left[\mathbf{A}_{i,j} \left(T_{ij}, m\right) \right] =$$

$$\frac{1}{2} \left\{ \left[\prod_{k=1}^{T_{ij}} \left(\cos w_{itl_k} \gamma \cos w_{jtr_k} \gamma + \sin w_{itl_k} \gamma \sin w_{jtr_k} \gamma \right) \right] - \left[\prod_{k=1}^{T_{ij}} \cos \cos w_{itl_k} \gamma \cos w_{jtr_k} \gamma - \sin w_{itl_k} \gamma \sin w_{jtr_k} \gamma \right] \right\} \tag{8.6.82}$$

which is a unproven conjecture based on the generalisation of sum of odd terms of a binomial expansion. A rigorous proof of equation 8.6.82 shall be postponed for future research.

Figure 8.6.5: The explicit derivation of the result of weighted $\langle + | e^{i\gamma \hat{C}} \hat{Y}_i \hat{Y}_j e^{-i\gamma \hat{C}} | + \rangle$.

All Plus Simplification of the Gradient of the Expectation Value (Weighted)

$$\nabla \langle \phi | \hat{C} | \phi \rangle = \sum_{(i,j) \in \mathrm{E}} \frac{w_{ij}}{2} \begin{pmatrix} \frac{\partial}{\partial \beta} \\ \frac{\partial}{\partial \gamma} \end{pmatrix} \langle \phi | \hat{Z}_i \hat{Z}_j | \phi \rangle \tag{8.6.83}$$

where,

$$\frac{\partial}{\partial \beta} \langle \phi | \hat{Z}_i \hat{Z}_j | \phi \rangle = 2\cos 4\beta \langle \psi' | \hat{Y}_i \hat{Z}_j + \hat{Z}_i \hat{Y}_j | \psi' \rangle + 2\sin 4\beta \langle \psi' | \hat{Y}_i \hat{Y}_j | \psi' \rangle \tag{8.6.84}$$

$$\frac{\partial}{\partial \gamma} \langle \phi | \hat{Z}_i \hat{Z}_j | \phi \rangle = \frac{1}{2} \sin 4\beta \frac{\partial}{\partial \gamma} \langle \psi' | \hat{Y}_i \hat{Z}_j + \hat{Z}_i \hat{Y}_j | \psi' \rangle + \sin^2 2\beta \frac{\partial}{\partial \gamma} \langle \psi' | \hat{Y}_i \hat{Y}_j | \psi' \rangle \tag{8.6.85}$$

and,

$$\frac{\partial}{\partial \gamma} \langle \psi' | \hat{Y}_i \hat{Z}_j | \psi' \rangle = \sin w_{ij}\gamma \left(\pi_{cifl}\right) \left(\pi_{citl}\right) \left[t_{ifl} + t_{itl} + \left(w_{ij} \cot w_{ij}\gamma\right)\right] \tag{8.6.86}$$

$$\frac{\partial}{\partial \gamma} \langle \psi' | \hat{Z}_i \hat{Y}_j | \psi' \rangle = \sin w_{ij}\gamma \left(\pi_{cjfr}\right) \left(\pi_{\lambda cjtr}\right) \left[t_{jfr} + t_{jtr} + \left(w_{ij} \cot w_{ij}\gamma\right)\right] \tag{8.6.87}$$

$$\frac{\partial}{\partial \gamma} \langle \psi' | \hat{Y}_i \hat{Y}_j | \psi' \rangle = -\frac{1}{2} \left(\pi_{cifl}\right) \left(\pi_{cjfr}\right) \left\{ \left[t_{ifl} + t_{jfr} + s_-\right] \left(\pi^-_{cijt}\right) - \left[t_{ifl} + t_{jfr} + s_+\right] \left(\pi^+_{cijt}\right) \right\} \tag{8.6.88}$$

note,

$$t_{ifl} = \sum_{k=1}^{L_{ij}} -w_{ifl_k} \tan w_{ifl_k}\gamma \tag{8.6.89}$$

$$t_{itl} = \sum_{k=1}^{T_{ij}} -w_{itl_k} \tan w_{itl_k}\gamma \tag{8.6.90}$$

$$t_{jfr} = \sum_{k=1}^{R_{ij}} -w_{jfr_k} \tan w_{jfr_k}\gamma \tag{8.6.91}$$

$$t_{jtr} = \sum_{k=1}^{T_{ij}} -w_{jtr_k} \tan w_{jtr_k}\gamma \tag{8.6.92}$$

$$s_- = \sum_{k=1}^{T_{ij}} -\left(w_{itl_k} - w_{jtr_k}\right) \sin\left(w_{itl_k}\gamma - w_{jtr_k}\gamma\right) \tag{8.6.93}$$

$$s_+ = \sum_{k=1}^{T_{ij}} -\left(w_{itl_k} + w_{jtr_k}\right) \sin\left(w_{itl_k}\gamma + w_{jtr_k}\gamma\right) \tag{8.6.94}$$

such that,

$$\frac{\partial}{\partial \gamma} \pi_{cifl} = \left(\pi_{cifl}\right) \left(t_{ifl}\right) \tag{8.6.95}$$

$$\frac{\partial}{\partial \gamma} \pi_{citl} = \left(\pi_{citl}\right) \left(t_{itl}\right) \tag{8.6.96}$$

$$\frac{\partial}{\partial \gamma} \pi_{cjfr} = \left(\pi_{cjfr}\right) \left(t_{jfr}\right) \tag{8.6.97}$$

$$\frac{\partial}{\partial \gamma} \pi_{\lambda cjtr} = \left(\pi_{\lambda cjtr}\right) \left(t_{jtr}\right) \tag{8.6.98}$$

$$\frac{\partial}{\partial \gamma} \pi^+_{cijt} = \left(\pi^+_{cijt}\right) \left(s_+\right) \tag{8.6.99}$$

$$\frac{\partial}{\partial \gamma} \pi^-_{cijt} = \left(\pi^-_{cijt}\right) \left(s_-\right) \tag{8.6.100}$$

All Plus Simplification of the Hessian of the Expectation Value (Unweighted)

$$\nabla^2 \langle \phi | \hat{C} | \phi \rangle = \sum_{(i,j)\in \mathrm{E}} \frac{w_{ij}}{2} \begin{pmatrix} \frac{\partial^2}{\partial \beta^2} & \frac{\partial^2}{\partial \gamma \partial \beta} \\ \frac{\partial^2}{\partial \beta \partial \gamma} & \frac{\partial^2}{\partial \gamma^2} \end{pmatrix} \langle \phi | \hat{Z}_i \hat{Z}_j | \phi \rangle \tag{8.6.101}$$

where,

$$\frac{\partial^2}{\partial \beta^2} \langle \phi | \hat{Z}_i \hat{Z}_j | \phi \rangle = -8 \sin 4\beta \langle \psi' | \hat{Y}_i \hat{Z}_j + \hat{Z}_i \hat{Y}_j | \psi' \rangle + 8 \cos 4\beta \langle \psi' | \hat{Y}_i \hat{Y}_j | \psi' \rangle \tag{8.6.102}$$

$$\frac{\partial^2}{\partial \gamma^2} \langle \phi | \hat{Z}_i \hat{Z}_j | \phi \rangle = \frac{1}{2} \sin 4\beta \frac{\partial^2}{\partial \gamma^2} \langle \psi' | \hat{Y}_i \hat{Z}_j + \hat{Z}_i \hat{Y}_j | \psi' \rangle + \sin^2 2\beta \frac{\partial^2}{\partial \gamma^2} \langle \psi' | \hat{Y}_i \hat{Y}_j | \psi' \rangle \tag{8.6.103}$$

$$\frac{\partial^2}{\partial \beta \partial \gamma} \langle \phi | \hat{Z}_i \hat{Z}_j | \phi \rangle = 2 \cos 4\beta \frac{\partial}{\partial \gamma} \langle \psi' | \hat{Y}_i \hat{Z}_j + \hat{Z}_i \hat{Y}_j | \psi' \rangle + 2 \sin 4\beta \frac{\partial}{\partial \gamma} \langle \psi' | \hat{Y}_i \hat{Y}_j | \psi' \rangle \tag{8.6.104}$$

$$= \frac{\partial^2}{\partial \gamma \partial \beta} \langle \phi | \hat{Z}_i \hat{Z}_j | \phi \rangle \tag{8.6.105}$$

and,

$$\frac{\partial^2}{\partial \gamma^2} \langle \psi' | \hat{Y}_i \hat{Z}_j | \psi' \rangle =$$
$$\sin w_{ij}\gamma \left(\pi_{cifl}\right) \left(\pi_{citl}\right) \left\{ \left[t_{ifl} + t_{itl} + \left(w_{ij} \cot w_{ij}\gamma \right) \right]^2 + \left[t'_{ifl} + t'_{itl} + \left(-w_{ij}^2 \csc w_{ij}\gamma \right) \right] \right\} \tag{8.6.106}$$

$$\frac{\partial^2}{\partial \gamma^2} \langle \psi' | \hat{Z}_i \hat{Y}_j | \psi' \rangle =$$
$$\sin w_{ij}\gamma \left(\pi_{cjfr}\right) \left(\pi_{\lambda cjtr}\right) \left\{ \left[t_{ifl} + t_{itl} + \left(w_{ij} \cot w_{ij}\gamma \right) \right]^2 + \left[t'_{ifl} + t'_{itl} + \left(-w_{ij}^2 \csc w_{ij}\gamma \right) \right] \right\} \tag{8.6.107}$$

$$\frac{\partial^2}{\partial \gamma^2} \langle \psi' | \left(\hat{Y}_i \hat{Y}_j \right) | \psi' \rangle =$$
$$-\frac{1}{2} \left(\pi_{cifl}\right) \left(\pi_{cjfr}\right) \left\{ \left[\left(t_{ifl} + t_{jfr} + s_- \right)^2 + \left(t'_{ifl} + t'_{jfr} + s'_- \right) \right] \left(\pi^-_{cijt} \right) \right.$$
$$\left. - \left[\left(t_{ifl} + t_{jfr} + s_+ \right)^2 + \left(t'_{ifl} + t'_{jfr} + s'_+ \right) \right] \left(\pi^+_{cijt} \right) \right\} \tag{8.6.108}$$

note,

$$t'_{ifl} = \sum_{k=1}^{L_{ij}} -w_{ifl_k}^2 \sec^2 w_{ifl_k}\gamma \tag{8.6.109}$$

$$t'_{itl} = \sum_{k=1}^{T_{ij}} -w_{itl_k}^2 \sec^2 w_{itl_k}\gamma \tag{8.6.110}$$

$$t'_{jfr} = \sum_{k=1}^{R_{ij}} -w_{jfl_k}^2 \sec^2 w_{jfl_k}\gamma \tag{8.6.111}$$

$$t'_{jtr} = \sum_{k=1}^{T_{ij}} -w_{jtr_k}^2 \sec^2 w_{jtr_k}\gamma \tag{8.6.112}$$

$$s'_- = \sum_{k=1}^{T_{ij}} -\left(w_{itl_k} - w_{jtr_k} \right) \sin \left(w_{itl_k}\gamma - w_{jtr_k}\gamma \right) \tag{8.6.113}$$

$$s'_+ = \sum_{k=1}^{T_{ij}} -\left(w_{itl_k} + w_{jtr_k} \right) \sin \left(w_{itl_k}\gamma + w_{jtr_k}\gamma \right) \tag{8.6.114}$$